

**What do we know about the quark gluon plasma  
from lattice gauge theory ?**

**E.-M. Ilgenfritz**

**Veksler-Baldin LHEP, JINR Dubna**

Helmholtz International Summer School 2013  
“Physics of Heavy Quarks and Hadrons”

BLTP, JINR, Dubna, Russia  
July 15 - 26

## Outline :

1. Introduction : Answers from analog simulations
2. Lattice formulation for QCD thermodynamics : some basic facts
3. The order parameters of two abstract phase structure problems
4. Searching for a transition along a line in the phase diagram
5. Phase transition and thermodynamics of twisted-mass fermions
6. Gluon and ghost propagators : a link to continuum approaches
7. Scanning the full phase diagram : finite baryonic density
8. Deep inside the phase diagram : properties of dense matter
9. Outlook

## 1. Introduction : Answers from analog simulations

How to characterize different phases of **Quantum Chromodynamics** ?

- thermodynamics
- symmetry
- topology
- functionality

### 1.1. Thermodynamics, Hamiltonian or Lagrangian approach ?

thermal density matrix or partition function:

$$\rho = \exp^{-\frac{1}{T}(H - \mu_i N_i)} , \quad Z = \hat{\text{Tr}}\rho , \quad \hat{\text{Tr}}(\dots) = \sum_n \langle n | (\dots) | n \rangle$$

$\mu_i$  are chemical potentials for some conserved charges  $N_i$

The trace is taken over the Hilbert space, but this might be different for different phases ! The single- or many-particle eigenstates of the (macroscopic) Hamiltonian are not known.

No such *a priori* knowledge should be necessary to proceed !

From the **partition function**  $Z(T, \mu_i)$ , we could obtain

$$\begin{aligned} F &= -T \ln Z, & \bar{N}_i &= \frac{\partial(T \ln Z)}{\partial \mu_i} \\ p &= \frac{\partial(T \ln Z)}{\partial V}, & E &= -pV + TS + \mu_i \bar{N}_i \\ S &= \frac{\partial(T \ln Z)}{\partial T}, \end{aligned}$$

Since the free energy is extensive,  $F = fV$ , in the thermodynamic limit it is more convenient to deal with the corresponding densities:

$$f = \frac{F}{V}, \quad p = -f, \quad s = \frac{S}{V}, \quad n_i = \frac{\bar{N}_i}{V}, \quad \epsilon = \frac{E}{V}$$

In particular **pressure  $p$  and energy density  $\epsilon$**  define together the trace anomaly, the entropy density, and the velocity of sound :

$$I(T) = T^{\mu\mu}(T) = T^5 \frac{\partial p(T)}{\partial T T^4} = \epsilon - 3p, \quad s = \frac{\epsilon + p}{T}, \quad c_s^2 = \frac{dp}{d\epsilon}$$

The **trace anomaly** will take a central position for the description of thermodynamic properties (by integrating the first relation).

**Lagrangian formulation in Euclidean space** (via path integral) allows to address these questions from first principles.

We believe to know the fundamental theory: take the **path integral over the fundamental fields of QCD** (**no matter whether these are confined or can exist – asymptotically – as free particles !**).

Neither quarks nor gluons are “physical” particles in this sense !

Their **lattice propagators** show this by **violation of spectral positivity** !

**Lattice simulation** means generation of **huge ensembles of 4-dimensional field specimen (“configurations”)**. Each ensemble represents the actual situation characterized by few parameters :

- **physically** : temperature, number and masses of quarks, eventually chemical potential of charges
- **lattice-technically** : lattice spacing and finite volume

Such ensembles can be stored, albeit only the gluonic field !

Quark fields (Grassmann fields) cannot be stored, are easily “added”.

## International Lattice Data Grid :

A library of field ensembles for use in the community

in US: <http://www.usqcd.org/ildg/>

in Europe: <http://hpc.desy.de/ldg/>

first pioneering steps : <http://qcd.nersc.gov/nersc/default/search>

An interested physicist/group can search according to metadata tags

- $\beta$  (the inverse coupling) of the simulation, determining the lattice spacing  $a$ ,
- the number of active (dynamical) flavors,
- the masses of the corresponding quarks,
- the volume  $N_x, N_y, N_z$  and  $N_t$  (in units of  $a$ , the latter determining the temperature  $aN_t = 1/T$ ,
- the collaboration that has produced the ensemble,
- the algorithm that has been used,

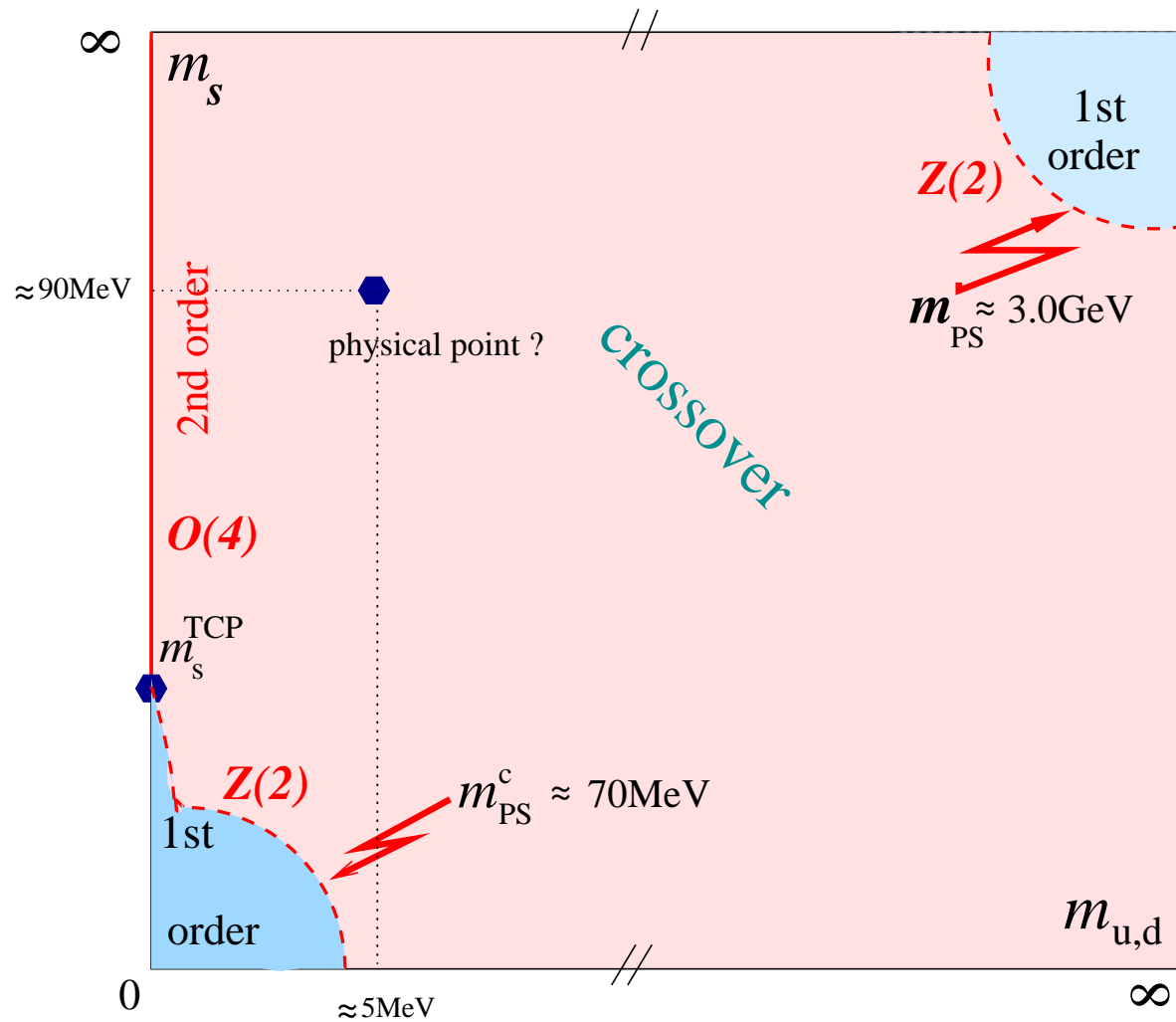
what he needs in order to start to do his/its own physical project.



By inspection of configurations one can study which phases are actually realized for the given parameters ! What one can expect ?

- **Thermodynamic functions** can witness only the sudden changes accompanying phase changes, cannot show structural details !
- To recognize **structural changes**, other observables are necessary (signals of symmetry breaking) : **order parameters**.
- **Hadronic correlators** are more general indicators of phase changes. Splitting between masses signals **breaking of symmetries**.
- Change of **topological structure** characterizes the different phases.
- Warning : all symmetry-related signals will become **clearly visible** in the corresponding limit  $m_q \rightarrow \infty$  (**tantamount to gluodynamics**) or in the limit  $m_q \rightarrow 0$  (**chiral limit of QCD**) only, not in real QCD !

The QCD transition at  $\mu = 0$  as function of quark masses  
 (so-called Columbia plot) from arXiv:1203.5320 Petreczky



## 1.2. Some words about path integrals and partition functions

For non-interacting systems (quadratic action), a **path integral** can be easily evaluated (see the textbooks) :

$$Z_0 = N \int D\phi e^{-S_0(\phi)} = N'(\det \Delta^{-1})^{-1/2}$$

$\Delta^{-1} = (\omega_n^2 + \omega^2)/T^2$  is the inverse propagator in momentum space with  $\omega^2 = m^2 + \vec{p}^2$ . This leads to the **more familiar expression** :

$$\lim_{V \rightarrow \infty} \ln Z_0 = V \int \frac{d^3p}{(2\pi)^3} \left[ \frac{-\omega}{2T} - \ln \left( 1 - e^{-\frac{\omega}{T}} \right) \right]$$

The integral over the first term diverges in the UV since  $\omega \sim |\mathbf{p}|$ .

**Renormalisation condition** : zero-point energy contribution must be subtracted, vacuum has to have zero pressure

$$p_{\text{phys}}(T) = p(T) - p(T = 0)$$

**Partition function for a free gas of spinless bosons**

$$\ln Z_0 = -V \int \frac{d^3p}{(2\pi)^3} \ln \left( 1 - e^{-\frac{\omega}{T}} \right)$$

For the  $m = 0$  case, the momentum integral can be done exactly.

**Pressure per bosonic degree of freedom** (no chemical potential,  $\mu = 0$ )

$$p = \frac{\pi^2}{90} T^4$$

## Counting the gluon degrees of freedom

For **non-abelian gauge fields**  $A_\mu^a$ , each field component corresponds to one bosonic mode, i.e. sum over  $a = 1, \dots, N^2 - 1$  and  $\mu = 1 \dots 4$ . This yields a **factor of**  $4(N^2 - 1)$ .

For gauge theories **gauge fixing is necessary** in order to invert the two-point function. For the free photon or Yang-Mills gas, two of the four bosonic Lorentz degrees of freedom get **cancelled by the corresponding ghost contributions**.

Thus a **factor of**  $2(N^2 - 1)$  instead of  $4(N^2 - 1)$  (with two polarisation states per massless vector particle) results.

Similar steps for a free Dirac field lead to the result

$$\ln Z_0 = 2V \int \frac{d^3p}{(2\pi)^3} \left[ \ln \left( 1 + e^{-\frac{\omega-\mu}{T}} \right) + \log \left( 1 + e^{-\frac{\omega+\mu}{T}} \right) \right]$$

Counting the quark degrees of freedom

**Factor of two** : represents the **two spin states** of a fermion.

**The two log-terms** (with  $\pm\mu$ ) are coming from **fermion and anti-fermion**.

Momentum integration for **one massless fermionic degree of freedom** (with  $\mu = 0$ ) gives the **fermionic pressure per d.o.f.**

$$p = \frac{7\pi^2}{890} T^4$$

Stefan-Boltzmann pressure of  $N_f$  flavors of quarks and antiquarks (counting their  $N$  colors) plus corresponding gluons :

$$\frac{p}{T^4} = \left( 2(N^2 - 1) + 4NN_f \frac{7}{8} \right) \frac{\pi^2}{90}$$

This limit is hardly reached at any foreseeable collision energy.

Interaction prevents all degrees of freedom from being fully activated !

Moreover, hadrons are the relevant degrees of freedom at low  $T$ .

For arbitrary masses  $m_i$  ( $\omega_i^2 = m_i^2 + \vec{p}^2$ ) one can write  $\ln Z_i^1(V, T)$  as

$$\ln Z_i^1(V, T) = \eta V \nu_i \int \frac{d^3p}{(2\pi)^3} \ln(1 + \eta e^{-(\omega_i - \mu_i)/T})$$

$\eta = -1$  for bosons and  $\eta = 1$  for fermions,  $\nu_i$  counts the degeneracy (spin) for particle of type  $i$ . Applicable for non-interacting hadrons as long as the internal d. o. f. are not excited.

### 1.3. Simplest models describing confined and deconfined phases

Hadron Gas Model (HGM, an approximation for the confined phase)

non-interacting hadrons, mesons = bosons and (anti-)baryons = fermions.

The confinement phase is interpreted as gas of individual hadrons.

This is reasonable as long as the energy density is not very high.

The deconfinement transition then seems to be not more than a sudden proliferation of degrees of freedom at some temperature  $T_{\text{dec}}$ .

These new d. o. f. remain “frozen” in the confinement phase (i.e. quarks inside hadrons, gluons in glueballs/usual hadrons).

Freezing (confinement) and deconfinement cannot be “explained” just by these thermodynamic formulae.



## Bag model

The “**bag pressure**”  $B$  is merely a trick to make the two pressure functions (hadron gas vs. quark-gluon gas) intersecting at some  $T_{\text{dec}}$ , by downshifting of the steeper one (first order transition) :

$$p_{\text{hadron}}(T_{\text{dec}}) = p_{\text{plasma}}(T_{\text{dec}}) - B \quad \text{or} \quad \left( c_{\text{SB}}^{\text{plasma}} - c_{\text{SB}}^{\text{hadron}} \right) T_{\text{dec}}^4 = B.$$

## Hadron Resonance Gas Model (HRGM)

This is an attempt to take into account the **interactions between hadrons, increasing with increasing density**, by including more (and more massive) resonance states in the sum over  $\ln Z_i^1(V, T)$  (including Particle Data Group Table states up to  $\approx 2$  GeV).

The model **describes reasonably well the onset of the phase transition from the hadronic side** (by an increasing number of effective degrees of freedom, of hadron species becoming “active”).

## Hagedorn model

exponential mass spectrum  $\rightarrow$  “maximal” hadronic temperature when singularities of the partition function are reached.

Such a spectrum was enforced by the selfconsistent bootstrap condition postulated 1965-68 by R. Hagedorn and reformulated by S. C. Frautschi in 1971 (meant to comprise hadron physics)

**Alternative view : no maximal temperature, quark liberation !**

**Two important papers in 1974/1975 : lattice, high temperature and high density** described this change of paradigm :

- “Confinement of Quarks”,  
Kenneth G. Wilson, Phys. Rev. D10 (1974) 2445
- “Exponential Hadronic Spectrum and Quark Liberation”,  
N. Cabibbo and G. Parisi, Phys. Lett. B59 (1975) 67

Application of LGT to the QCD at finite  $T$  : has provided the first real prediction of LGT : the  $SU(2)$  deconfinement transition

- “A Monte Carlo Study of  $SU(2)$  Yang-Mills Theory at Finite Temperature”, L. D. McLerran and B. Svetitsky, Phys. Lett. B98 (1981) 195
- “Monte Carlo Study of  $SU(2)$  Gauge Theory at Finite Temperature”, J. Kuti, J. Polonyi, and K. Szlachanyi, Phys. Lett. B98 (1981) 199

Both discovered deconfinement in the sense of center symmetry breaking (to be described later).

## 2. Lattice formulation for QCD thermodynamics : some basic facts

### 2.1. Path integral expression for the partition function

$$Z(V, \mu_f, T; g, m_f) = \int DA D\bar{\psi} D\psi e^{-S_g[A_\mu]} e^{-S_f[\bar{\psi}, \psi, A_\mu]}$$

Euclidean formulation here natural, not just a **trick (Wick rotation)** to avoid the oscillating weight in Minkowski space (reappears for  $\mu \neq 0$ ) !

Euclidean gauge and fermion actions :

$$S_g[A_\mu] = \int_0^{1/T} d\tau \int_V d^3x \frac{1}{2} \text{Tr} F_{\mu\nu}(x) F_{\mu\nu}(x),$$
$$S_f[\bar{\psi}, \psi, A_\mu] = \int_0^{1/T} d\tau \int_V d^3x \sum_{f=1}^{N_f} \bar{\psi}_f(x) (\gamma_\mu D_\mu + m_f - \mu_f \gamma_0) \psi_f(x)$$

Covariant derivative with  $A_\mu$  field and gauge coupling  $g$

$$D_\mu = (\partial_\mu - igA_\mu), \quad A_\mu = T^a A_\mu^a(x), \quad a = 1, \dots, N^2 - 1$$

Field strength, non-linear in  $A_\mu$  (non-Abelian)

$$F_{\mu\nu}(x) = \frac{i}{g}[D_\mu, D_\nu] = \partial_\mu A_\nu - \partial_\nu A_\mu - ig[A_\mu, A_\nu]$$

Bosonic fields (commuting) and fermionic fields (anticommuting, defined by Grassmann calculus) have **different temporal boundary conditions over the finite “time” interval of length  $1/T$  :**

$$A_\mu(\tau, \mathbf{x}) = A_\mu(\tau + \frac{1}{T}, \mathbf{x}), \quad \psi_f(\tau, \mathbf{x}) = -\psi_f(\tau + \frac{1}{T}, \mathbf{x})$$

In a finite volume  $V = L^3$  and at temperature  $T$

- allowed spatial momenta are discrete  $p_\mu = (2n_\mu\pi)/L$  for  $\mu = 1, 2, 3$
- allowed “Matsubara” frequencies are  
 $\omega = 2n_4\pi T$  for bosons (gluons) with periodic boundary conditions  
 $\omega = (2n_4 + 1)\pi T$  for fermions (quarks) with antiperiodic b. c.

By discretizing space and time, a lattice of  $N_s^3 \times N_t$  sites is replacing the continuum, making it accessible for numerical simulation.

$$n_\mu = 0, \dots, N_s - 1 \text{ and } n_4 = 0, \dots, N_t - 1$$

The lattice spacing  $a$  relates this to the continuum box :

$$L = N_s a \quad V = L^3 \quad \text{and} \quad \frac{1}{T} = N_t a$$

What replaces the gluon field  $A_\mu(x)$  ?

Fundamental degrees of freedom are links (“transporters”) between neighboring lattice sites  $x$  and  $x + \hat{\mu}$ :

$$U_\mu(x) = P \exp \left( \int_0^1 i a d\lambda A_\mu(x + (1 - \lambda)\hat{\mu}) \right)$$

The standard Wilson gauge action in terms of links

$$S_g[U] = \sum_x \sum_{1 \leq \mu < \nu \leq 4} \beta \left( 1 - \frac{1}{3} \text{ReTr} U_p \right)$$

is expressed via elementary plaquettes (discrete version of curl !)

$$U_p = U_\mu(x) U_\nu(x + a\hat{\mu}) U_\mu^\dagger(x + a\hat{\nu}) U_\nu^\dagger(x)$$

ReTr takes the square !  $\beta$  related to gauge coupling  $g$  via  $\beta = 2N/g^2$ .

The relation between  $a$  and  $\beta$  is set by the **renormalisation group** :

$$a\Lambda_L = \left(\frac{6 b_0}{\beta}\right)^{-b_1/2b_0^2} e^{-\frac{\beta}{12b_0}}, \quad \text{for } N = 3 \text{ colors}$$

$$b_0 = \frac{1}{16\pi^2} \left(11 - \frac{2}{3}N_f\right), \quad b_1 = \left(\frac{1}{16\pi^2}\right)^2 \left[102 - \left(10 + \frac{2}{3}\right)N_f\right]$$

$\Lambda_L$  characterizes the kind of lattice actions (mainly gluonic action).

**Deviations from this “two-loop asymptotic scaling”** formula are unavoidable at low  $\beta$  ! They can be fixed by ***ad hoc* calibration simulations at  $T = 0$**  (i.e.  $N_s \leq N_t$ ), which are necessary to obtain the function  $a(\beta)$ , by fixing either ...



Find the function  $a(\beta)$  by fixing ...

- ... either the “**Sommer scale**”  $r_0$  or its variant  $r_1$  defined by

$$\left( r^2 \frac{dV_{\bar{Q}Q}(r)}{dr} \right)_{r=r_0} = 1.65 \quad \left( r^2 \frac{dV_{\bar{Q}Q}(r)}{dr} \right)_{r=r_1} = 1.00$$

to a generally agreed physical value, say  $r_0 \approx 0.48$  fm.

- ... or a **measured vector meson mass**, say  $m_\rho$ , to the physical value.
- For most settings, the **measured pseudoscalar masses**  $m_\pi$  **etc.** would differ strongly from the physical values (not suitable) !
- The **ratio**  $m_\pi/m_\rho$  is an *a posteriori* **measure of quality assessment**, describing how good the simulation approaches physical QCD.

- The simulation time behaves

$$\text{CPU time} \propto (N_s^3 N_t)^{\frac{5}{4}} \left(\frac{r_0}{a}\right)^7 \left(\frac{m_\rho}{m_\pi}\right)^{z_\pi}$$

with high exponent  $z_\pi \approx 6$ , the “Berlin wall” behavior !

- The limit  $m_\pi \rightarrow m_\pi^{\text{physical}}$  is extremely costly !

Chiral perturbation theory ( $\chi$ PT) may do the **extrapolation of lattice results to their physical counterpart.**

- For all finite-temperature studies it is important to **record the would-be pion mass  $m_\pi$  to characterize the setting in use !**
- Typically, **many sets of simulations are done, with varying  $m_\pi$ ,** in order to get the corresponding crossover/transition temperatures  $T_\chi$  and to find a suitable **chiral extrapolation.**

## Hamiltonian and transfer matrix view of the time lattice :

The definition of **transfer matrix in “coordinate  $U_i$  representation”**

$$T[U_i(\tau + 1), U_i(\tau)] = e^{-aH} = \int DU_0(\tau) \exp(-L[U_i(\tau + 1), U_0(\tau), U_i(\tau)])$$

includes the **integration over all timelike links linking 2 time slices.**

$$S_g = \sum_{\tau} L[U_i(\tau + 1), U_0(\tau), U_i(\tau)]$$

with

$$L[U_i(\tau + 1), U_0(\tau), U_i(\tau)] = \frac{1}{2}L_1[U_i(\tau + 1)] + L_2[U_i(\tau + 1), U_0(\tau), U_i(\tau)] \\ + \frac{1}{2}L_1[U_i(\tau)]$$

$$L_1[U_i(\tau)] = -\frac{\beta}{N} \sum_{p(\text{fixed } \tau)} \text{ReTr}U_p \quad (\text{spacelike at a single time})$$

$$L_2[U_i(\tau + 1), U_0(\tau), U_i(\tau)] = -\frac{\beta}{N} \sum_{p(\text{linking } \tau, \tau+1)} \text{ReTr}U_p \quad (\text{timelike only})$$

Partition function expressed as “matrix product” by multiple integration over spacelike links  $U_i$  (located within time slices) :

$$Z = \int \prod_{\tau} (DU_i(\tau, \mathbf{x}) T[U_i(\tau + 1), U_i(\tau)]) = \hat{\text{Tr}}(T^{N_{\tau}}) = \hat{\text{Tr}}(e^{-N_{\tau}aH})$$

A time slice  $\{U_i(\tau)\}$  encodes **all possible states of the Hilbert space**. Importance sampling exhibits the essence of respective phases. Does the overlap between the respective Hilbert spaces vanish in the limit  $V \rightarrow \infty$  ?

Qualitative changes are physically recognizable (but not only !) in **equal-time correlators ! (screening lengths)**

For  $Z$ , taking the trace requires periodicity, :

$$U_i(\tau = 1) = U_i(\tau = N_{\tau} + 1)$$

which plays an important role in understanding QCD at finite  $T$ .

## 2.2. Dynamical fermions

Including “dynamical fermions” means inclusion of a bilinear fermion action in terms of Grassmann fields (interacting only through the gauge field !)

$$S_f = \sum_{x,y} \bar{\psi}(x) D_{xy}^f(\{U\}; m_f) \psi(y)$$

into the total action.  $D$  is the Dirac operator (first derivatives).

The **Grassmann Gauss integral can be done (only !) formally.**

In observables which contain  $\psi$  and  $\bar{\psi}$ , these can be **contracted by inserting everywhere fermion propagators**  $(D^f)^{-1}(\{U\})$  which are supposed to be known for any given gauge field background  $U$ .

The full partition function contains the “fermion determinants” coming from Grassmann Gaussian integration :

$$Z(N_s, N_t; \beta, m_f) = \int \prod_{\tau=1}^{N_t} \prod_{\mathbf{x}, \mu} dU_\mu(\tau, \mathbf{x}) \prod_f \det D^f(\{U\}; m_f) e^{-S_g[U]}$$

with thermal (timelike) boundary conditions

$$\begin{aligned} U_\mu(\tau, \mathbf{x}) &= U_\mu(\tau + N_t, \mathbf{x}) \\ \psi(\tau, \mathbf{x}) &= -\psi(\tau + N_t, \mathbf{x}) \end{aligned}$$

and with the bosonic integration measure

$$dU = \text{Haar measure on the compact Lie group } SU(N)$$

For example,  $N_f$  degenerate Wilson fermions described by

$$\begin{aligned}
 S_f^W &= \sum_{x,y,f} a^4 \bar{\psi}_f(x) D_{xy}^f(\{U\}; m_f) \psi_f(y) \\
 &= \frac{1}{2a} \sum_{x,\mu,f} a^4 \bar{\psi}_f(x) [(\gamma_\mu - r) U_\mu(x) \psi_f(x + \hat{\mu}) \\
 &\quad - (\gamma_\mu + r) U_\mu^\dagger(x - \hat{\mu}) \psi_f(x - \hat{\mu})] \\
 &\quad + \sum_{x,f} \left(m + 4\frac{r}{a}\right) a^4 \bar{\psi}_f(x) \psi_f(x)
 \end{aligned}$$

For  $m = 0$  and without Wilson's  $r$ , the Dirac operator fulfills chiral invariance :  $\gamma_5 D + D \gamma_5 = 0$ .

Effective action includes the determinants :

$$S_{\text{eff}}[U] = S_g[U] - \sum_f \ln \det D^f(\{U\}; m_f)$$

## 2.3. General terminology (for all kinds of lattice fermions)

- **Gluodynamics/Yang-Mills theory** :  $N_f = 0$ , no dynamical fermions; “quenched approximation” of QCD, feedback of quarks impossible.
- $N_f = 2$  “**full QCD**” :  $N_f = 2$  degenerate flavors of first generation ( $u$  and  $d$  quarks) made dynamical; chiral limit  $m_u = m_d \rightarrow 0$ .
- $N_f = 2 + 1$  “**full QCD**” : one heavier flavor ( $s$  quark) added to the first generation.
- $N_f = 3$  **QCD** : all three flavors taken mass-degenerate, eventually the chiral limit  $m_u = m_d = m_s \rightarrow 0$  is intended.
- $N_f = 4$  **QCD** : four flavors taken mass-degenerate, eventually all massless. Then the critical endpoint sits at  $(T = T_\chi, \mu_q = 0)$ .



- $N_f = 2 + 1 + 1$  “real QCD” : inclusion of two generations of light (degenerate  $u$  and  $d$ ) and heavy (non-degenerate  $s$  and  $c$ ) quarks.  $c$  quarks contribute to EoS already at temperature  $T > 200$  MeV.

## 2.4. Complications due to dynamical fermions

- Nonlocal updates of the gauge field necessary !
- Why chiral symmetry of the Dirac operator must be given up ?
- How to simulate with non-vanishing baryonic chemical potential ?  
Sign problem ! Change the order of integration from “fermions first” to gauge field first ? Strong coupling versions of lattice QCD have a weaker sign problem.

## Euclidean measure

positive as long as  $\mu_B = 0$ , fermion determinants are real-valued.

Great advantage : importance sampling of gauge fields is still possible !

- for pure gauge theories : local updates (heat bath or Metropolis)
- for theories with fermions : non-local, global “smart updates”  
obtained by solving **Hamilton’s equations of motion** for  $U_\mu(x)$   
 (“trajectories” running in **5-th dimension**  $\tau$  over  $\Delta\tau = \mathcal{O}(1)$ ) with
  - a “potential energy”  $U_{\text{pot}} = S_{\text{eff}}[U]$
  - a “kinetic energy”  $T_{\text{kin}} = \frac{1}{2} \sum_{x,\mu} \text{tr} [\Pi_\mu(x)]^2$ ,

applying **Metropolis acceptance check** w.r.t. the positive measure

$$\text{weight} \propto \exp(-T_{\text{kin}} - U_{\text{pot}})$$

Hybrid Monte Carlo algorithm solves the first fermion problem !

Lattice fermions present a deeper theoretical problem, however :

In order to circumvent the **fermion doubling problem**, one has to sacrifice **chiral symmetry**,  $\gamma_5 D + D \gamma_5 = 0$ , of the (massless) action.

**Chiral symmetry is - after that step is done - either**

- reduced, as for **staggered** (Kogut-Susskind) fermions, or
- broken completely, as for **Wilson fermions**.

**This renders the study of the behaviour in the chiral limit difficult.**

**Chiral symmetry is optimally realized on the lattice using**

- **overlap** (Neuberger) fermions, with  $\gamma_5 D + D \gamma_5 = \frac{a}{\rho} D \gamma_5 D$  ( $D$  as solution of this “Ginsparg-Wilson relation”) or
- **domain wall** (Kaplan) fermions (**in 4+1 dimensions**).

Overlap and domain wall fermions optimally saturate the principal limit for chiral symmetry that is imposed by the discretization !

However, apart from other delicate algorithmic problems, present day computing capacity is hardly sufficient for mass production of gauge field ensembles.

Chemical potential  $\mu_B \neq 0$  presents the **third, hard practical problem !**

**This “sign problem” is not restricted to fermionic field theories !**

A chemical potential, counting any kind of **conserved charge**, is introduced by the **substitution** (Karsch and Hasenfratz, 1982)

$$\begin{aligned} U_0(\mathbf{x}, \tau) &\rightarrow U_0(\mathbf{x}, \tau) \exp(+\mu_q a) && \text{timelike forward link} \\ U_0^\dagger(\mathbf{x}, \tau) &\rightarrow U_0^\dagger(\mathbf{x}, \tau) \exp(-\mu_q a) && \text{timelike backward link} \end{aligned}$$

$\mu_q$  acts as **time component of an external imaginary Abelian gauge field**, while the same  $\mu_q$  counts **quark-minus-antiquark (baryon charge)**.

Along a forward **Wilson line** a weight  $\exp(\mu_q/T)$  is accumulated, for a **baryon loop** the weight factor is  $\exp(\mu_B/T) = \exp(3\mu_q/T)$ .

**Complex valuedness of fermion determinants** can be concluded from the  **$\gamma_5$ -hermiticity of Dirac operators** (precisely, its violation) :

$$\gamma_5 D \gamma_5 = D^\dagger \quad \text{implies} \quad \det D = [\det D]^*$$

$\gamma_5$ -hermiticity is **spoiled for  $\mu_q \neq 0$** , when one has instead

$$\gamma_5 D(\mu_q) \gamma_5 = D^\dagger(-\mu_q) \quad \rightarrow \quad \text{determinant is complex}$$

This is the **universal origin** of the **sign problem** appearing in all **fermionic problems**.

Presence of two flavors would not render the weight factor real.

## 2.5. Exceptional cases without sign problem :

**A. Imaginary chemical potential** : for  $\mu_q = i\eta$  the determinant is real. Then (at least for two flavors) the weight is positive.

Optimistic approach : **simulate at  $\mu_q^2 < 0$  and extrapolate to  $\mu_q^2 > 0$ .**

Examples for analytic continuation : **transition temperature, screening lengths** etc. can be represented as analytic functions of  $\mu^2$

**But no direct access available to gauge field configurations that would be corresponding to real  $\mu_q \neq 0$  ! (the “no-overlap problem”)**

**B. Isospin chemical potential** : if for two flavors, the species have opposite isospin charge,  $\mu_u = \mu_I$  and  $\mu_d = -\mu_I$ .

The **Dirac operator of both flavors** has block-diagonal form

$$\begin{pmatrix} D(\mu_I) & 0 \\ 0 & D(-\mu_I) \end{pmatrix}$$

or

$$\begin{pmatrix} D(\mu_I) & 0 \\ 0 & \gamma_5 D^\dagger(\mu_I) \gamma_5 \end{pmatrix}$$

The **common determinant** is

$$\det[D(\mu_I)] \det[\gamma_5 D^\dagger(\mu_I) \gamma_5] = \det[D(\mu_I)] \det[D^\dagger(\mu_I)] = |\det[D(\mu_I)]|^2$$

**Lesson :**

“For finite isospin chemical potential, the determinantal weight factor in the presence of two flavors (opposite in isospin) is real and positive.”



### C. Chiral (or axial) chemical potential $\mu_5$

Creates an **imbalance between left handed and right handed matter** mimicking the presence of a topologically charged background field :

$$D(\mu_5) = \gamma_\mu D_\mu + m + \mu_5 \gamma_4 \gamma_5 \quad \text{in continuum}$$

in lattice notation like Karsch/Hasenfratz :

$$\begin{aligned} [D_W(\mu_5)]_{x,y} &= \delta_{x,y} - \kappa \sum_i \left[ (1 - \gamma_i) U_i(x) \delta_{x+\hat{i},y} + (1 + \gamma_i) U_i^\dagger(x - \hat{i}) \delta_{x-\hat{i},y} \right] \\ &\quad - \kappa \left[ (1 - \gamma_4 e^{a\mu_5 \gamma_5}) U_4(x) \delta_{x+\hat{4},y} + (1 + \gamma_4 e^{-a\mu_5 \gamma_5}) U_4^\dagger(x - \hat{4}) \delta_{x-\hat{4},y} \right] \end{aligned}$$

with

$$e^{\pm a\mu_5 \gamma_5} = \cosh(a\mu_5) \pm \gamma_5 \sinh(a\mu_5)$$

This again **satisfies  $\gamma_5$ -hermiticity** :  $\gamma_5 D(\mu_5) \gamma_5 = D^\dagger(\mu_5)$

**Consequently, the determinant is real-valued !**

Simulation result : **A current is induced through the chiral magnetic effect (CME)** in presence of an external magnetic field  $\vec{B}$  acting on electrical charges  $e$  :

$$\vec{j} = \frac{1}{2\pi^2} \mu_5 e \vec{B}$$

#### D. Other gauge groups than $SU(3)$ :

For example, the gauge groups  $SU(2)$ ,  $G_2$  and  $SO(N)$  do not have a sign problem !

One might be tempted to escape to such “toy models”.

### 3. The order parameters of two abstract phase structure problems

#### 3.1. Quenched limit of QCD and $Z(N)$ -symmetry

quarks infinitely heavy  $\rightarrow$  pure gauge theory plus static quark fields;  
action must be invariant under standard gauge transformations

$$S_g[U^g] = S_g[U] \quad \text{with} \quad U_\mu^g(x) = g(x)U_\mu(x)g^{-1}(x + \hat{\mu}), \quad g(x) \in SU(N)$$

with **periodic boundary conditions** both for  $U$  and  $g$  :

$$U_\mu(\tau, \mathbf{x}) = U_\mu(\tau + N_\tau, \mathbf{x}), \quad g(\tau, \mathbf{x}) = g(\tau + N_\tau, \mathbf{x})$$

Additionally, gauge transformations  $g'(x)$  of **“topologically non-trivial kind”**  
can be permitted, **which are periodic only up to a constant matrix  $h$**  :

$$g'(\tau + N_\tau, \mathbf{x}) = hg'(\tau, \mathbf{x}), \quad h \in SU(N)$$

Thus,  $g'(x)$  picks up a **“twist” factor  $h$**  winding once around the torus.

The gauge links, after an extended gauge transformation, would behave across the temporal boundary as

$$U_{\mu}^{g'}(\tau + N_{\tau}, \mathbf{x}) = h U_{\mu}^{g'}(N_{\tau}, \mathbf{x}) h^{-1}$$

This is **consistent with periodicity** if and only if  $[h, U_i^{g'}] = 0$ , i.e.

$$h = z\mathbf{1} \in Z(N), \quad \text{center of } SU(N) \quad z = \exp\left(i\frac{2\pi n}{N}\right), \quad n \in \{0, 1, 2, \dots, N-1\} .$$

**Lesson :**

“Pure gauge theory at finite temperature is invariant under gauge transformations with non-trivial winding, for any global twist factor  $h \in Z(N)$ , the center of the gauge group  $SU(N)$ .”

Gauge invariant observables are sensitive to twists if and only if they wind around the torus, too.

Example : “Wilson line” in the temporal direction closing onto itself, nowadays called (un-traced) “Polyakov loop”:

$$L(\mathbf{x}) = \prod_{x_0}^{N_\tau} U_0(x) .$$

Physically, this is the “propagator” of a static quark.

Under gauge transformations of the two sorts, it behaves

$$\begin{aligned} L^g(\mathbf{x}) &= g(x)L(\mathbf{x})g^{-1}(x), \\ L^{g'}(\mathbf{x}) &= g'(1, \mathbf{x})L(\mathbf{x})g'^{-1}(1 + N_\tau, \mathbf{x}) = g'(1, \mathbf{x})L(\mathbf{x})g'^{-1}(1, \mathbf{x})h^{-1} . \end{aligned}$$

such that for the trace holds

$$\mathrm{Tr} L^g = \mathrm{Tr} L, \quad \mathrm{Tr} L^{g'} = z^* \mathrm{Tr} L .$$

We conclude that the **traced Polyakov loop**

- is gauge invariant w.r.t. topologically trivial gauge transformations,
- picks up a center element  $z^*$  when transformed with a non-trivial, winding gauge transformation,

The Polyakov loop emerges as observable in the **QCD path integral with heavy quarks** (to leading order in the hopping expansion).

Consider : partition function for pure gauge theory with a single static quark sitting at  $\mathbf{x}$ :

$$Z_Q = \int DU \text{Tr} L(\mathbf{x}) e^{-S_g[U]} .$$

Hence, the **expectation value** of  $\text{Tr} L$  is :

$$\langle \text{Tr} L \rangle = \frac{1}{Z} \int DU \text{Tr} L e^{-S_g} = \frac{Z_Q}{Z} = e^{-(F_Q - F_0)/T} ,$$

Lesson :

“VEV of Polyakov loop = exponential of free energy difference between the Yang-Mills plasma with and without a static quark embedded.”

Two limiting cases make clear how center symmetry can be realized :

- For  $T \rightarrow 0$  Yang-Mills theory is confining. It would cost infinite energy to place a single quark into the gluon plasma,  $F_Q = \infty$ , and

$$\langle \text{Tr } L \rangle = 0$$

“Center symmetry is manifest !”

- $T \rightarrow \infty$  corresponds to  $\beta \rightarrow \infty$ , for which  $U_0 \rightarrow 1$  and

$$\langle \text{Tr } L \rangle \rightarrow \text{Tr } \mathbf{1} = N .$$

A non-zero expectation value cannot be invariant under center transformations  $\rightarrow$  “Center symmetry is spontaneously broken !”

**Lesson :**

“QCD in the quenched limit has a true (non-analytic) deconfinement phase transition, corresponding to the breaking of the global center symmetry. The average of the Polyakov loop is the corresponding order parameter.”

If **dynamical quark fields are added**, they will behave as

$$\psi^g(x) = g(x)\psi(x), \quad \psi(\tau + N_\tau, \mathbf{x}) = -\psi(\tau, \mathbf{x}), \quad \psi^{g'}(\tau + N_\tau, \mathbf{x}) = -h\psi(\tau, \mathbf{x})$$

Statistical mechanics requires anti-periodic boundary conditions for fermions, therefore **trivial  $h = 1$  is the only permissible choice.**

**There is no center symmetry in the presence of dynamical quarks !**



- Physically, if there are dynamical quarks, their pair production screens the confining force (it leads to string breaking):  
 $F_Q$  is finite, and the  $Q\bar{Q}$  potential stops rising at  $R = R_{\text{string-breaking}}$ .
- Correspondingly,  $\langle \text{Tr } L \rangle \neq 0$  for all temperatures, and the Polyakov loop is no longer a true order parameter.
- In this case, a non-analytic phase transition as a function of temperature is not realized; confined and deconfined regions may be then analytically connected by a smooth crossover.

Example: With heavy quarks ( $m_q = \mathcal{O}(3 \dots 10)$  GeV) the first order phase transition line, beginning with pure  $SU(3)$  Yang-Mills theory, terminates and goes over into a crossover at some critical endpoint. The would-be physics is governed by competition between explicit and spontaneous breaking of center symmetry.

## 3.2. The chiral limit of QCD

Classical QCD Lagrangian in the limit of zero quark masses is invariant under **global chiral symmetry transformations** with the symmetry group  $U_A(1) \times SU_L(N_f) \times SU_R(N_f)$ .

- **axial  $U_A(1)$  is anomalous**, quantum corrections break it down to  $Z(N_f)$
- remainder gets **spontaneously broken to the diagonal subgroup**,  $SU_L(N_f) \times SU_R(N_f) \rightarrow SU_V(N_f)$ , giving rise to  $N_f^2 - 1$  massless **pseudoscalar Goldstone bosons** (pions, kaons etc.)
- the **order parameter of chiral symmetry** is the chiral condensate,

$$\langle \bar{\psi}\psi \rangle = \frac{1}{N_s^3 N_t} \frac{\partial}{\partial m_f} \ln Z = \frac{1}{N_s^3 N_t} \langle \text{tr} D_f^{-1} \rangle \propto \langle \rho(\lambda = 0) \rangle$$

This is the “**Banks-Casher relation**”, it holds since

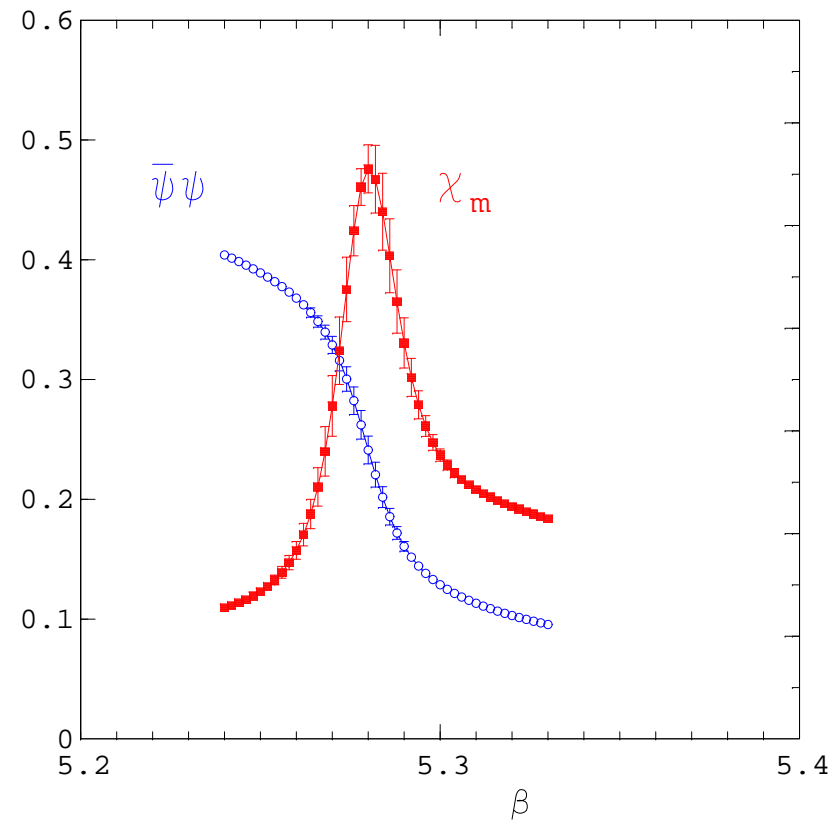
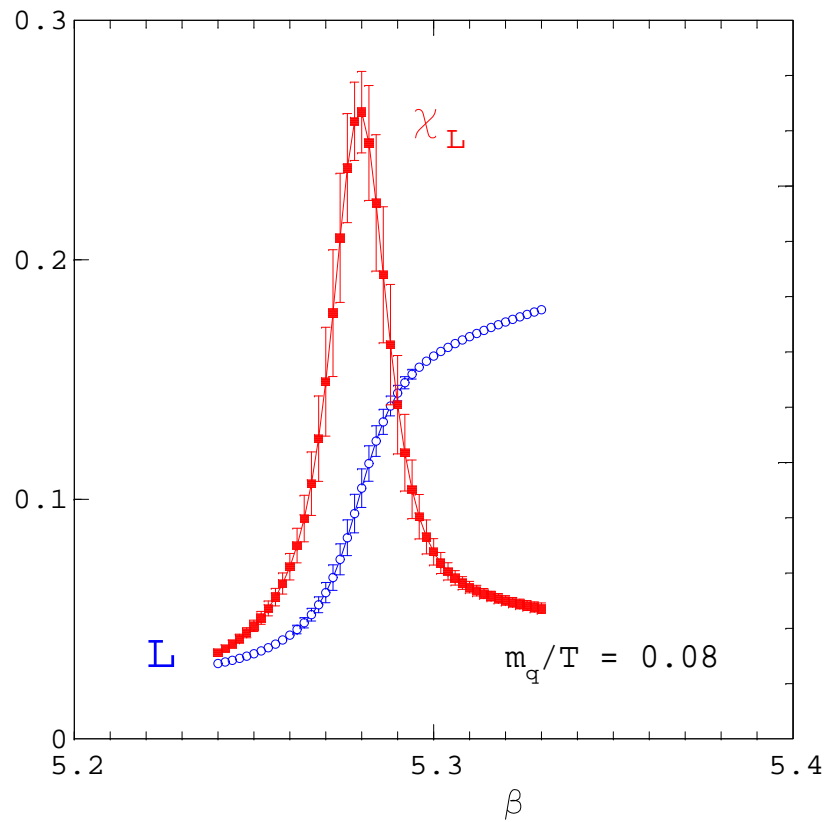
$$\langle \bar{\psi}\psi \rangle \propto \lim_{m \rightarrow 0} \left\langle \sum_{\text{eigenvalue } i} \frac{1}{i \lambda_i + m} \right\rangle = \lim_{m \rightarrow 0} \int d\lambda \langle \rho(\lambda) \rangle \frac{2m}{\lambda^2 + m^2} = \langle \rho(\lambda = 0) \rangle$$

- **A clear order parameter would mean :**  
 $\langle \bar{\psi}\psi \rangle \neq 0$  for  $T < T_\chi$  (chiral symmetry is **spontaneously broken** )  
and  $\langle \bar{\psi}\psi \rangle = 0$  for  $T > T_\chi$  (when **chiral symmetry is restored** ).
- for **zero quark mass** there is a **non-analytic finite temperature phase transition** corresponding to chiral symmetry restoration.
- For **non-zero quark masses**, chiral symmetry is broken explicitly.  
The chiral condensate is then  $\langle \bar{\psi}\psi \rangle \neq 0$  for all temperatures.
- Again, in this case a **non-analytic phase transition** related to **chiral symmetry** is not realized : **there is an analytical crossover.**

### 3.3. Physical QCD

- QCD with physical quark masses is **very different both from the chiral or quenched limit.**
- $Z(3)$  symmetry as well as **chiral symmetry** are explicitly broken.
- Still, physical QCD possesses **confinement (in the sense of absence of colored states, also of gluons)** as well as **three light pions** as “remnants” of **chiral symmetry (and its breaking).**
- In the presence of mass terms there is **no true order parameter.** The expectation values of **Polyakov loop and chiral condensate are non-vanishing at any temperature.**
- Hence, the **deconfined and chirally symmetric phase** is **analytically connected** with the **confined and chirally broken phase.**

Polyakov loop  $L$  (left) and chiral condensate  $\langle \bar{\psi}\psi \rangle$  (right) together with their susceptibilities show both transitions in two-flavour QCD.  
from Karsch et al. 2001



### 3.4. How center (a-)symmetry is intertwined with chiral symmetry breaking in quenched and real QCD ?

see: E. Bilgici, F. Bruckmann, J. Danzer, C. Gattringer, C. Hagen, E.-M. I., A. Maas, Few Body Syst. 47 (2010) 125 , arXiv:0906.3957

**Experiment** : Calculate fermionic observables (chiral condensate etc.) with valence quarks, which may differ from sea quarks by **modified temporal boundary conditions** :

- for antisymmetric b. c. the standard result is reobtained;
- for periodic b. c. a fictive (valence) result is obtained;
- at which temperatures the results start to depend on b. c. ?
- how does the chiral condensate of valence quarks depend on their (continuously varied) boundary condition ?

We consider general b. c.

$$\psi(\mathbf{x}, N_t) = e^{i\phi} \psi(\mathbf{x}, 0)$$

**Observation :**

In the low-temperature phase the boundary condition applied to (valence) fermions does not play any role ! In the high-temperature phase various quantities (the spectral gap or - if it vanishes - the spectral density near zero eigenvalue  $\rho(0)$ ) depend on  $\phi$  !

**Notice !** This is not real QCD. **For quenched QCD all fermions are valence quarks.** The above observations hold when full QCD configurations are analysed by valence quarks !

**In other words :** The way **how center symmetry is broken or not** in the gauge system can be **visualized by non-standard b. c. for fermions** (focusing the zero modes on different types of topological excitations).

Define a **generalized quark condensate** :

$$S(\phi) = -\langle \bar{\psi}\psi \rangle|_{\phi} = \frac{1}{V} \sum_j \frac{1}{i \lambda_j(\phi) + m}$$

with Dirac eigenvalues  $\lambda_j(\phi)$  depending on  $\phi$  (modified temporal b. c.)

**True quark condensate (quenched or dynamic) :**

$$\Sigma^{(0)} = S(\phi = \pi) \quad \text{for antiperiodic b. c.}$$

The **dual quark condensate** is the first Fourier component of  $S(\phi)$ :

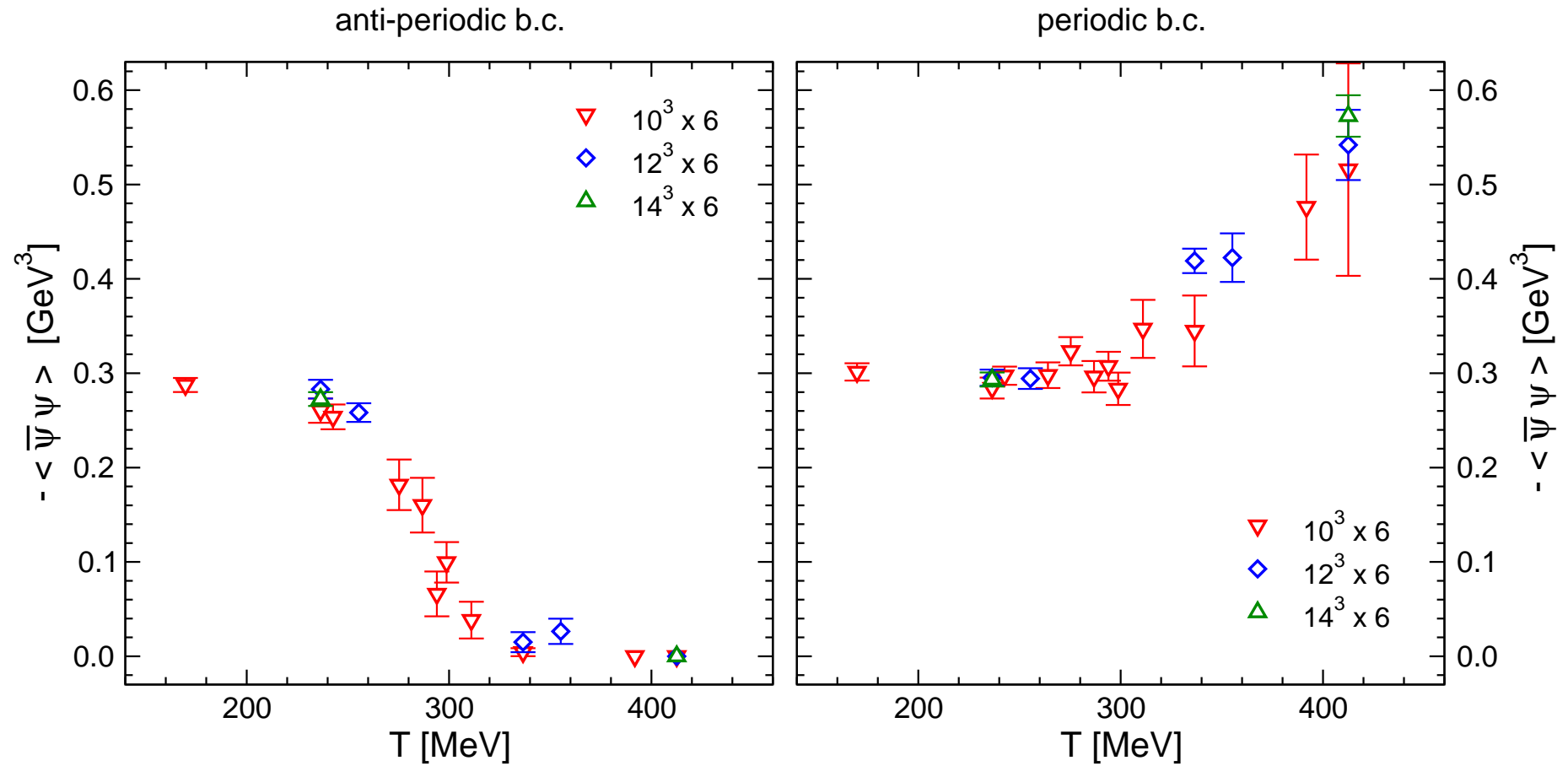
$$\Sigma^{(1)} = \int_0^{2\pi} \frac{d\phi}{2\pi} S(\phi) e^{-i\phi}$$

It behaves like the renormalized Polyakov loop. In literature:

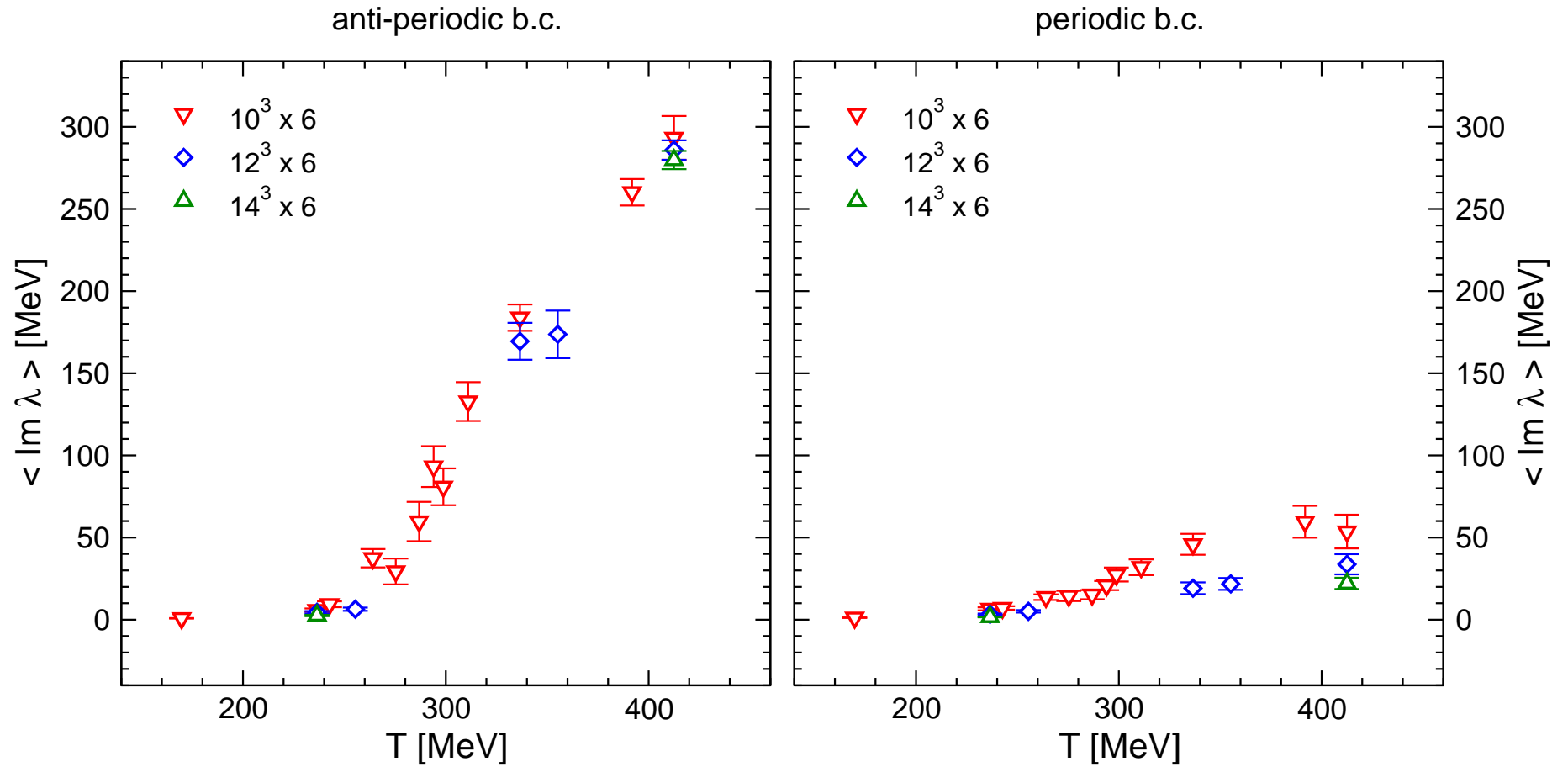
**“dual quark condensate” synonymous with “dressed Polyakov loop”**



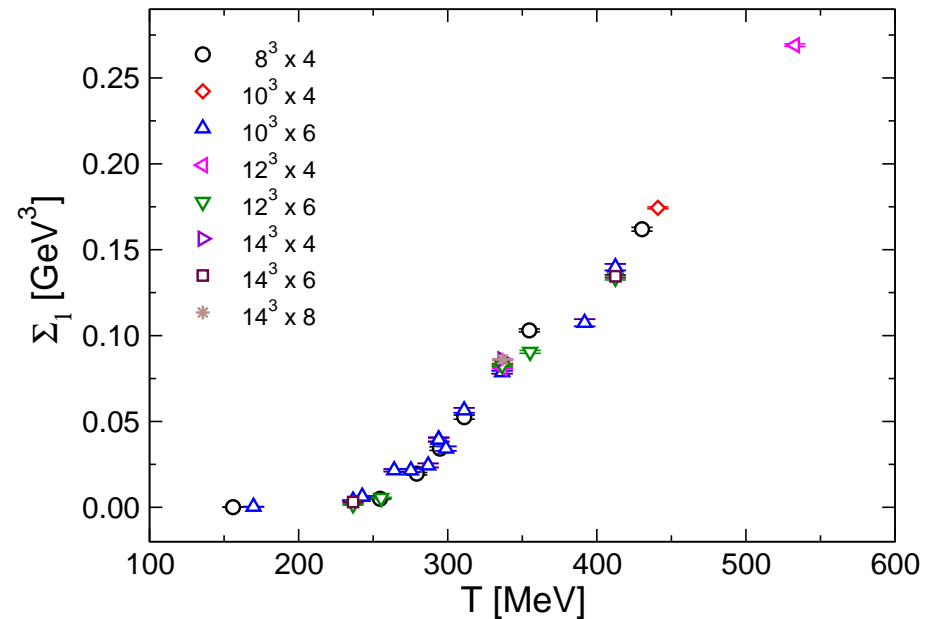
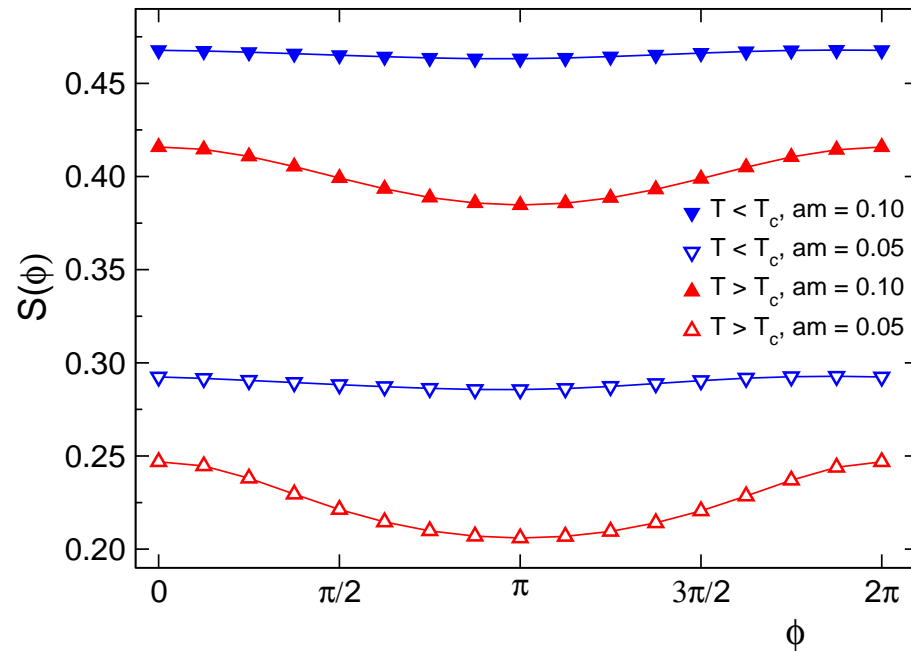
Quenched chiral condensate  $-\langle\bar{\psi}\psi\rangle$  for anti-periodic (left) and periodic (right) temporal fermion boundary conditions as a function of temperature. (from arXiv:0906.3957)



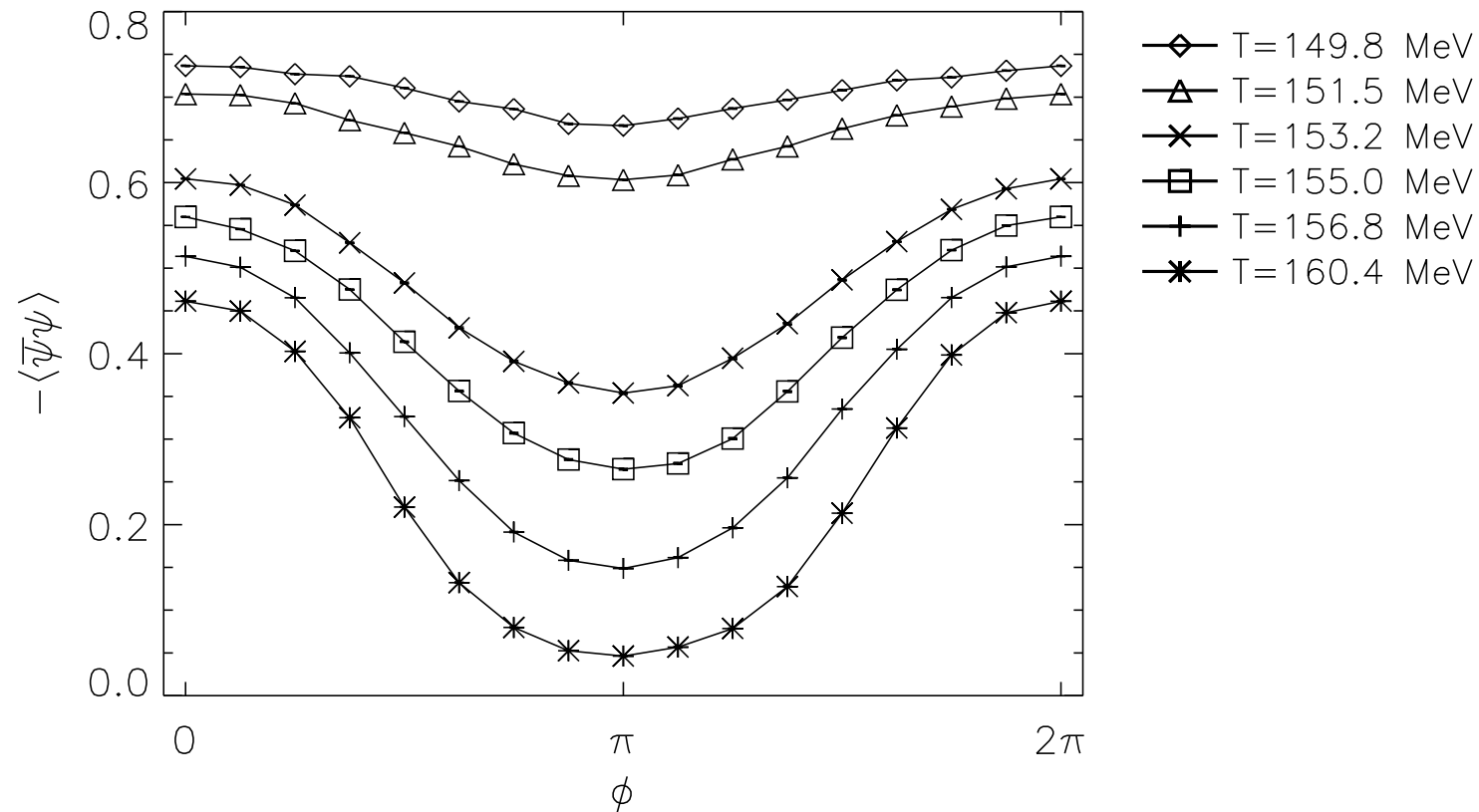
Quenched spectral gap for anti-periodic (left) and periodic (right) temporal fermion boundary conditions as a function of temperature.  
(from arXiv:0906.3957)



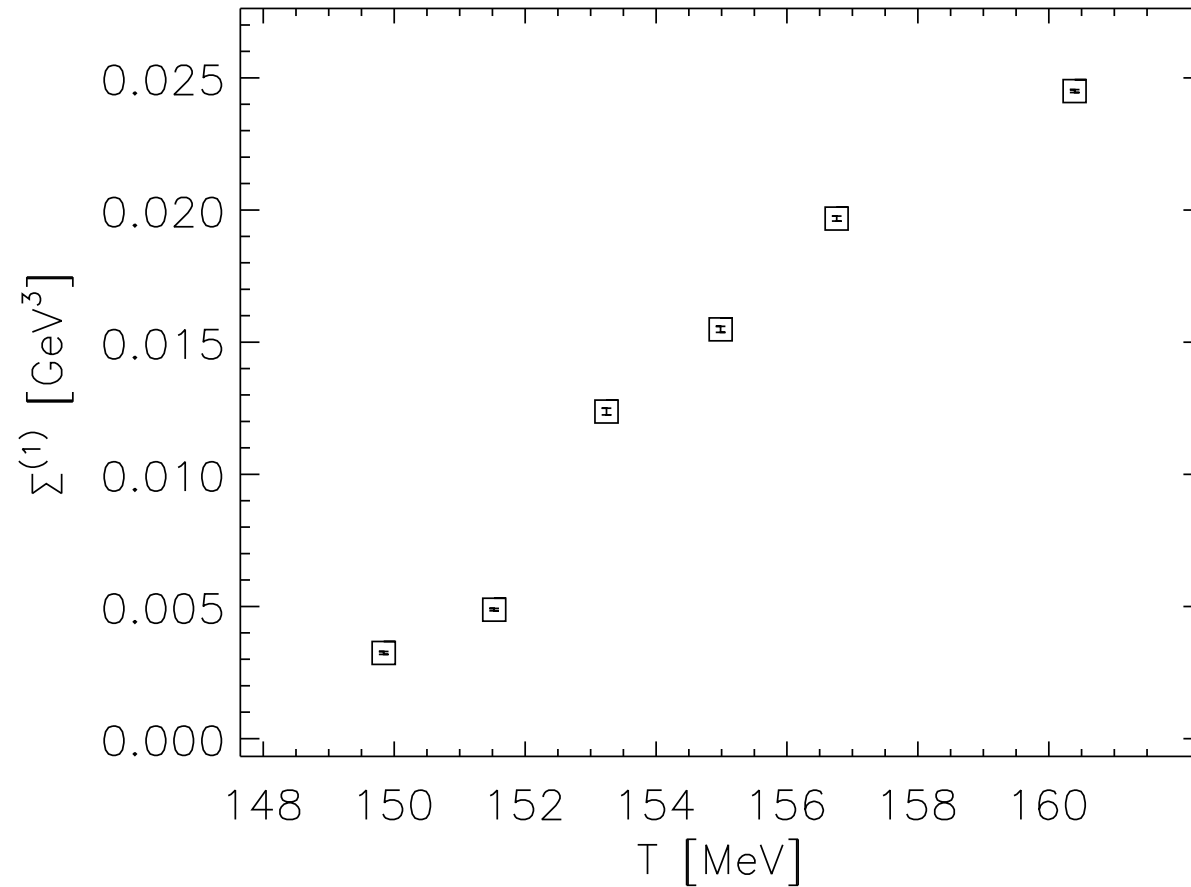
Left: the integrand  $S(\phi)$  of the dual chiral condensate in the quenched case as function of the boundary angle  $\phi$ . (two bare quark masses and two temperatures below and above  $T_{\text{dec}}$ . Right: the quenched dual chiral condensate as function of the temperature. (from arXiv:0906.3957)



The chiral condensate of the dynamical theory as function of the boundary angle  $\phi$  for various temperatures. (from arXiv:0906.3957)



The bare dual chiral condensate  $\Sigma^{(1)}$  for the dynamical theory as function of the temperature. (from arXiv:0906.3957)



#### 4. Searching for a transition along a line in the phase diagram

- Searching for the crossover/the crossovers done by means of the Polyakov loop, the chiral condensate and the corresponding susceptibilities. For example, **varying  $T$  along the axis  $\mu_q = 0$ .**
- For **light quark masses and large  $N_t$  the Polyakov loop loses much of its analytic power** to describe “the (de)confinement aspect” of the transition. Polyakov loop is not a derivative of  $\ln Z$  !
- One might ask: Is the **center symmetry really important for confinement, if the theory contains light quarks ?** The dual condensate relates light quarks to center symmetry, as seen before !
- **How can we imagine “deconfinement” ?** The light quark number  $n_q - n_{\bar{q}}$  may start to fluctuate “freely”. Thus, the **quark number susceptibility supersedes the Polyakov loop** as deconfinement signal.

- **Renormalized Polyakov loop** (intention : removal of the finite- $a$  effects)

$$\langle \text{Re}(L) \rangle_R = \langle \text{Re}(L) \rangle \exp (V(r_0)/2T)$$

$V(r_0)$  is the zero-temperature potential at distance  $r_0$ .

**Aim:** search for inflection point and for a Gaussian peak of susceptibility above background.

- **Renormalized quark condensate** (aim : remove divergent part  $\propto a^{-2}$ )

$$\langle \bar{\psi}\psi \rangle_R = Z_p \left( \langle \bar{\psi}\psi \rangle + c(g_0) \frac{\mu_0}{a^2} \right)$$

practically used

$$R_{\bar{\psi}\psi} = \frac{\langle \bar{\psi}\psi \rangle(T, \mu_0) - \langle \bar{\psi}\psi \rangle(0, \mu_0) + \langle \bar{\psi}\psi \rangle(0, 0)}{\langle \bar{\psi}\psi \rangle(0, 0)}$$

The corresponding (disconnected) susceptibility of the quark condensate is obtained as the variance over the ensemble. It shows a maximum at the transition.

- **Quark number susceptibility** : second derivative w.r.t  $\mu_q$  (taken at  $\mu_q = 0$ ) of  $\ln \det D = \text{tr} \ln D$

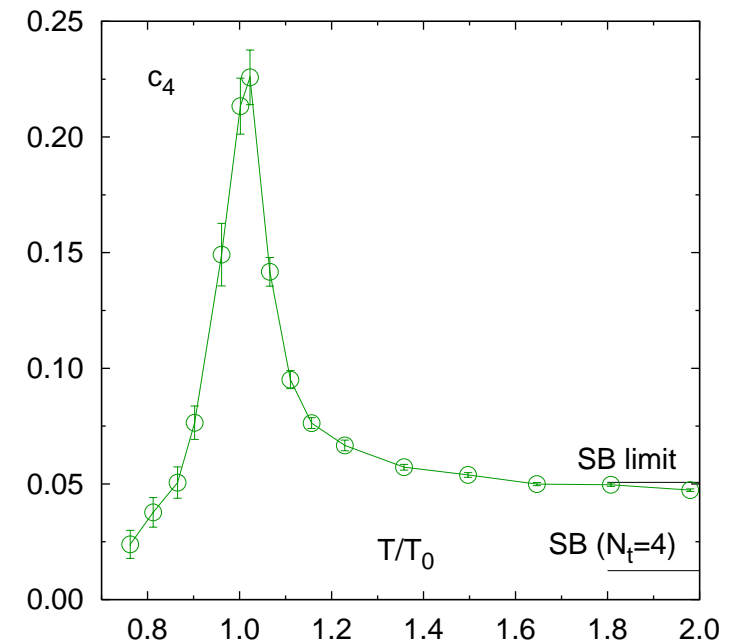
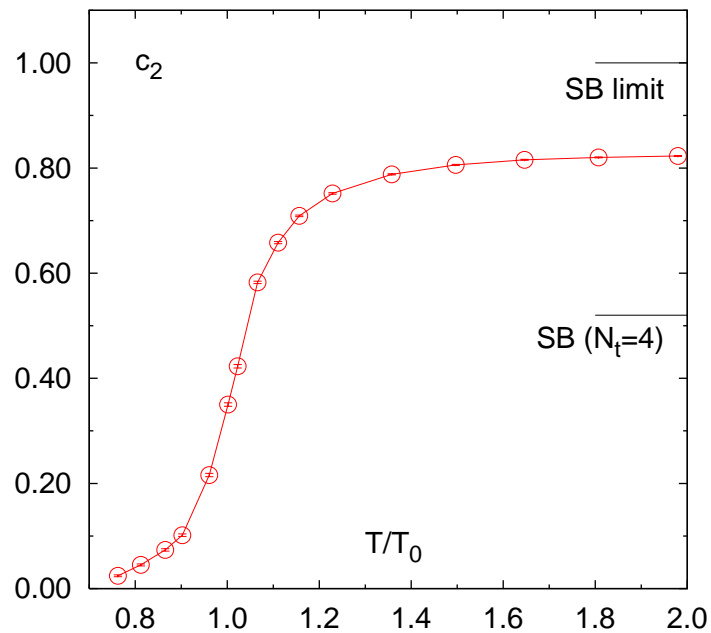
$$c_2 = \frac{\partial^2 \ln \det D(\mu_q)}{\partial \mu_q^2} = -\text{tr} \left[ D^{-1} \frac{\partial D}{\partial \mu_q} D^{-1} \frac{\partial D}{\partial \mu_q} \right] + \text{tr} \left[ D^{-1} \frac{\partial^2 D}{\partial \mu_q^2} \right]$$

These expressions are standard for the Taylor expansion in  $\mu_q$  used to explore the region of non-vanishing baryonic density.

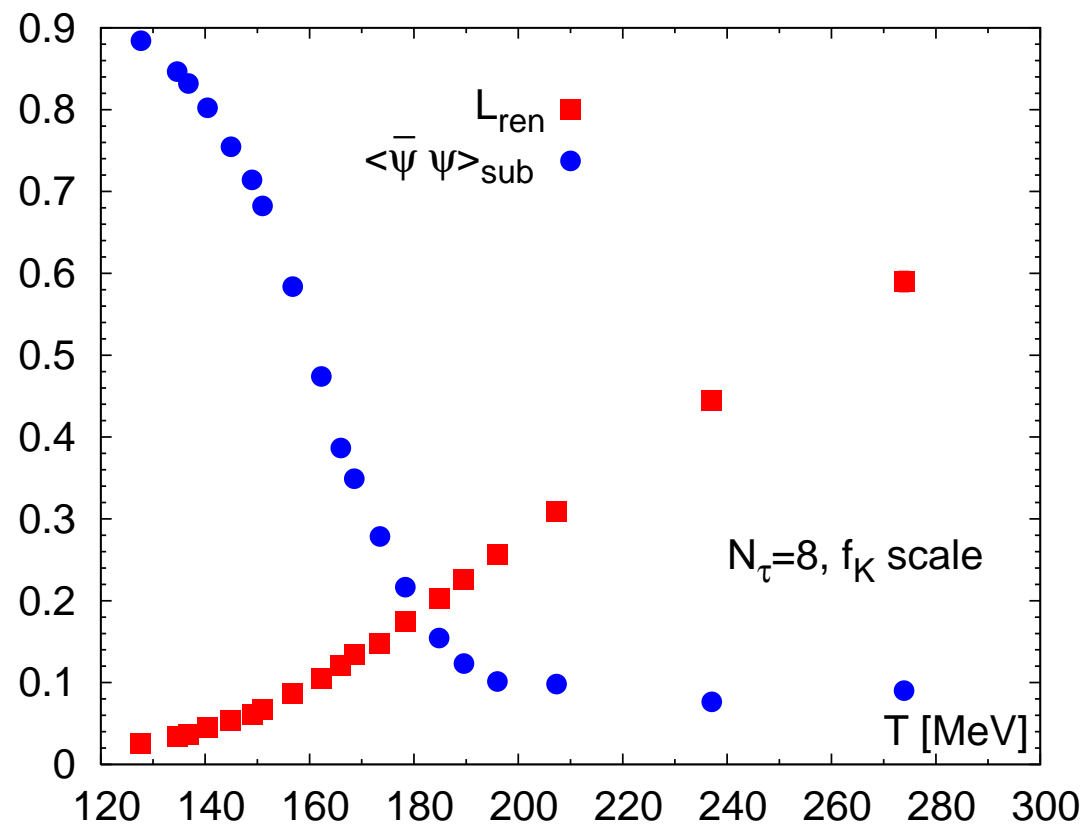
**Useful also as an observable emphasizing the deconfinement at vanishing baryonic density !**



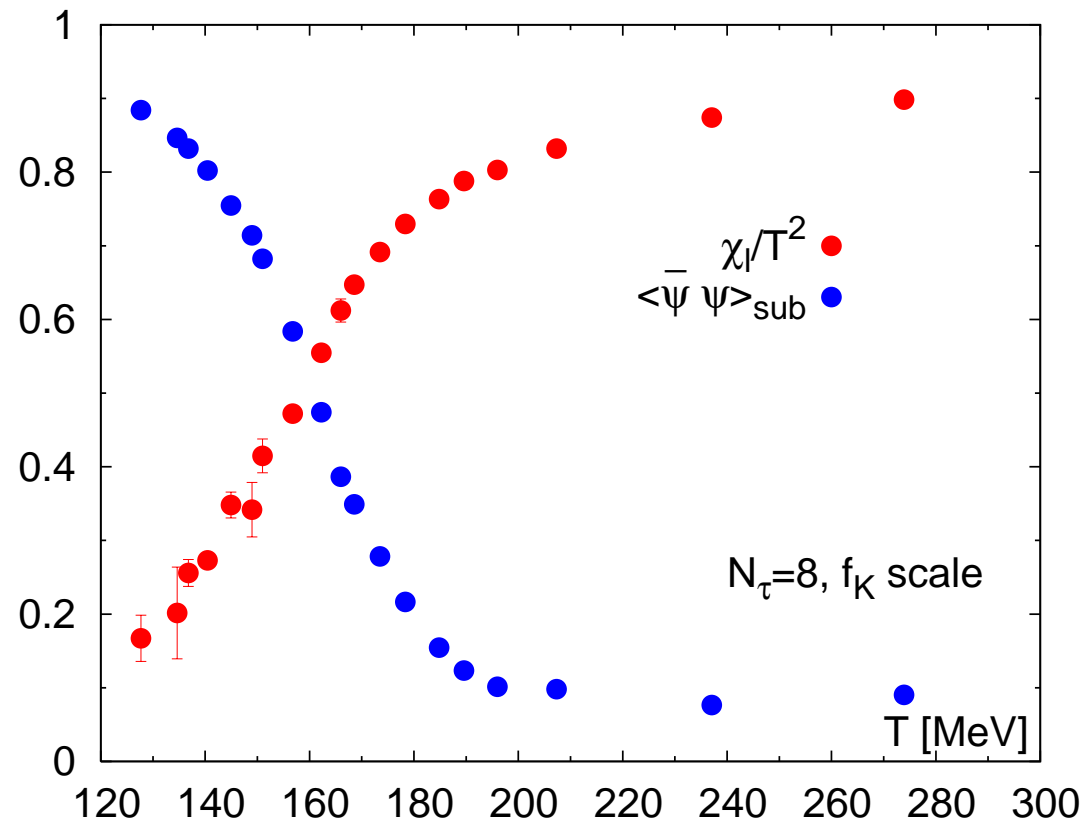
The second and fourth derivatives  $c_2$  and  $c_4$  as functions of temperature  
Quark number susceptibility behaves like step function, the next higher  
moment like a “usual” susceptibility. (from Ch. Schmidt hep-lat/0610116)



The chiral condensate compared to the renormalized Polyakov loop in full QCD from arXiv:1203.5320 Petreczky



The chiral condensate compared to the light quark number susceptibility in full QCD from arXiv:1203.5320 Petreczky



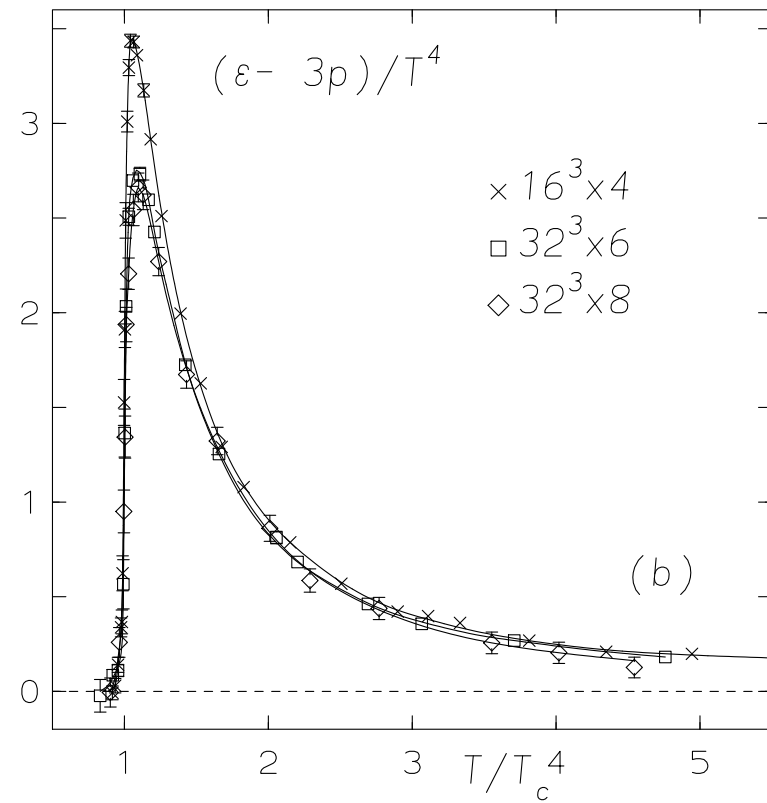
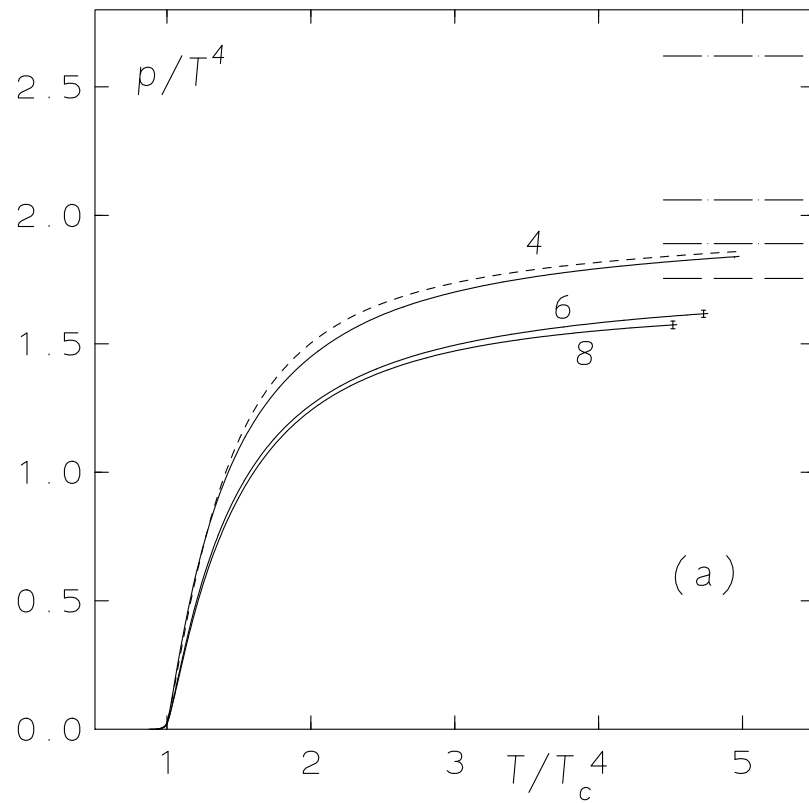
What follows after the transition ? The so-called quark-gluon-plasma

What distinguishes high from low temperature in real QCD ?

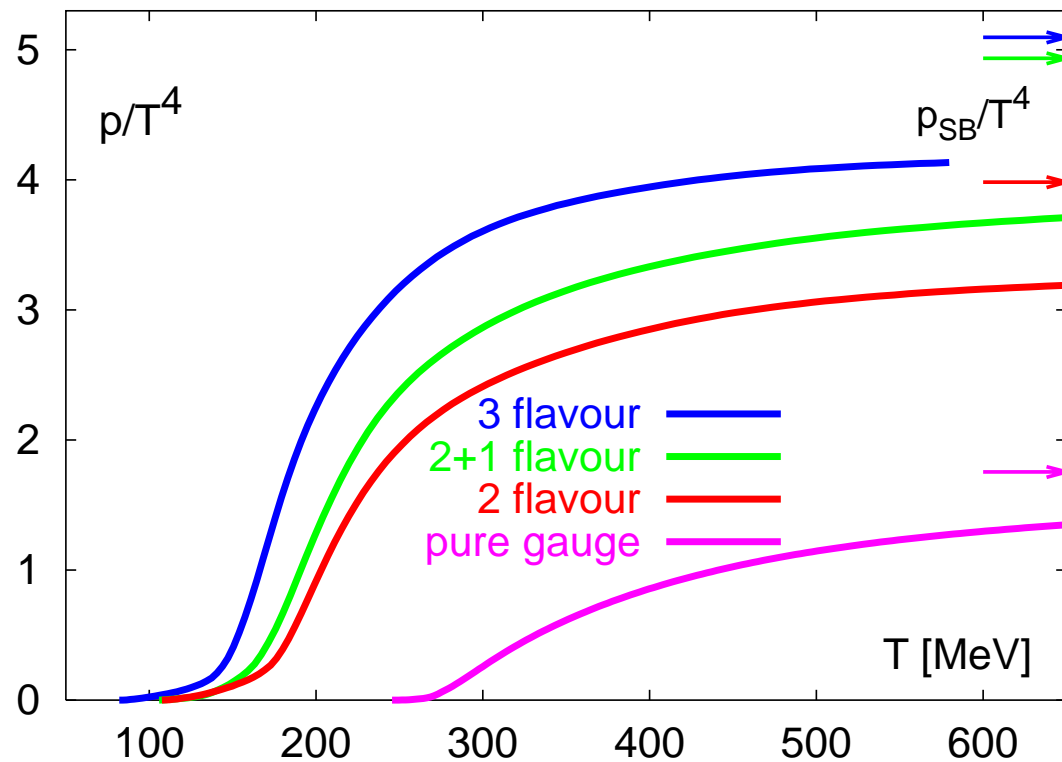
- The renormalized **Polyakov loop** is large.
- The renormalized **quark condensate** is small.
- The **quark number susceptibility** is large.
- The **pressure and the energy density** are large, however still far from the Stefan-Boltzmann limit.
- The **signal (driving force)** for the “liberation of degrees of freedom” is the **trace anomaly** (“interaction measure”).
- For pure Yang-Mills theory (no quarks) this is a **very sharp signal** !

**The trace anomaly induces the rise of pressure and energy density.**

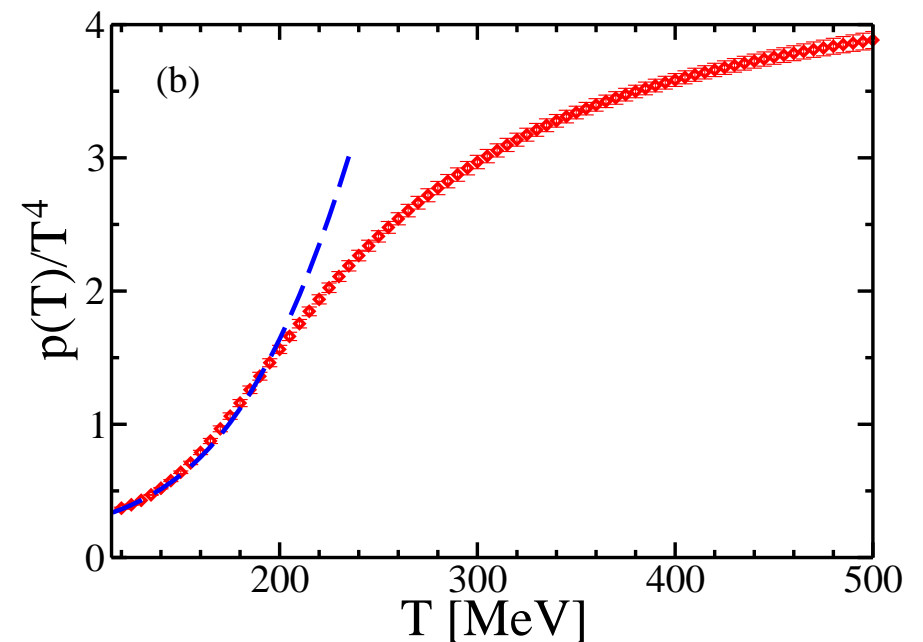
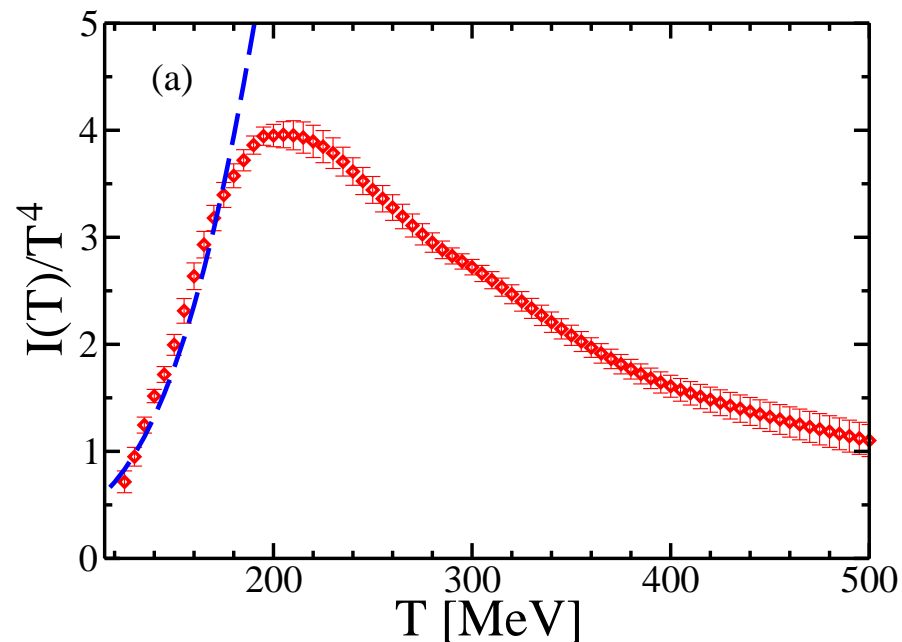
The pressure (left) versus  $T/T_c$  for  $N_t = 4, 6$  and  $8$  in pure gluodynamics.  
The interaction measure of gluons (trace anomaly)  $(\epsilon - 3p)/T^4$  (right).  
from Boyd et al. 1995



The pressure : gluons only, 2 light, 2 light + 1 heavy and 3 light flavors from Karsch, Laermann and Peikert (2000) (the quark contribution is important !)



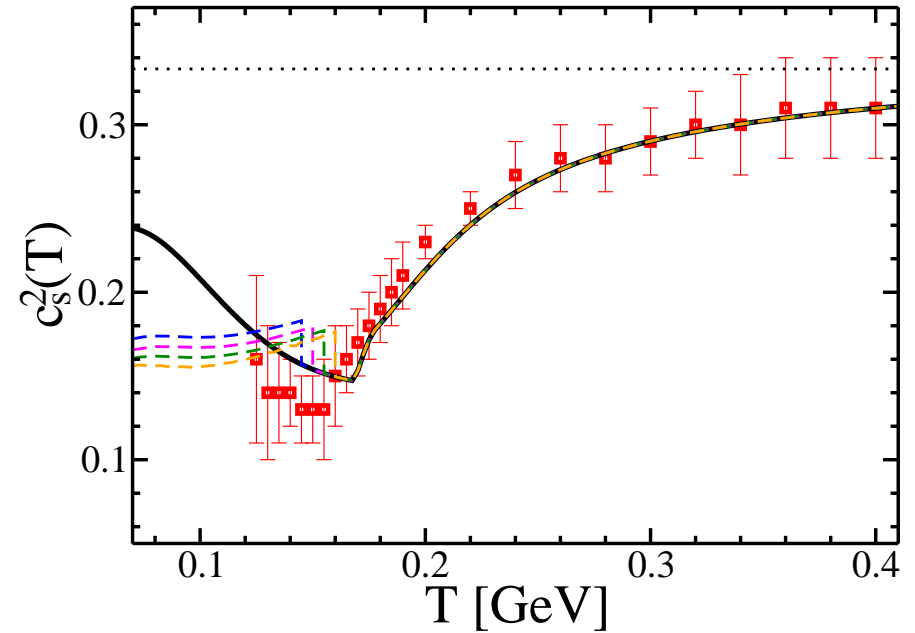
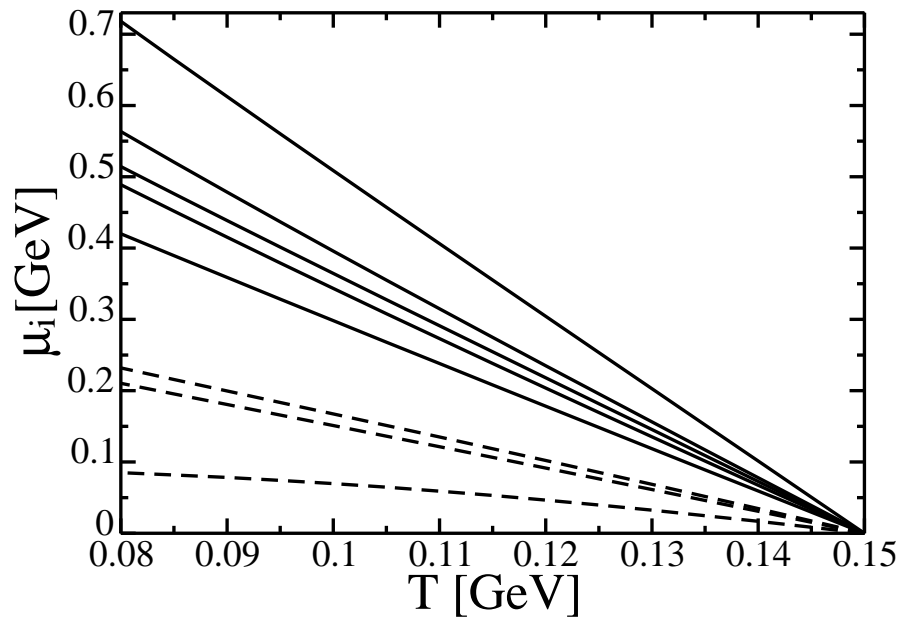
**EoS recently obtained from lattice data at  $n_B = 0$  and  $N_f = 2 + 1$  flavors !**  
Interaction measure (left) and pressure (right) from  $N_f = 2+1$  lattice data with physical quark masses (S. Borsanyi et al. Wuppertal-Budapest collaboration) from Bluhm, Alba, Alberico, Beraudo, Ratti, arXiv:1306.6188



Left:  $T$ -dependent effective chemical potential for freezeout at  $T_{\text{freeze}} = 150$  MeV (solid: for baryons  $\Omega^-$ ,  $\Xi^-$ ,  $\Lambda^0$  and  $p$ ; dashed: for mesons  $\eta$ ,  $K^-$  and  $\pi^+$ ).

Right: speed of sound  $c_s^2(T)$  (solid: HRG in equilibrium, dashed: partial chem. equilibrium in hadronic phase, symbols: equilibrium lattice data).

from Bluhm, Alba, Alberico, Beraudo, Ratti, arXiv:1306.6188





## 5. Phase transition and thermodynamics of twisted-mass fermions

For  $\mu_q = 0$  lattice QCD, importance sampling by Hybrid Monte Carlo works perfectly.

The only problem left is to control systematic effects of different fermion formulations.

### 5.1. Staggered (Kogut-Susskind) quarks

- Lattice thermodynamics is **dominated by staggered fermions** and improved variants of this formulation (p4, asqtad, stout and HISQ). This is computationally the cheapest method.
- The **improvements ameliorate problems** like taste symmetry breaking.
- The **fundamental problem, however, remains unanswered** : rooting, locality of the action .... Theoretically not completely clear !

- **Basic staggered action : 4 (degenerate) flavors, 16 d.o.f. per  $2^4$  cell.**  
 “Rooting” is the trick to get the action for  $N_f$  independent flavors :

$$\det D \text{ for } N_f \text{ flavors} = \left( (\det D_{\text{staggered}})^{\frac{1}{4}} \right)^{N_f}$$

→ can make the flavors non-degenerate (different charges etc.)

## 5.2. Wilson fermions

- Advantage : **clear flavor interpretation.**
- **Break chiral symmetry completely**, hopefully restored in continuum.
- **Phase structure complicated, partly irrelevant** at finite  $a$ .
- **Considerably more CPU-intensive !**
- Twisting probes spontaneous parity-flavor breaking that leads to the **Aoiki phase at very strong coupling (keep away from this !!)**.

## Two ways to improve Wilson fermion simulations to $\mathcal{O}(a)$ :

- **Clover improvement** (adding a Pauli term, Sheikholeslami/Wohlert)  
CP-PACS, WHOT, DIK (DESY-ITEP-Kanazawa) collaborations.  
In this case, the hopping parameter  $\kappa$  drives the transition !
- **Twisted mass fermions** (chiral rotation within doublets, even number of flavors): ETMC, tmfT-Collaboration (HU Berlin, Frankfurt, INFN Frascati).

## Advantage of twisted mass:

- **at maximal twist**, with  $\kappa$  set to  $\kappa_c(\beta)$  (then  $\beta$  drives the transition !)  
the twisted mass term takes the role of the mass term,  
while **automatic  $\mathcal{O}(a)$  improvement is guaranteed**.  
Observed first by R. Frezzotti, G. C. Rossi, JHEP 0408 (2004) 007

### 5.3. What is twisted mass ?

Fermion action in the **physical basis**  $\bar{\Psi}, \Psi$  written (see **Wilson's  $r$ -term**)

$$S_F[\Psi, \bar{\Psi}, U] = a^4 \sum_x \left[ \bar{\Psi}(x) \left( \gamma_\mu \frac{1}{2a} (\nabla_\mu + \nabla_\mu^*) - \frac{ar}{2} e^{-i\omega\gamma_5\tau^3} \nabla_\mu^* \nabla_\mu + M_0 \right) \Psi(x) \right]$$

The **physical basis**  $\bar{\Psi}, \Psi$  is related to the **twisted basis**  $\bar{\psi}, \psi$  by the non-anomalous chiral rotation

$$\begin{aligned} \Psi &= \exp\left(i\frac{\omega}{2}\gamma_5\tau^3\right) \psi, \\ \bar{\Psi} &= \bar{\psi} \exp\left(i\frac{\omega}{2}\gamma_5\tau^3\right) \end{aligned}$$

with

$$M_0 = \sqrt{m_0^2 + \mu_0^2}, \quad \tan(\omega) = \mu_0/m_0,$$

(with  $M_0$ , the bare polar quark mass and  $\omega$ , the bare twist angle).

For maximal twist, both bases related through :

$$\Psi = \frac{1}{\sqrt{2}}(1 + i\gamma_5\tau^3)\psi \quad \text{and} \quad \bar{\Psi} = \bar{\psi}\frac{1}{\sqrt{2}}(1 + i\gamma_5\tau^3)$$

Introducing Wilson's **hopping parameter**  $\kappa = 1/(2am_0 + 8r)$

and rescaling as usual  $\sqrt{a^3/(2\kappa)}\psi \rightarrow \chi$  leads to the **standard form of the twisted fermion action (in the twisted basis) appearing in the simulation code :**

$$S_F[\chi, \bar{\chi}, U] = \sum_x \left[ \bar{\chi}(x) (1 + i2\kappa a\mu_0\gamma_5\tau^3) \chi(x) - \kappa \sum_{\mu} \bar{\chi}(x) \left( (r - \gamma_{\mu})U_{x,\mu}\chi(x + \hat{\mu}) + (r + \gamma_{\mu})U_{x-\hat{\mu},\mu}^{\dagger}\chi(x - \hat{\mu}) \right) \right]$$

This fermionic action is simulated together with **tree-level Symanzik improved gauge action** : (Iwasaki action)

**public code available**, see <https://github.com/etmc/tmLQCD/>

$$S_G[U] = \beta \left[ c_0 \sum_P \left( 1 - \frac{1}{3} \text{Re} (\text{tr} [U(P)]) \right) + c_1 \sum_R \left( 1 - \frac{1}{3} \text{Re} (\text{tr} [U(R)]) \right) \right]$$

where  $\beta = 6/g_0^2$  and  $U(P)$ ,  $U(R)$  are **plaquette and rectangle loops**.

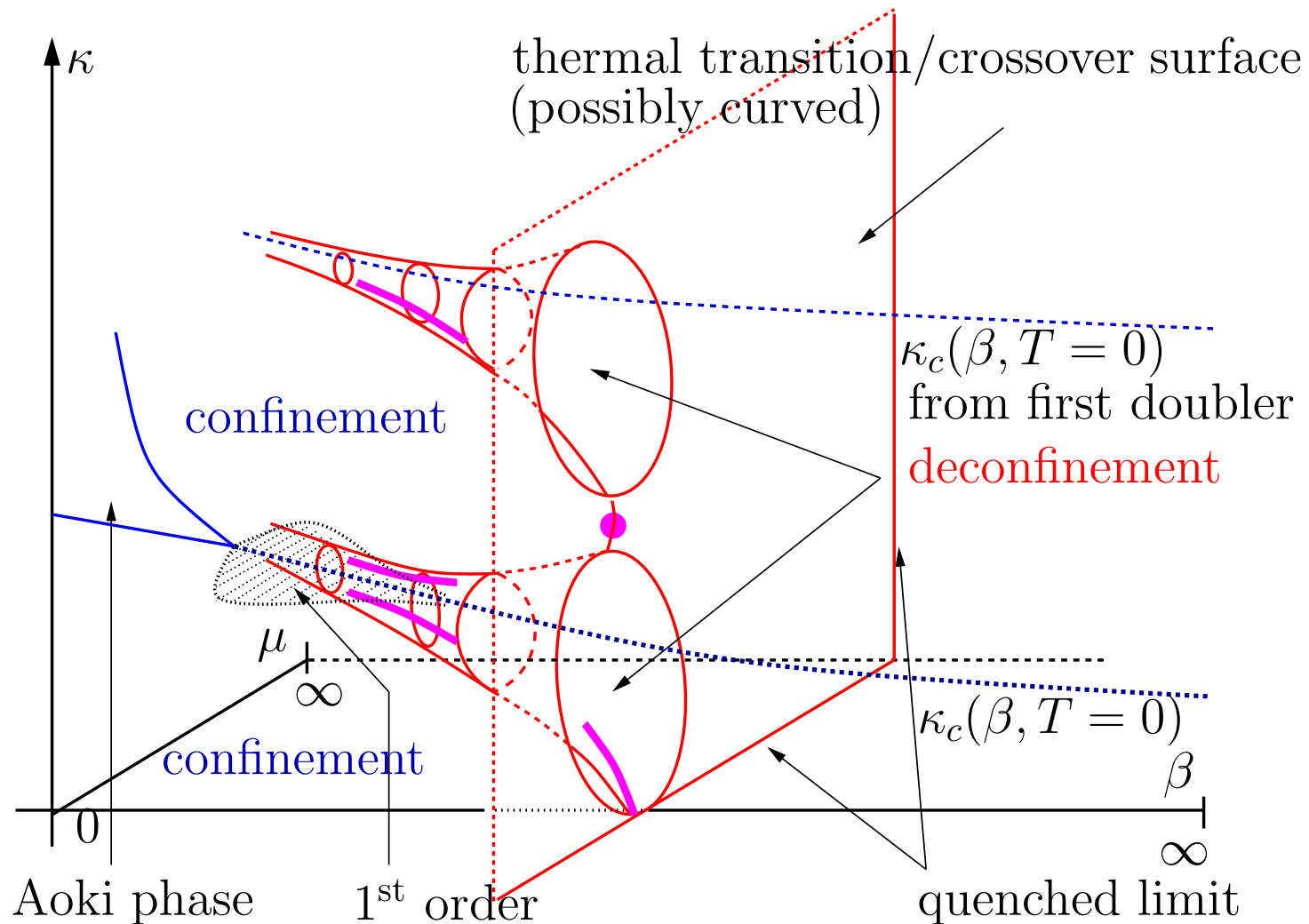
**Tree-level improvement condition** :  $c_0 + 8c_1 = 1$ , and  $c_1 = -1/12$ .

**Outlook to future work of tmfT** :

In order to describe  $N_f = 2 + 1 + 1$  **flavors**, add a second, non-degenerate doublet:

$$S_F[\psi, \bar{\psi}, U] = a^4 \sum_x [\bar{\psi}_l(x) (D_W[U] + m_{0,l} + i\mu_l \gamma_5 \tau^3) \psi_l(x)] \\ + a^4 \sum_x [\bar{\psi}_h(x) (D_W[U] + m_{0,h} + i\mu_\sigma \gamma_5 \tau^1 + \mu_\delta \tau^3) \psi_h(x)]$$

5.4. The global, fully 3-dimensional phase diagram for  $N_f = 2$   
 (illustrating Creutz' "cone conjecture")



**Global phase structure (for all  $\beta, \kappa, \mu_0$ ) had been discussed earlier in :**

- **arXiv:0905.3112 (E.-M. I., K. Jansen et al.) Phys. Rev. D 80 (2009) 094502**



## What is the physically relevant branch ?

- Only the **lowest cone is connected with the quenched limit !**  
Varying the quark mass  $\rightarrow \infty$ , a **critical endpoint** is passed, at which the crossover goes over to a first order (under investigation).  
The first order line ends in the **quenched endpoint** at  $\kappa = 0$ .
- How does a **line of constant physics (LCP)** pierce Creutz' cone ?
  - LCP **should run** at maximal twist !
  - LCP **must not run** at  $\mu_0 = \text{const}$  !

The details for this analysis rest on **calibration simulations at  $T = 0$ ,**

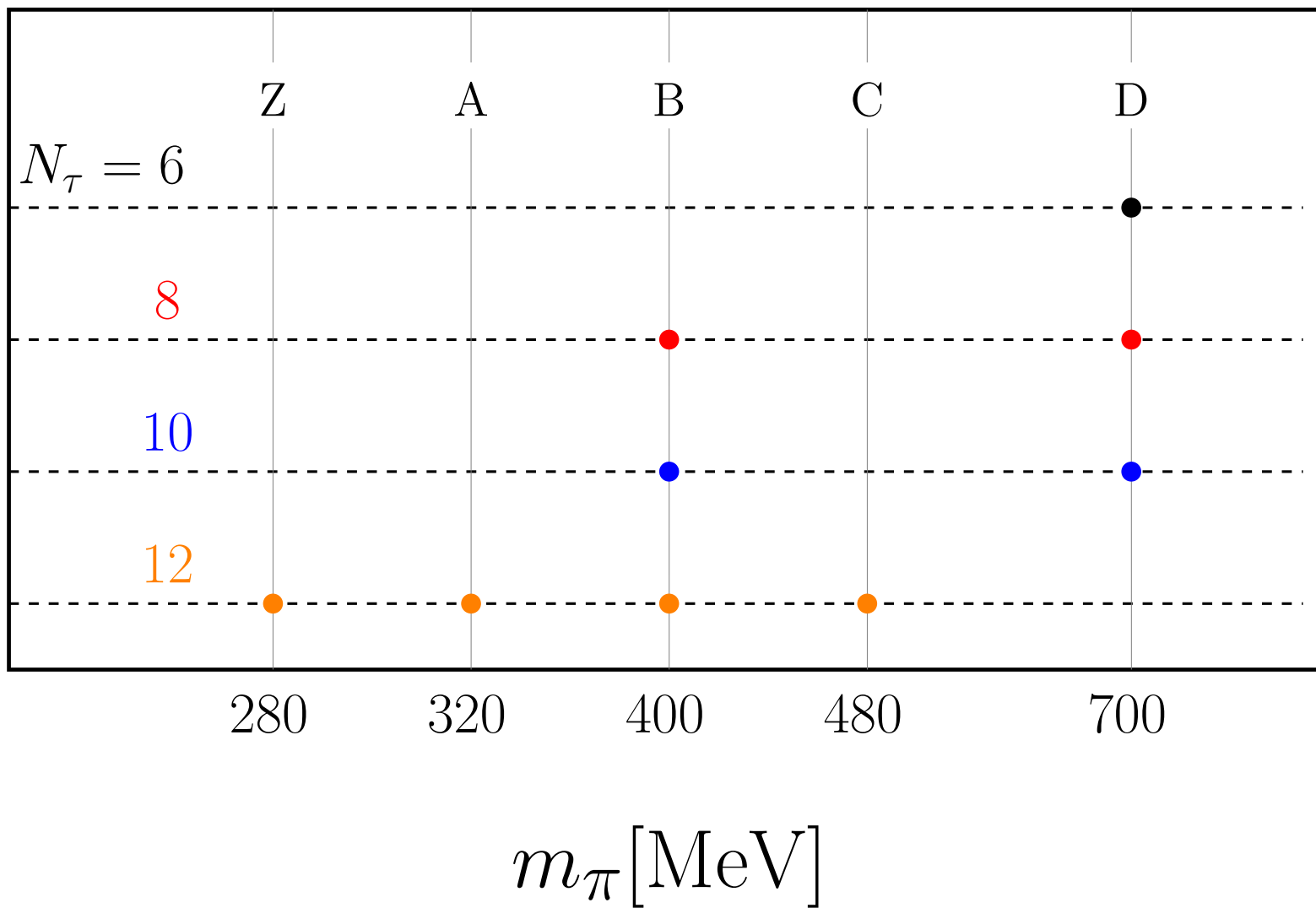
- done by the ETM Collaboration
- own simulations of the tmfT Collaboration

## 5.5. Locating the crossover on the lowest cone

- Evaluated : **three families of ensembles** : A12, B12, C12  
(one more becoming finished now : Z12)
- populate the **three-dimensional phase diagram**  $\beta, \kappa, \mu_0$
- a  **$\beta$  scan** should fix the position of the crossover line
- maximal twist: requires **tuning of**  $\kappa = \kappa_c(T = 0, \beta)$
- fixed pion mass: requires **tuning of**  $a\mu_0 = (a\mu_0)(\beta) = C \exp(-\beta/(12\beta_0))$

(obtained from a one-loop fit with  $\beta_0 = \frac{11-2N_f/3}{(4\pi)^2}$  or from a two-loop fit)

- such **fits for various families of  $T = 0$  simulations** based on data of the ETM-Collaboration exist [published JHEP 08 097 (2010)]



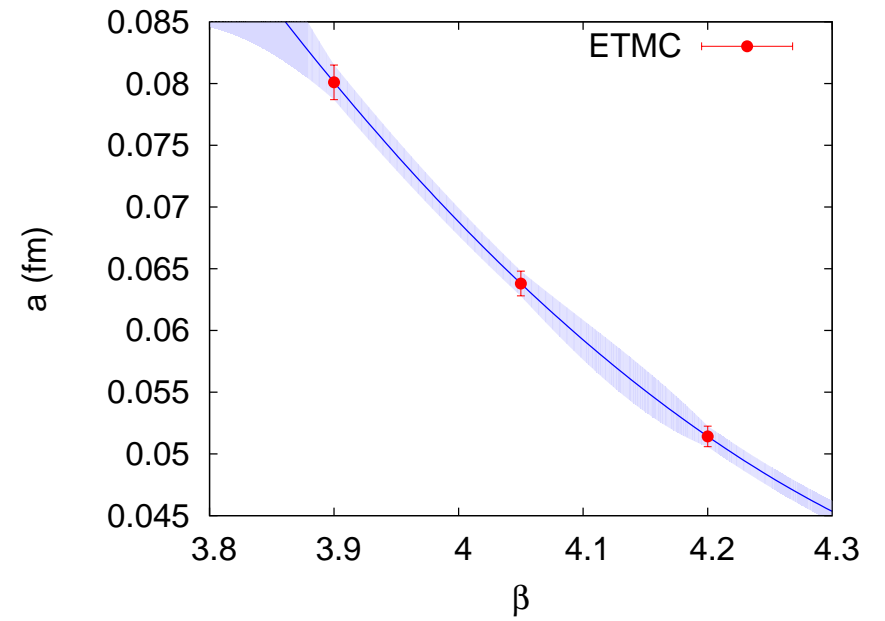
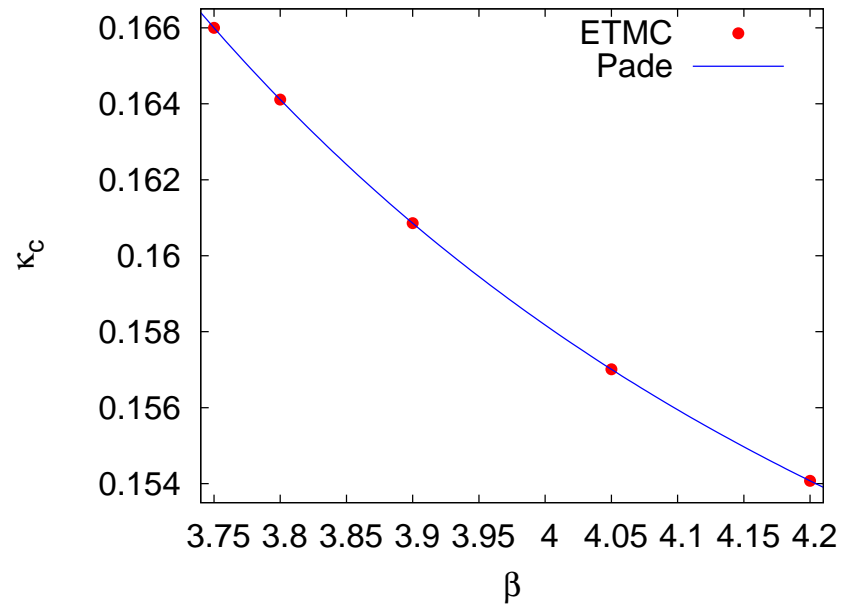
## List of $\beta$ -scans

- **A12:**  $32^3 \times 12$ ,  $3.84 \leq \beta \leq 3.99$ ,  
 $m_\pi = 316(16)$  **MeV**,  $r_0 m_\pi = 0.673(42)$   
 $\beta_\chi = 3.89(3)$ ,  $T_\chi = 202(7)$  **MeV**
- **B12:**  $32^3 \times 12$ ,  $3.86 \leq \beta \leq 4.35$ ,  
 $m_\pi = 398(20)$  **MeV**,  $r_0 m_\pi = 0.847(53)$   
 $\beta_\chi = 3.93(2)$ ,  $T_\chi = 217(5)$  **MeV**  
 $\beta_{\text{deconf}} = 4.027(14)$ ,  $T_{\text{deconf}} = 249(5)$  **MeV**
- **C12:**  $32^3 \times 12$ ,  $3.90 \leq \beta \leq 4.07$ ,  
 $m_\pi = 469(24)$  **MeV**,  $r_0 m_\pi = 0.998(62)$   
 $\beta_\chi = 3.97(3)$ ,  $T_\chi = 229(5)$  **MeV**  
 $\beta_{\text{deconf}} = 4.050(15)$ ,  $T_{\text{deconf}} = 258(5)$  **MeV**

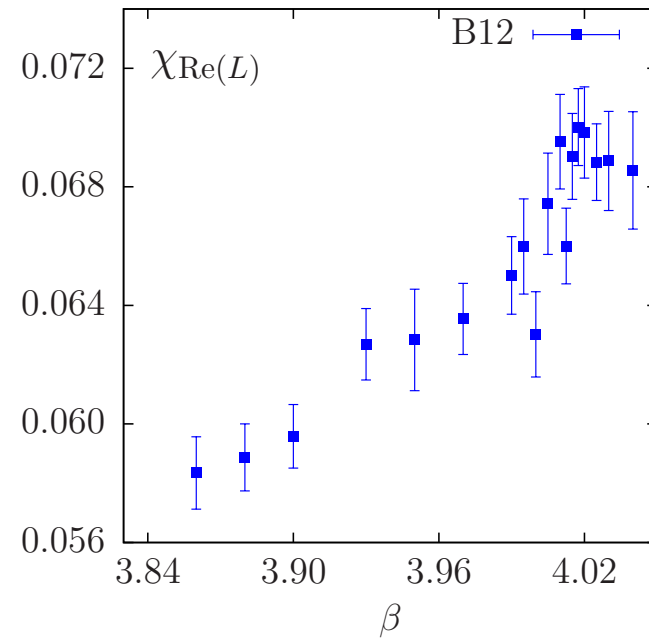
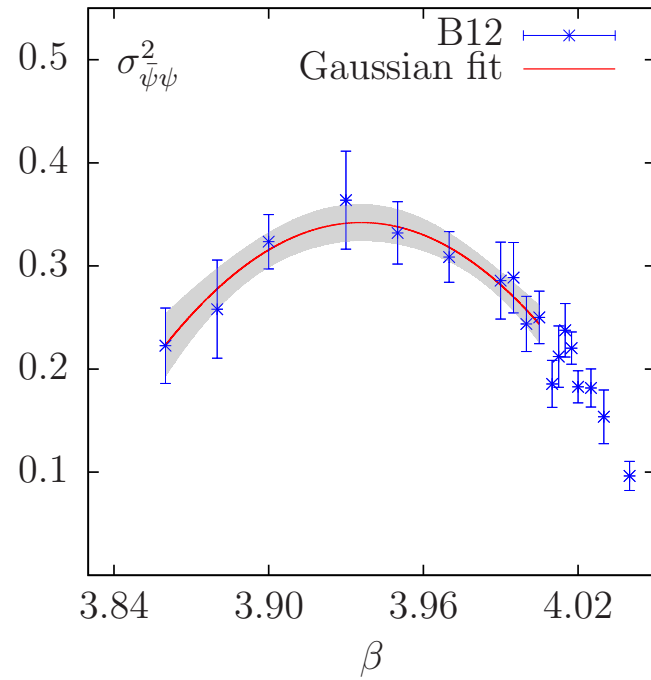
$m_\pi$ -dependence and chiral extrapolations are discussed in papers :

- arXiv:1102.4530v2 (F. Burger et al.) Phys. Rev. D 87 (2013) 074508
- arXiv:1212.0982 (F. Burger at Lattice 2012)

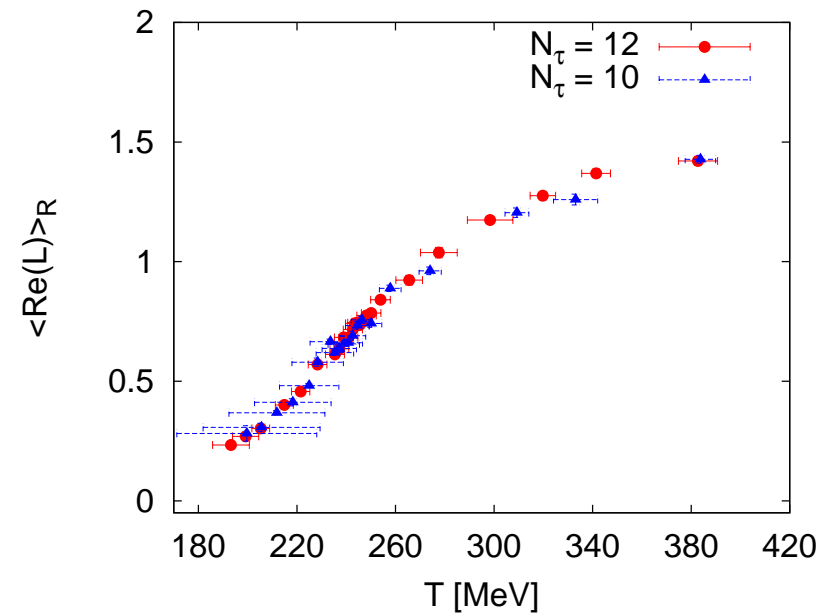
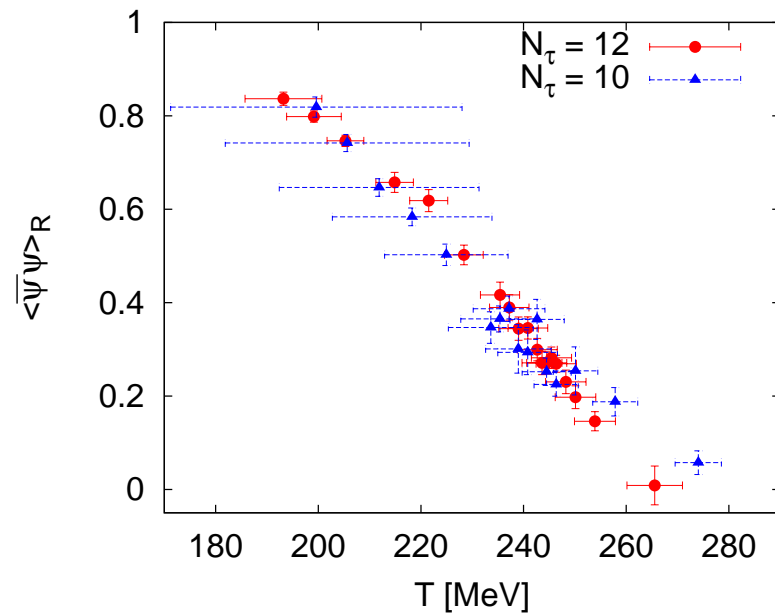
$\kappa_c(T=0, \beta)$  and the lattice spacing  $a(\beta)$



## Chiral susceptibility and Polyakov loop susceptibility for B12



Renormalized  $\langle \bar{\psi}\psi \rangle_R$  and renormalized Polyakov loop  $\langle \text{Re}(L) \rangle_R$   
(combining data from B12 and B10,  $N_t = 10$  and  $N_t = 12$ )





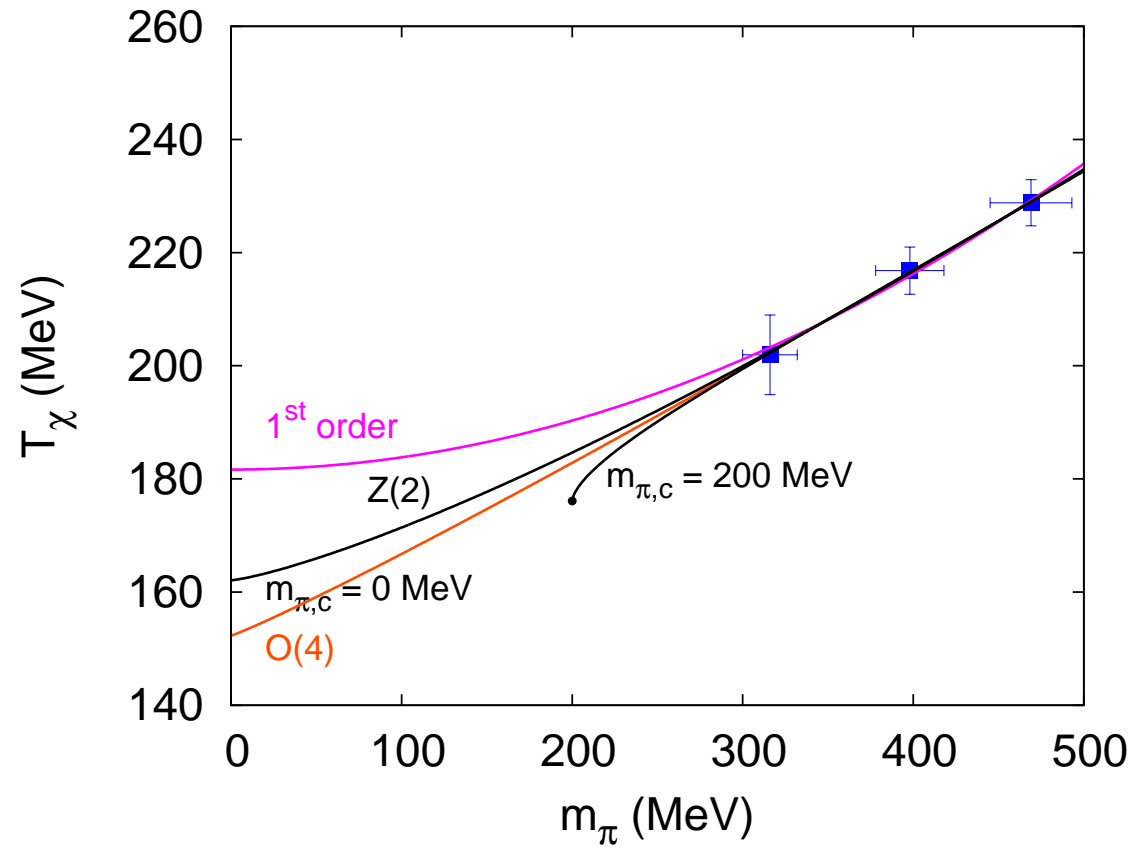
## 5.6. Chiral extrapolations for $T_\chi(m_\pi)$ for various scenarios ( $\chi$ PT)

$$T_\chi(m_\pi) = T_\chi(m_\pi = 0) + A m_\pi^{2/(\tilde{\beta}\delta)}$$

with critical indices  $\tilde{\beta}$ ,  $\delta$  corresponding to the respective equivalence classes of **three-dimensional spin models**.

- $O(4)$  :  $2/(\tilde{\beta}\delta) = 1.08$  leads to  $T_\chi(m_\pi = 0) = 152(26)$  MeV
- $Z(2)$  : two cases  $m_{\pi,c} = 0$  or  $m_{\pi,c} \neq 0$ ;  
lead to  $T_\chi(m_\pi \rightarrow 0)$  **between  $O(4)$  and 1-st order scenario**
- **first order** : in literature formally  $2/(\tilde{\beta}\delta) = 2$  is taken;  
leads to  $T_\chi(m_\pi = 0) = 182(14)$  MeV  
(applicability of these “critical indices” unclear !)

# Chiral extrapolations for $T_\chi(m_\pi)$ for various scenarios



## 5.7. Towards the Equation of State (EoS)

The trace anomaly is the primary quantity on the lattice

$$\begin{aligned} \frac{I}{T^4} &= \frac{\epsilon - 3p}{T^4} = -\frac{T}{VT^4} \left\langle \frac{d \ln Z}{d \ln a} \right\rangle_{\text{sub}} \\ &= N_\tau^4 B_\beta \frac{1}{N_\sigma^3 N_\tau} \left\{ \begin{aligned} &\frac{c_0}{3} \langle \text{ReTr} \sum_P U_P \rangle_{\text{sub}} \\ &+ \frac{c_1}{3} \langle \text{ReTr} \sum_R U_R \rangle_{\text{sub}} \\ &+ B_\kappa \langle \bar{\chi} D_W[U] \chi \rangle_{\text{sub}} \\ &- [2(a\mu) B_\kappa + 2\kappa_c(a\mu) B_\mu] \langle \bar{\chi} i \gamma_5 \tau^3 \chi \rangle_{\text{sub}} \end{aligned} \right\} \end{aligned}$$

$\langle \dots \rangle_{\text{sub}} \equiv \langle \dots \rangle_{T>0} - \langle \dots \rangle_{T=0}$  denotes **subtraction of vacuum contributions.**

$B_\beta$ ,  $B_\mu$  and  $B_\kappa$  are (related to) **derivatives of the bare parameters with respect to the lattice spacing :**

$$B_\beta = a \frac{d\beta}{da}, \quad B_\mu = \frac{1}{(a\mu)} \frac{\partial(a\mu)}{\partial\beta}, \quad B_\kappa = \frac{\partial\kappa_c}{\partial\beta}$$

**Evaluation of the pressure by integrating the identity**

$$\frac{I}{T^4} = T \frac{\partial}{\partial T} \left( \frac{p}{T^4} \right)$$

**along the line of constant physics (LCP):**

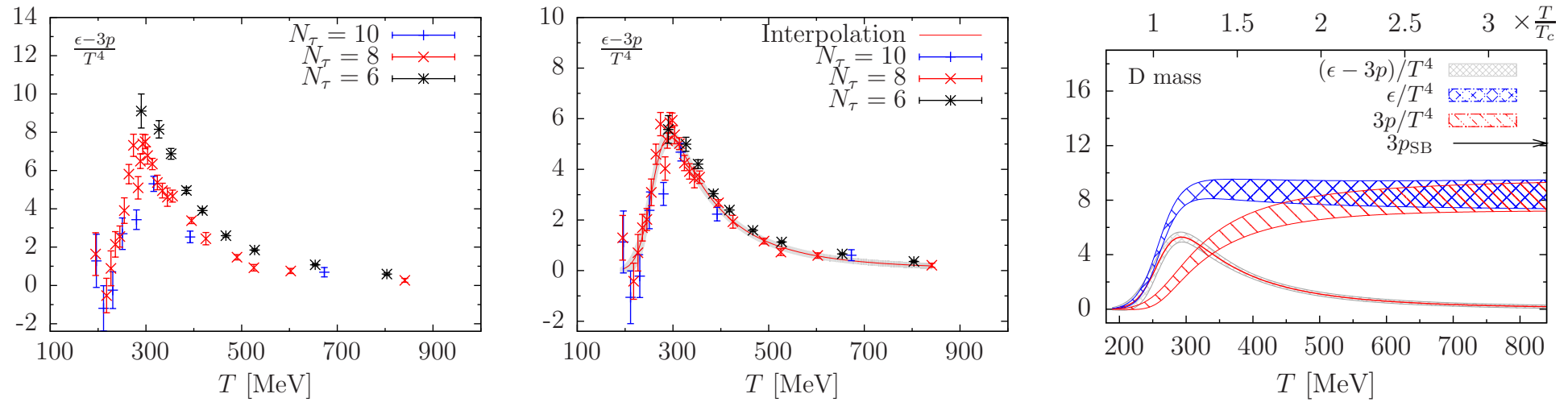
$$\frac{p}{T^4} - \frac{p_0}{T_0^4} = \int_{T_0}^T d\tau \frac{\epsilon - 3p}{\tau^5} \Big|_{\text{LCP}}$$

The available lattice data of  $\frac{I}{T^4}$  have been fitted to the ansatz

$$\frac{I}{T^4} = \exp(-h_1 \bar{t} - h_2 \bar{t}^2) \cdot \left( h_0 + \frac{f_0 \{ \tanh(f_1 \bar{t} + f_2) \}}{1 + g_1 \bar{t} + g_2 \bar{t}^2} \right)$$

where  $\bar{t} = T/T_0$  and  $T_0$  is a free parameter in the fit.

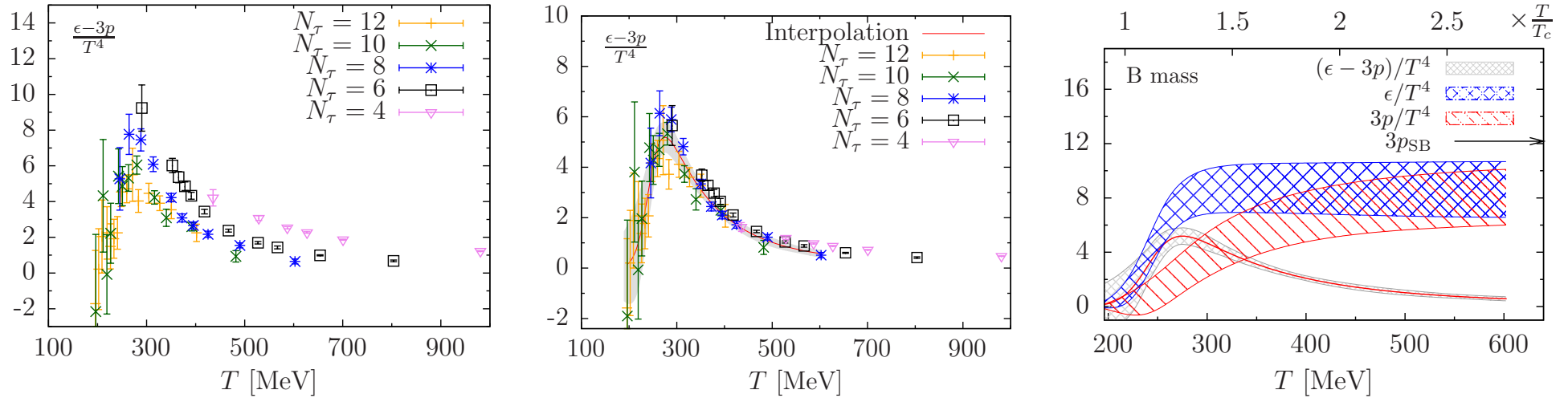
For the D ensembles data from  $N_\tau = 8, 10$  have been fitted simultaneously.



Still preliminary : EoS for the D ensembles ( $m_\pi \approx 700$  MeV)

Left: raw data for  $I$ , Middle: after tree-level corrections, Right: trace anomaly, pressure and energy density.

For the B ensembles data from  $N_\tau = 8, 10$  and 12 have been fitted simultaneously.



Still preliminary : EoS for the B ensembles ( $m_\pi \approx 400$  MeV)

Left: raw data for  $I$ , Middle: after tree-level corrections, Right: trace anomaly, pressure and energy density.

## 6. Gluon and ghost propagators : a link to continuum approaches

- Performing the Landau gauge fixing on a given ensemble of gauge field configurations gives the possibility to study gluon and ghost propagators in straightforward way. (Problem : Gribov ambiguity)
- We have done this for pure gluodynamics ( $N_f = 0$ ) in the vicinity of the first order phase transition, and later for the relevant ensembles of full QCD configurations ( $N_f = 2$ ) over the crossover region.
- Non-perturbative continuum techniques (DSE and FRG) are based on propagators and vertices : thermodynamics and various effective potentials, e.g. for the Polyakov loop, expressed through propagators.
- The propagators for gluodynamics and full QCD appear in Dyson-Schwinger equations (DSE). Lattice data allow crosschecks of the predictions by DSE relating quenched and non-quenched propagators.

## Landau gauge

$$\nabla_\mu A_\mu(x) = \sum_\mu (A_\mu(x + \hat{\mu}/2) - A_\mu(x - \hat{\mu}/2)) = 0$$

where

$$A_\mu(x + \hat{\mu}/2) = \frac{1}{2ia g_0} (U_{x\mu} - U_{x\mu}^\dagger)_{|traceless}$$

can be enforced by **maximization** of the functional

$$F_U[g] = \frac{1}{3} \sum_{x,\mu} \text{Re tr} \left( g_x U_{x\mu} g_{x+\mu}^\dagger \right)$$

with suitable gauge transformations  $g_x$  (including twisted ones  $g'_x$ !).

- **Gauge fixing** is performed for relevant ensembles of Monte Carlo configurations, **irrespective of their origin** (quenched or dynamic).
- **Ghosts are not explicit, studied only algebraically**, by inversion of the Faddeev-Popov operator.



- We have studied the quark propagator for the gluon configurations generated with twisted mass fermions by the TMC : F. Burger et al., Phys.Rev. D 87 (2013) 034514, arXiv:1210.0838 [hep-lat]
- Our aim was to study the effect of the crossover on the gluon (and ghost) propagator in presence of quarks.
- For quenched  $SU(3)$  gauge theory, the first order transition should lead to the strongest relative change of the propagator.
- To set a benchmark, we investigated first the finite  $T$  propagators for pure gauge theory !
- Later we have studied the gluon and ghost propagators for the ensembles generated in the twisted-quark search for the crossover.

Problem of Gribov copies turned out to be severe only in the **extreme infrared (IR) limit**, i.e. **practically irrelevant** for the following analyses !

The aim was to find a good **continuum parametrization** for the propagators,

- over a **relatively broad momentum interval**,
- for a **series of temperatures** around the transition/crossover temperature and **ranging up to  $3 T_{\text{deconf}}$** ,

in order to provide this to the practitioners of continuum approaches (SDE and FRG) enabling crosschecks for their methods and approximations.

First step : quenched propagator study at finite  $T$

R. Aouane et al., Phys. Rev. D 85 (2012) 034501

arXiv:1108.1735 [hep-lat] (with Wilson action, for various lattices)

**Glueon propagator** in momentum space as ensemble average :

$$D_{\mu\nu}^{ab}(q) = \left\langle \tilde{A}_\mu^a(k) \tilde{A}_\nu^b(-k) \right\rangle$$
$$q_\mu(k_\mu) = \frac{2}{a} \sin\left(\frac{\pi k_\mu}{N_\mu}\right) \quad \text{for Matsubara frequency } q_4 = 0$$

For non-zero temperature, Euclidean invariance is broken,  
useful to split  $D_{\mu\nu}^{ab}(q)$  into two components, ( $N_g = N_c^2 - 1$  and  $N_c = 3$ )

- **transversal  $D_T$  (“chromomagnetic”)** propagator
- **longitudinal  $D_L$  (“chromoelectric”)** propagator

$$D_{\mu\nu}^{ab}(q) = \delta^{ab} \left( P_{\mu\nu}^T D_T(q_4^2, \vec{q}^2) + P_{\mu\nu}^L D_L(q_4^2, \vec{q}^2) \right)$$

**Propagators**  $D_{T,L}$  (or their respective dimensionless **dressing functions**  $Z_{T,L}(q) = q^2 D_{T,L}(q)$ ) obtained from the Fourier transforms

$$D_T(q) = \frac{1}{2N_g} \left\langle \sum_{i=1}^3 \tilde{A}_i^a(k) \tilde{A}_i^a(-k) - \frac{q_4^2}{\vec{q}^2} \tilde{A}_4^a(k) \tilde{A}_4^a(-k) \right\rangle$$

and

$$D_L(q) = \frac{1}{N_g} \left( 1 + \frac{q_4^2}{\vec{q}^2} \right) \left\langle \tilde{A}_4^a(k) \tilde{A}_4^a(-k) \right\rangle$$

The **corresponding renormalized functions**, in momentum subtraction (MOM) schemes, can be obtained from

$$\begin{aligned} Z_{T,L}^{ren}(q, \mu) &\equiv \tilde{Z}_{T,L}(\mu) Z_{T,L}(q) \\ J^{ren}(q, \mu) &\equiv \tilde{Z}_J(\mu) J(q) \end{aligned}$$

with the  $\tilde{Z}$ -factors being defined such that

$$\begin{aligned} Z_{T,L}^{ren}(\mu, \mu) &= 1 \\ J^{ren}(\mu, \mu) &= 1 \end{aligned}$$

Our main emphasis : Finite-volume and discretization studies, providing continuum parametrizations for various temperatures, as input (or benchmark) for finite- $T$  continuum studies (within SDE and FRG), with eventual extensions to finite baryonic density !

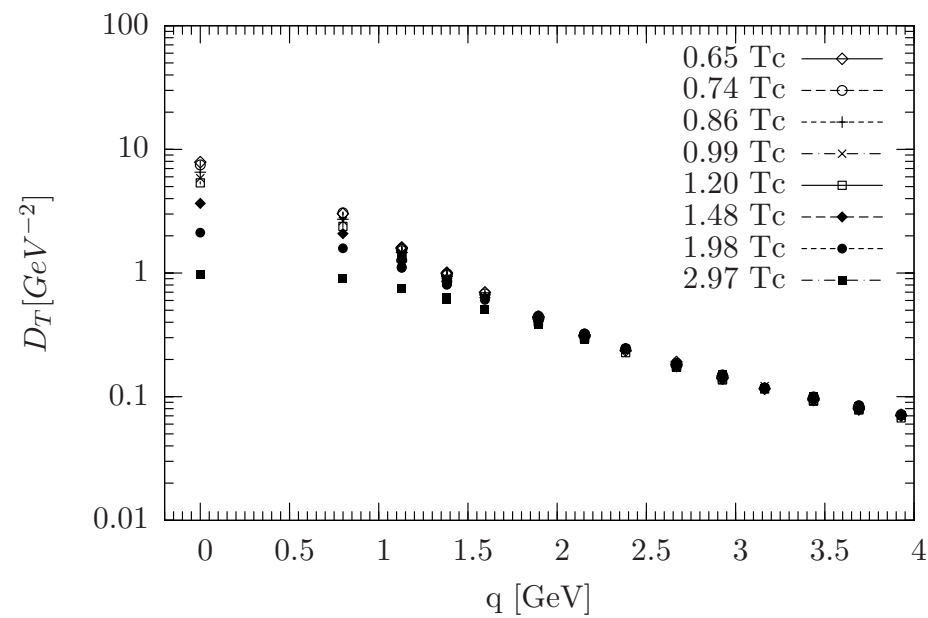
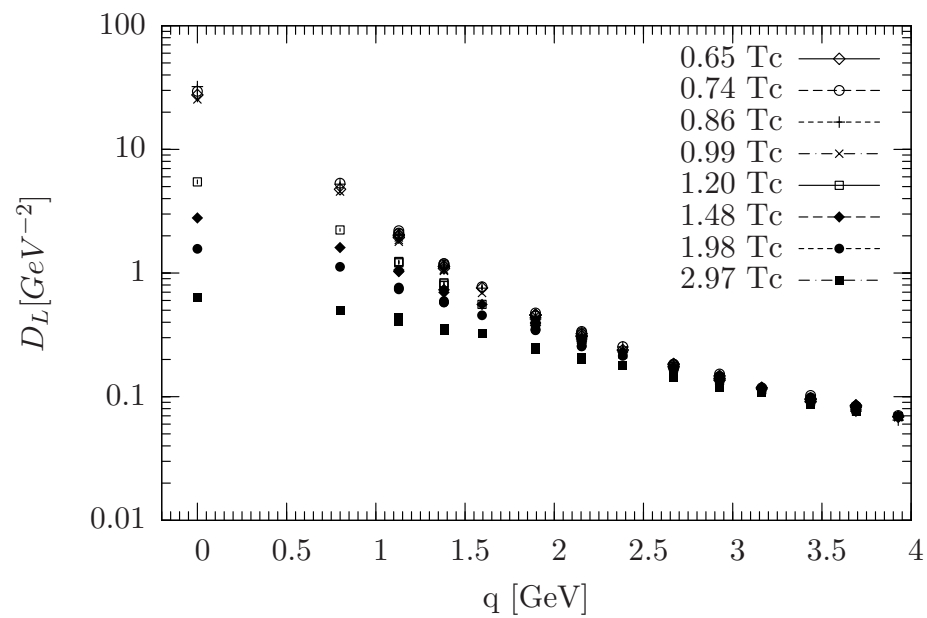
The gluon dressing function was fitted with the **Gribov-Stingl formula**

$$Z_{\text{fit}}(q) = q^2 \frac{c (1 + d q^{2n})}{(q^2 + r^2)^2 + b^2}$$

- fits of the momentum dependence of the propagators in the interval  $0.6 \text{ GeV} < q < 3.0 \text{ GeV}$
- in the temperature range up to  $3 T_{\text{dec}}$   
 $0.65 < T/T_{\text{deconf}} < 2.97$
- Gribov copy and finite volume effects of minor importance in the momentum range under study

While the first order nature of the phase transition is obvious,  
no abrupt changes have been found in the propagators !

## $q$ dependence of $D_L$ and $D_T$ for various temperatures







It is not difficult to reconcile the first order phase transition with the continuous  $T$ -dependence of the propagators !

Our finite-temperature results for pure Yang-Mills theory have been used by [K. Fukushima and K. Kashiwa, arXiv:1206.0685v5 \[hep-ph\]](#)

- for the **effective potential for the Polyakov loop**
- for **reconstructing the Equation of State (EoS)**

In leading order of the 2PI-formalism, the **thermodynamical potential can be approximated** as follows in terms of the gluon and ghost propagators :

$$\frac{1}{T}\Omega_{\text{glue}} \simeq -\frac{1}{2}\text{tr} \ln D_{\text{gl}}^{-1} + \text{tr} \ln D_{\text{gh}}^{-1}$$

For example, the inverse gluon propagator has been extracted from our data for  $T < 1.2 T_c$

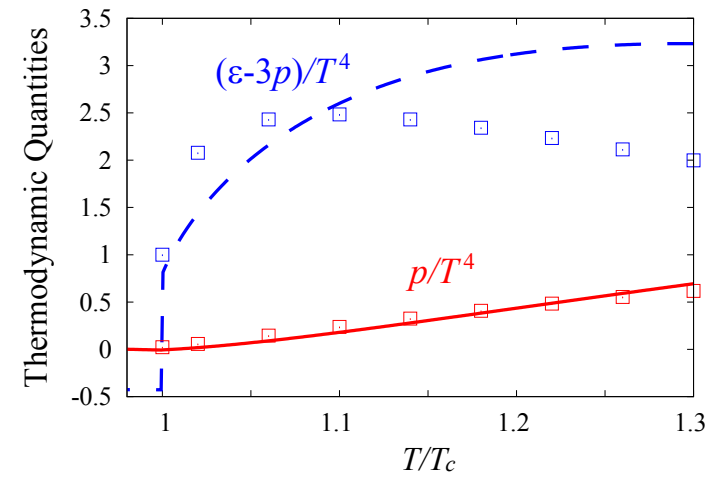
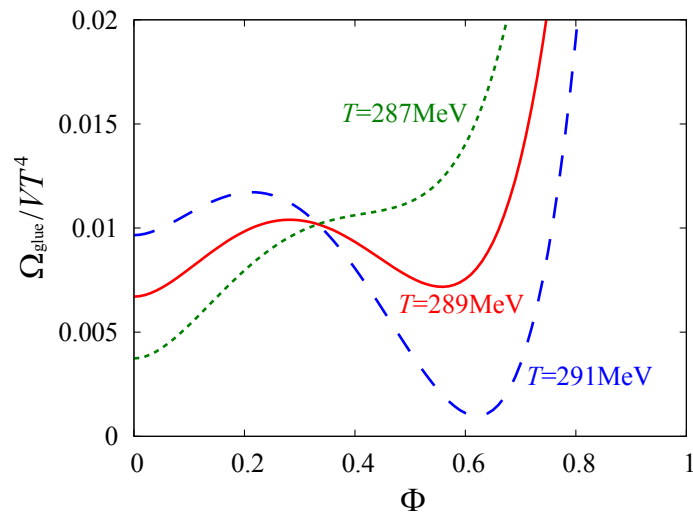
$$D_{\text{gl}}^{-1}(p^2) = \left[ p^2 Z_T(p^2) T_{\mu\nu} + \xi^{-1} p^2 Z_L(p^2) L_{\mu\nu} \right] \delta^{ab}$$

## Results :

- The transition temperature has been successfully reconstructed in terms of the Polyakov loop effective potential from the  $T$ -dependent propagator data.
- The pressure and trace anomaly are obtained, respectively, good and roughly correct.

## Order parameter and EoS of pure Yang-Mills

Transition temperature and first rise of pressure successfully reconstructed from the  $T$ -dependent propagator data !



## What about propagators from non-quenched simulations ?

How are non-quenched gluon propagators related to quenched ones ?

How good can SDE predict/postdict what will be/has been measured on the lattice ?

C. S. Fischer and J. Luecker, “Propagators and phase structure of  $N_f = 2$  and  $N_f = 2 + 1$  QCD”

Physics Letters B 718 (2013) 1036, arXiv:1206.5191,

also in: C. S. Fischer, L. Fister, J. Luecker, J. M. Pawłowski, “Polyakov loop potential at finite density”, arXiv:1306.6022

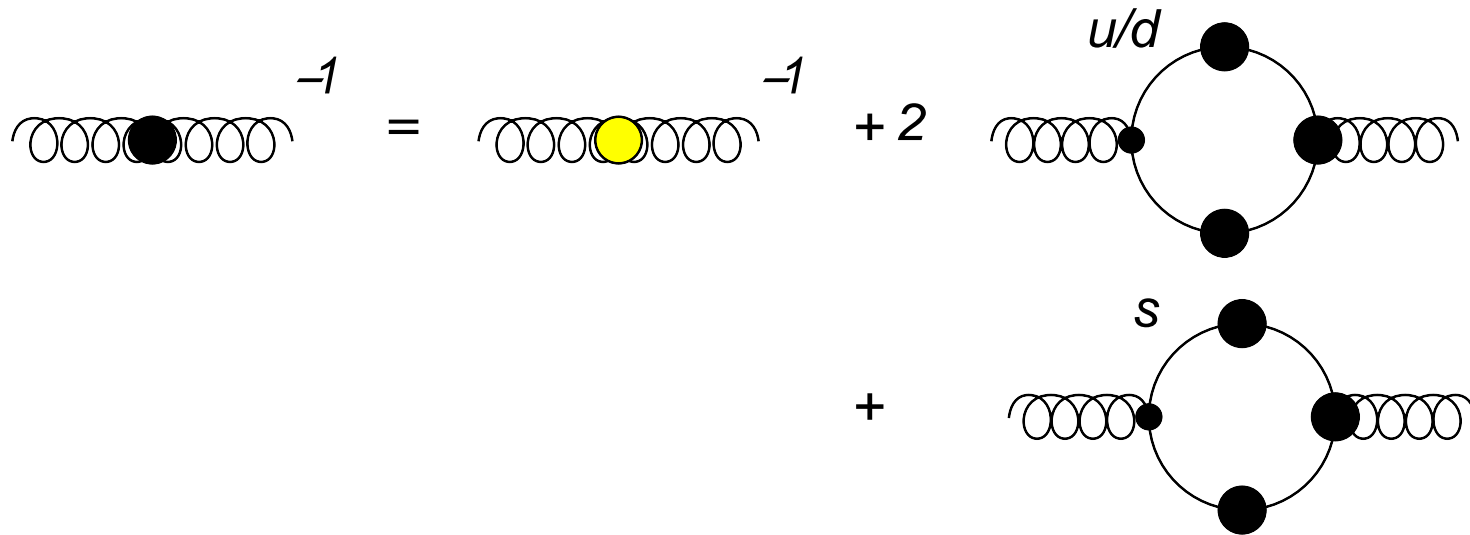
Full set of Schwinger-Dyson equations is used to predict the  $T$  dependence of full QCD propagators from the quenched ones, depending on  $m_\pi$  as a parameter to be measured in the non-quenched simulations (crossover).

# Full Dyson-Schwinger equations for the quark and the gluon propagator

The diagram shows the Dyson-Schwinger equation for the quark propagator. On the left, a solid horizontal line with a black dot in the middle is followed by an equals sign and a superscript  $-1$ . This is equal to a solid horizontal line with an arrow pointing to the right, followed by a plus sign and a superscript  $-1$ . This is then followed by a plus sign and a diagram of a self-energy loop: a solid horizontal line with two black dots, from which a wavy line (gluon) loops back to the first dot, with a black dot on the wavy line.

The diagram shows the Dyson-Schwinger equation for the gluon propagator. On the left, a wavy horizontal line with a black dot in the middle is followed by an equals sign and a superscript  $-1$ . This is equal to a wavy horizontal line with a superscript  $-1$ , followed by a plus sign and a diagram of a ghost loop: a wavy line with two black dots, from which a dashed line (ghost) loops back to the first dot, with a black dot on the dashed line. This is followed by a plus sign and a diagram of a quark loop: a wavy line with two black dots, from which a solid line (quark) loops back to the first dot, with two black dots on the solid line. This is followed by a plus sign and a diagram of a gluon loop: a wavy line with two black dots, from which a wavy line loops back to the first dot, with two black dots on the wavy line. This is followed by a plus sign and a diagram of a ghost-gluon loop: a wavy line with two black dots, from which a dashed line loops back to the first dot, with a black dot on the dashed line. This is followed by a plus sign and a diagram of a quark-gluon loop: a wavy line with two black dots, from which a solid line loops back to the first dot, with a black dot on the solid line.

Truncated gluon Dyson-Schwinger equation relating the quenched and the non-quenched gluon propagator (for  $u, d$  and evtl.  $s$  quarks)  
 (yellow insert = quenched gluon propagator)



By-product of this study : quark propagator at  $T \neq 0$   
(was not yet studied by us for twisted mass at  $T \neq 0$ )

Would be interesting to compare !

More recently: [Phys. Rev. D 87 \(2013\) 114502](#), [arXiv:1212.1102](#)

“Landau gauge gluon and ghost propagators from lattice QCD with  $N_f = 2$  twisted mass fermions at finite temperature”

R. Aouane, F. Burger, E.-M. I., M. Müller-Preussker, A. Sternbeck

has provided the unquenched propagators for twisted mass ensembles of the tmfT collaboration, leading to continuum parametrizations in the momentum ranges :

- $0.4 \text{ GeV} < q < 3.0 \text{ GeV}$  for the gluon propagators (perfect fit !)  
fitting parameter  $b^2$  in the Gribov-Stingl fit compatible with zero (no splitting in complex conjugate poles visible in this momentum range !)
- $0.4 \text{ GeV} < q < 4.0 \text{ GeV}$  for the ghost propagator (less good, fit correct within few percent, a mass term  $m_{\text{gh}}$  wouldn't help),

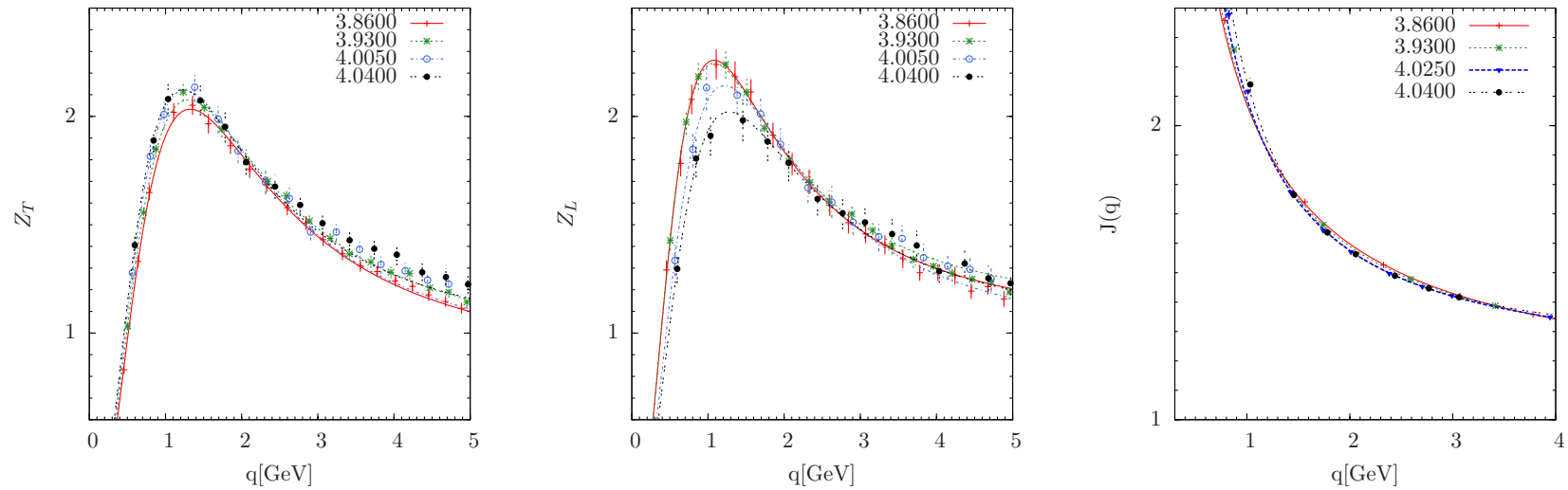


Temperature range covered :

- Done for various temperatures in the range  $180 \text{ MeV} < T < 260 \text{ MeV}$  which were investigated in the “phase transition project”.

Renormalized propagators given for renormalization scale  $\mu = 2.5 \text{ GeV}$ .

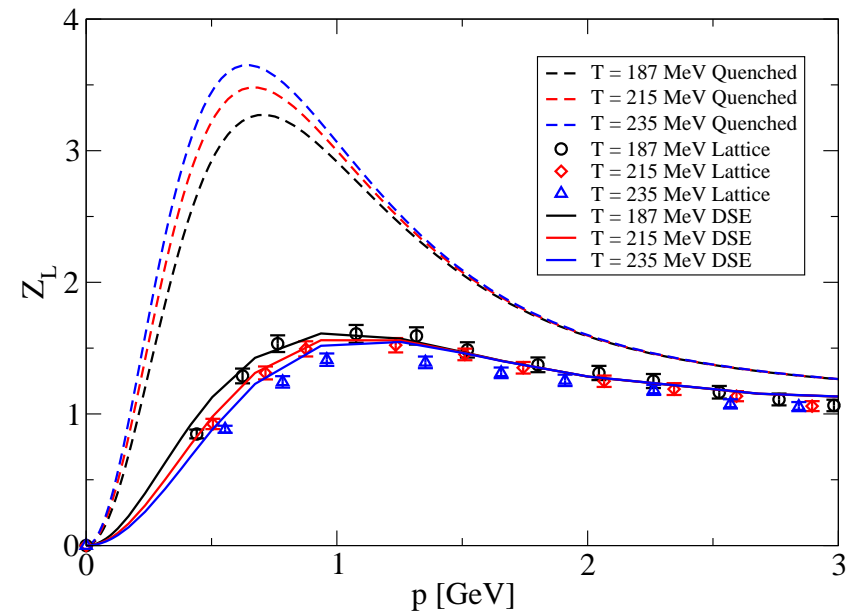
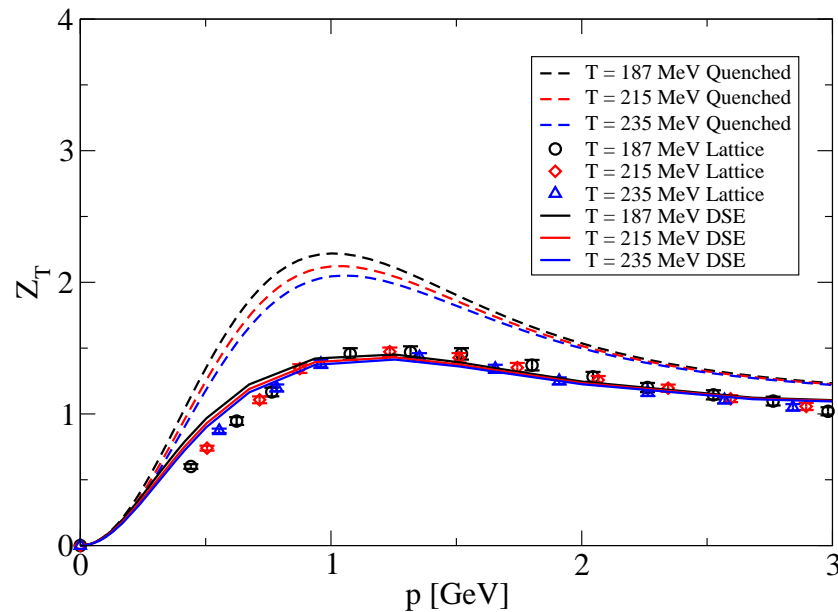
The unrenormalized dressing functions,  $Z_T$  (left panel),  $Z_L$  (middle panel) and for the ghost  $J$  (right panel) for various temperatures, B12 for  $m_\pi = 398$  MeV



How are non-quenched gluon propagators related to quenched ones throughout the crossover region ?

C. S. Fischer, L. Fister, J. Luecker, J. M. Pawłowski,  
“Polyakov loop potential at finite density”, arXiv:1306.6022

Dressing functions  $Z_T$  (left) and  $Z_L$  (right) with and without dynamical fermions from lattice and related through DSE



## Conclusions concerning twisted mass at finite temperature

- The  $N_f = 2$  **crossover structure** and the investigation of its chiral limit are **close to completion**.
- The results are in fair **agreement with** other results with **Wilson fermions** (DIK collaboration) and **other lattice fermions**.
- The **EoS** is will be presented **soon in full detail** (F. Burger).
- **Chiral crossover and deconfinement (hard to find) do not coincide**.
- The **effect of the crossover** on the gluon propagator is **visible**.  
Masses too large ! Longitudinal gluon propagator most sensitive.
- Interesting **cross-checks with SDE** (Ch. Fischer et al.) !
- Future orientation of the **tmfT collaboration** ?  
We will **turn to  $N_f = 2 + 1 + 1$  simulations**.

- Strange and charmed quarks are less important for finding the chiral transition temperature. However, they are **important for the thermodynamics of the deconfined phase !**

## 7. Scanning the full phase diagram : finite baryonic density

Let's next discuss the **generalization to non-zero baryon density**, the phase diagram in the  $T - \mu_q$  plane. It is sufficient to consider  $\mu_q \geq 0$ .

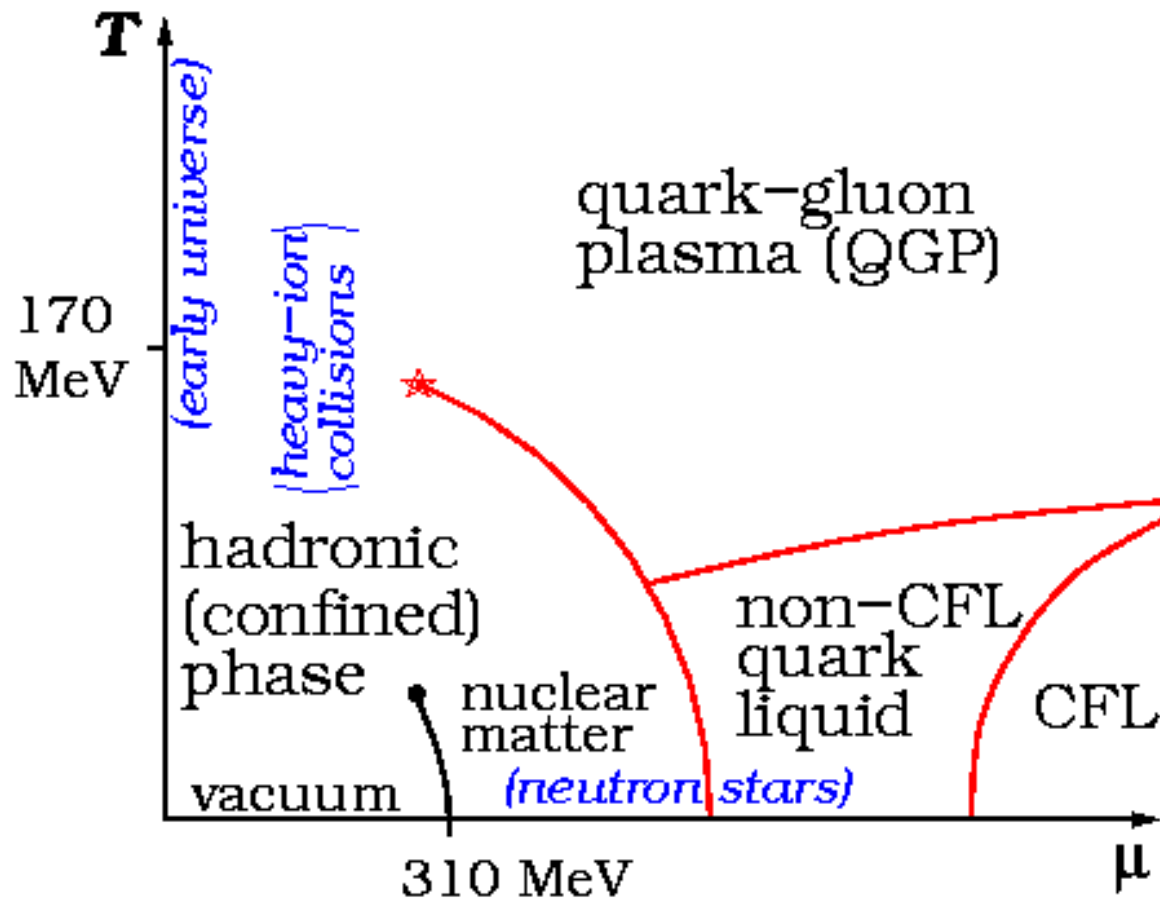
**If one could simply simulate at any  $\mu_q$** , one could map out the phase diagram by  **$\beta$ -scans for all interesting  $\mu_q$**  or **at fixed ratio  $\mu_q/T$** .

Unfortunately, **importance sampling simulation at  $\mu_q \neq 0$  is impossible !**

**Four main possibilities to fight the sign (complex weight) problem :**

- Analytical continuation from imaginary  $\mu_q = i\eta$  (for selected results)
- Phase quenching : neglecting the phase of the determinant during simulation, including it into the observable
- Reweighting across the  $\beta$ - $\mu_q$  plane
- Taylor expansion in  $\mu_q$  in points along the  $\beta$ -axis

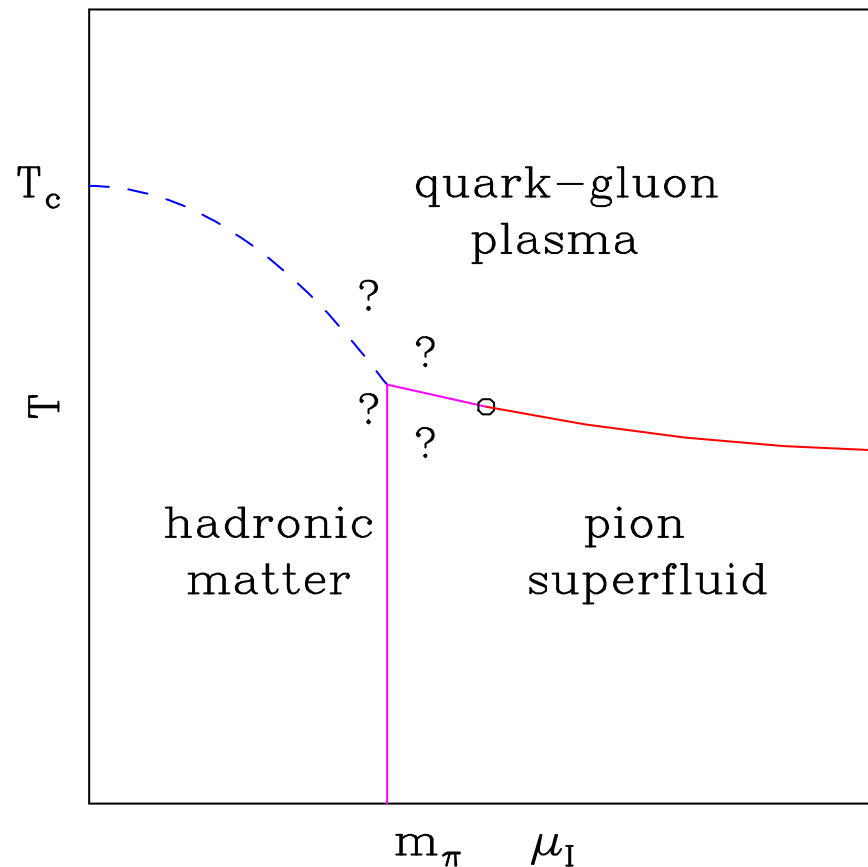
Hypothetic phase diagram of QCD (from Wikipedia)  
after Ph. de Forcrand arXiv:1005.0539



What if one ignores the phase of the fermion determinant ?

This would give the phase diagram for QCD at finite isospin density schematically, from Philipsen arXiv:1009.4089

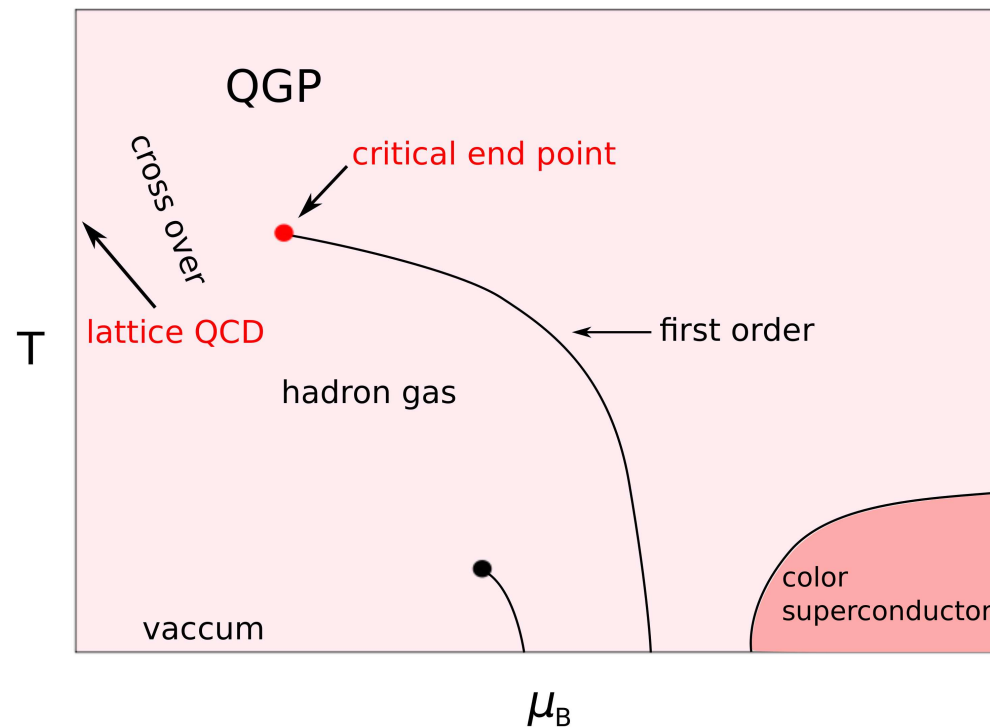
$N_f=2$  QCD at finite isospin density



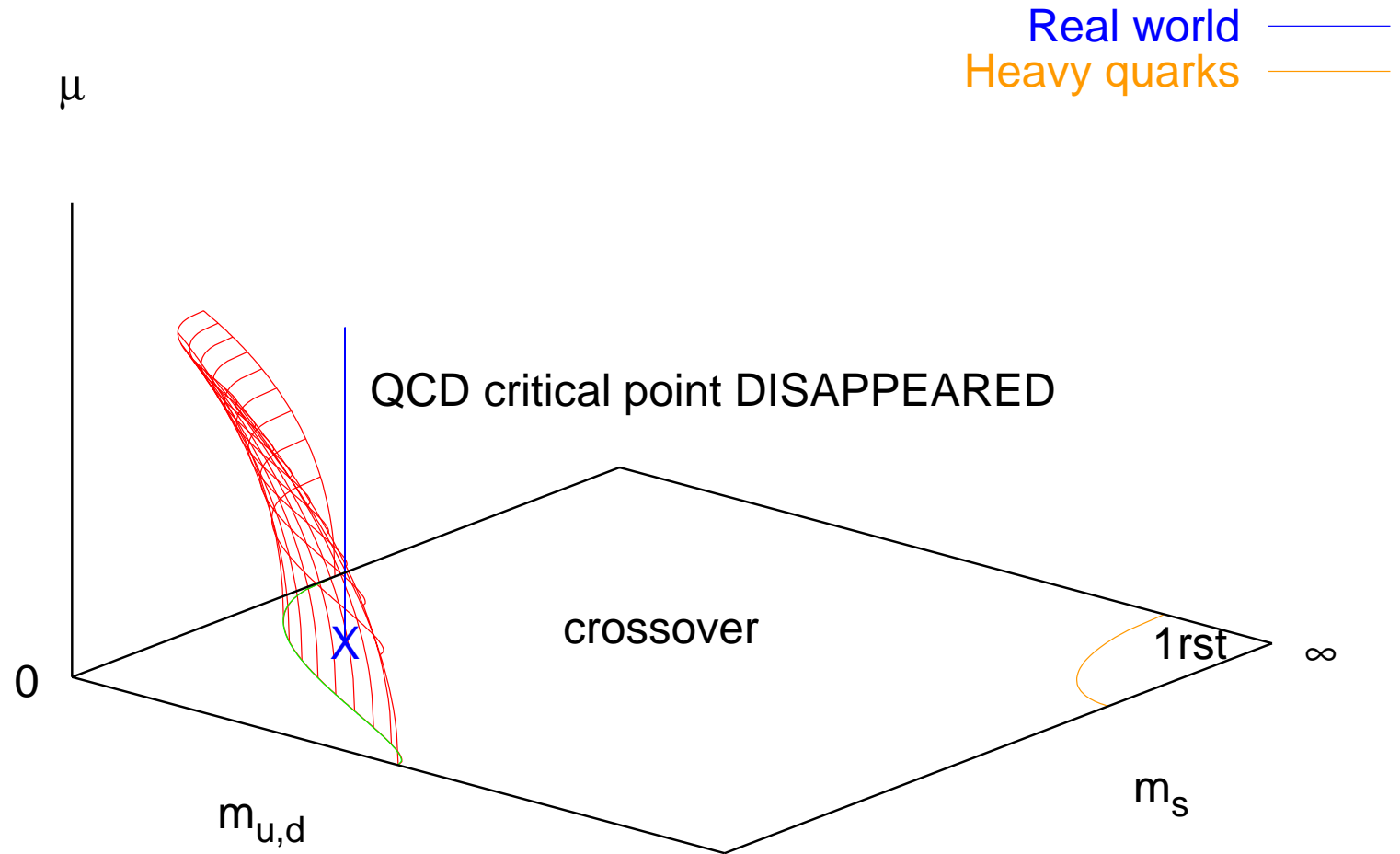


# Crossover vs. First Order Transition in the Phase Diagram of QCD

from Anyi Li arXiv:1002:4459



The Columbia plot extended into a third direction  $\mu$  : will there be a true phase transition (critical point) for physical quark masses ?  
from Ph. de Forcrand and O. Philipsen hep-lat/0607017



## 7.1. Analytical continuation from imaginary $\mu_q = i\eta$ to real $\mu_q$

Can we get the phase transition curve directly from experiment ?

From central Pb+Pb (Au+Au) collisions at SIS, AGS, SPS and RHIC the **collision energy dependence of temperature and baryonic chemical potential** (both obtained from particle yields, say via THERMUS) has been found in the form ( $s_{NN}$  is related to a single nucleon pair) ;

$$\mu_B = \frac{1.308}{1 + 0.273\sqrt{s_{NN}}}$$

This  $\mu_B$  enters the (chemical) “freeze-out” temperature  $T_{\text{freeze}}(\mu_B)$  close to the crossover temperature at vanishing baryon density,

$T_\chi(\mu = 0) = 0.166$  GeV which is then parametrized as follows :

$$\frac{T_{\text{freeze}}(\mu)}{T_\chi(\mu = 0)} = 1 - 0.023 \left(\frac{\mu_B}{T}\right)^2 - \mathcal{O}\left(\left(\frac{\mu}{T}\right)^4\right)$$

J. Cleymans Phys. Rev. C 63 (2006) 034905

This has motivated the interest in lattice results for the  $\mu$  dependence of the phase transition temperature  $T_\chi(\mu)$  near  $T_\chi(0)$  (it is not too hard).

$T_\chi(\mu)$  must be an even function of  $\mu$  near  $\mu = 0$ .

$$\frac{T_\chi(\mu)}{T_\chi(\mu = 0)} = 1 - \sum_k t_{2k} \left(\frac{\mu}{T}\right)^{2k}$$

The curvature found on the lattice is much smaller than that of the freeze-out curve :

$$\frac{T_\chi(\mu)}{T_\chi(\mu = 0)} = 1 - 0.0066(7) \left(\frac{\mu}{T}\right)^2$$

Similarly

$$\frac{\beta_\chi(\mu)}{\beta_\chi(\mu = 0)} = 1 - \sum_k b_{2k} \left(\frac{\mu}{T}\right)^{2k}$$

The coefficients have been determined at imaginary  $\mu = i\eta$ .

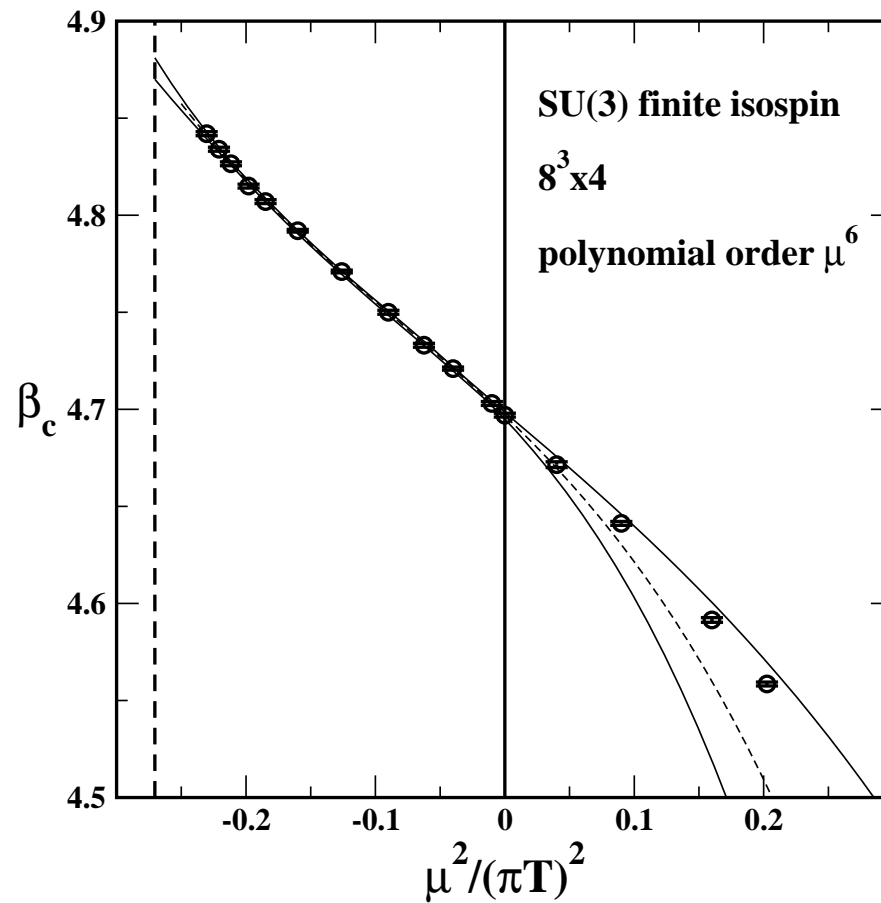
This is the first example for analytic continuation.

- It turns out, that the freeze-out temperature is three times more curved downward than  $T_\chi(\mu)$ .
- Moreover, the curvature seems to decrease in the continuum limit !
- However, the method is sensitive to the order of the series that is fitted to the imaginary- $\mu$  data :  
The coefficients at imaginary  $\mu$  are alternating in sign and can be determined only with large uncertainty.

Lesson :

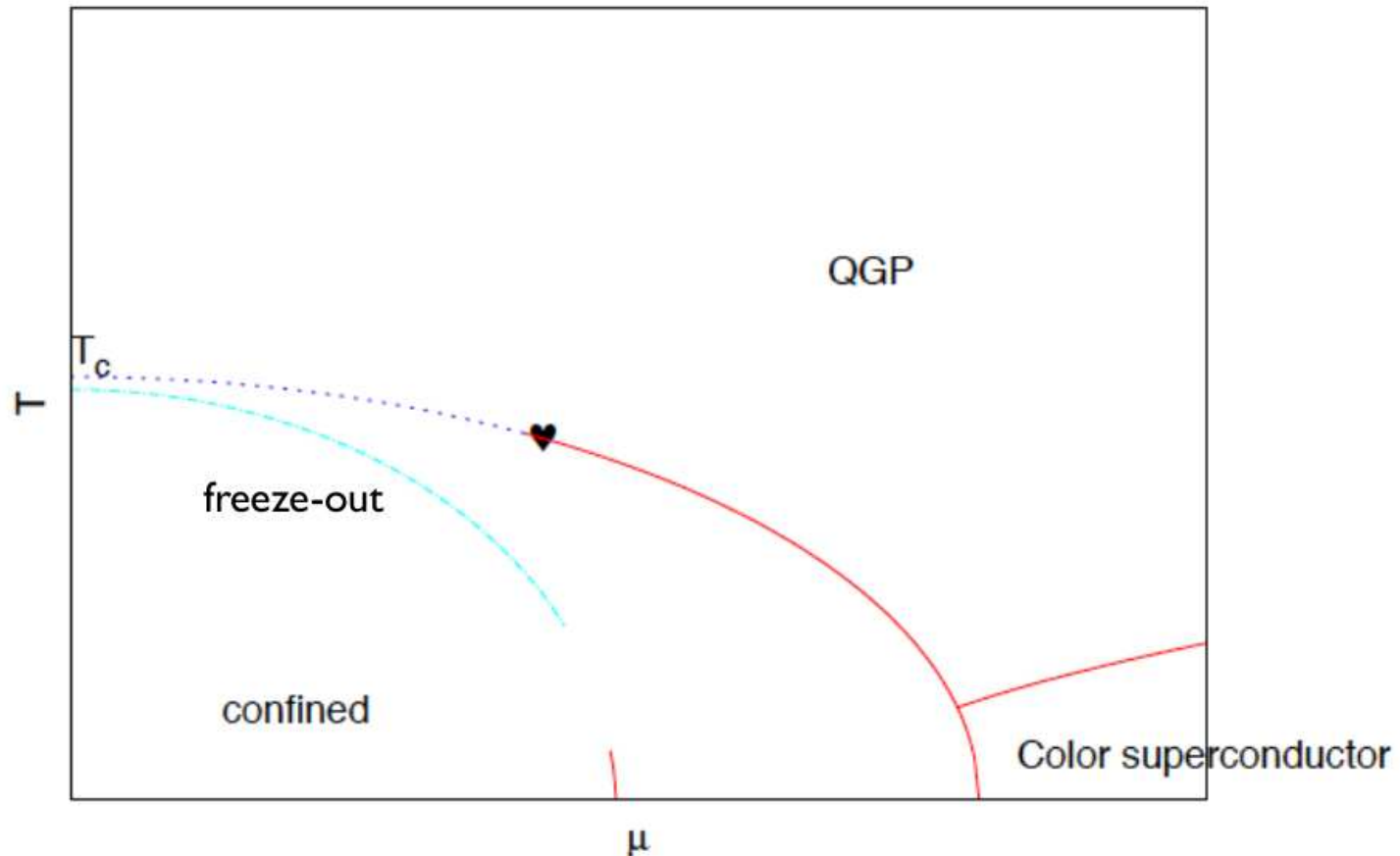
“The chemical freeze-out happens deep inside the hadronic phase and has no relation to the quark-gluon plasma.”

Continuation of  $\beta_c$  from negative  $\mu^2$  to positive  $\mu^2$   
from Ph. de Forcrand arXiv:1005.0539



Sketch of the QCD crossover line  $T_c(\mu)$  vs. the experimental freeze-out curve, which has a larger curvature, near  $T_c(0)$ .

from Ph. de Forcrand arXiv:1005.0539

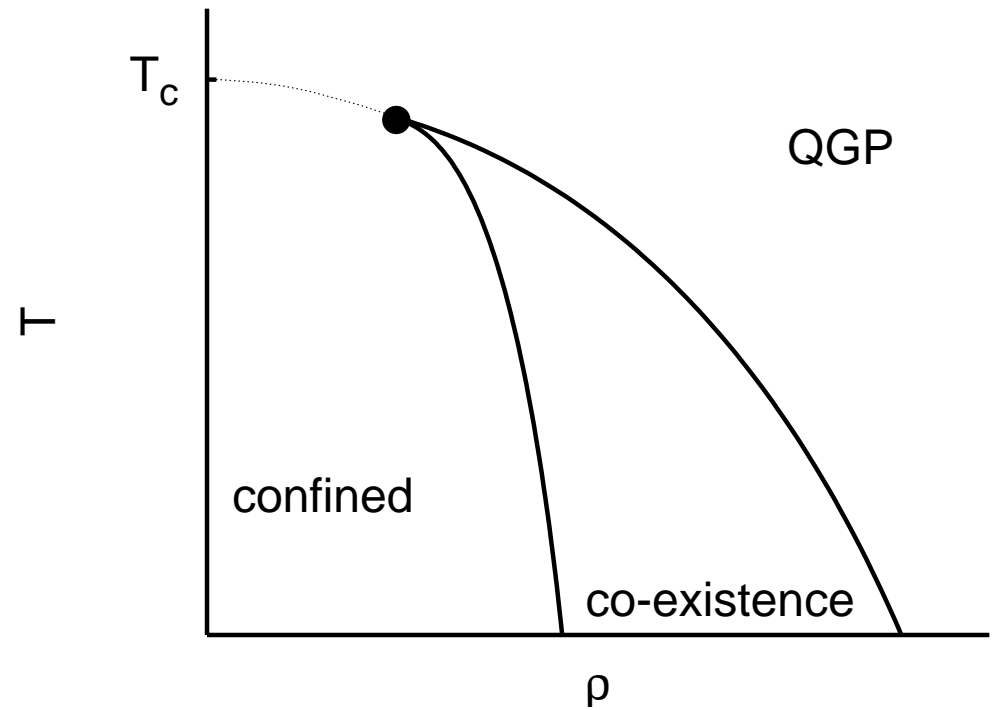
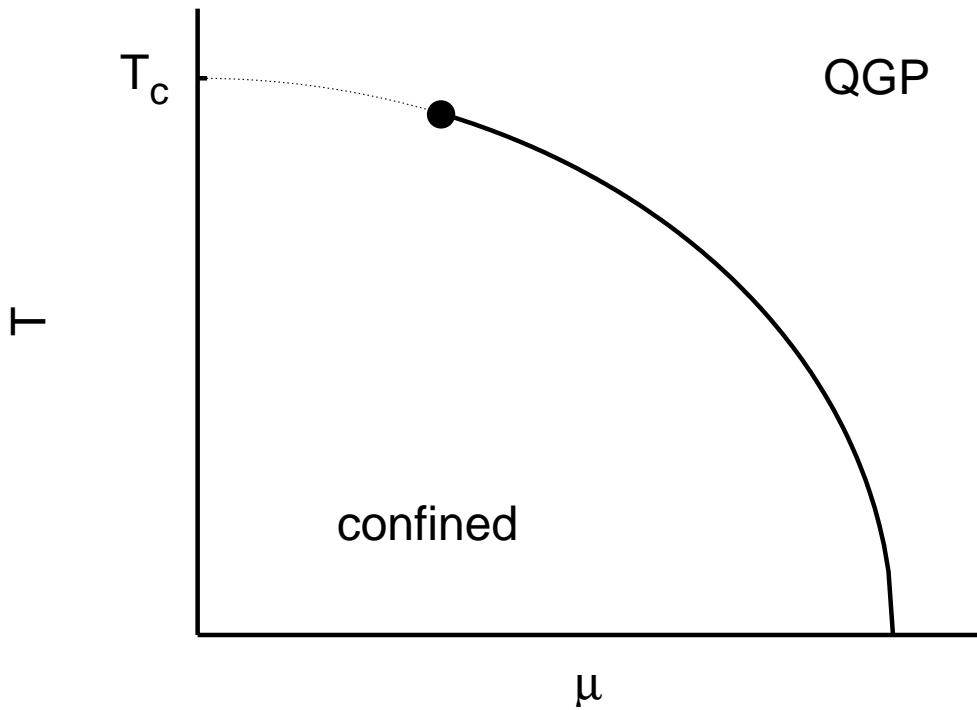


Much more could be said about imaginary chemical potential :

- a full view of the phase diagram with imaginary chemical potential
- the Roberge-Weiss periodicity :  $\frac{\eta}{T} \rightarrow \frac{\eta}{T} + \frac{2\pi}{3}$
- the construction of canonical ensembles for fixed numbers of baryons  $N_B$
- the phase diagram in the  $T$ - $n_B$  (baryonic density) plane : mixed phases



The QCD Phase Diagram: Grand Canonical and Canonical View  
from S. Kratochvila and Ph. de Forcrand hep-lat/0509143



Both thermodynamic ensembles should be equivalent in the infinite volume limit. However, this limit is difficult to achieve.

For large, **quasi-continuous baryon number**  $B$ ,  $Z_C$  becomes a function of the baryon density  $\rho$  :

$$Z_C^{(q)}(V, T, n = NB) = Z_C^{(B)}(V, T, B) = Z_C^{(dens)}(V, T, \rho)$$

Then

$$\begin{aligned} Z(V, T, \mu) &= \int_{-\infty}^{+\infty} d\rho e^{VN\rho\mu/T} Z_C^{(dens)}(V, T, \rho) \\ &= \lim_{V \rightarrow \infty} \int_{-\infty}^{+\infty} d\rho e^{-\frac{V}{T}(f(\rho) - \mu\rho)} \end{aligned}$$

with  $f(\rho)$  as the **free energy density in canonical ensemble**.

Finally,  $\mu$  can be expressed as function of the baryon density  $\rho$  :

$$\mu(\rho) = \frac{1}{N} \frac{\partial f(\rho)}{\partial \rho}$$

This function shows a behavior resembling the van der Waals gas.

This approach has been pursued numerically :

S. Kratochvila and Ph. de Forcrand, hep-lat/0509143

$6^3 \times 4$  lattice, four degenerate staggered quarks, volume  $(1.8 \text{ fm})^3$

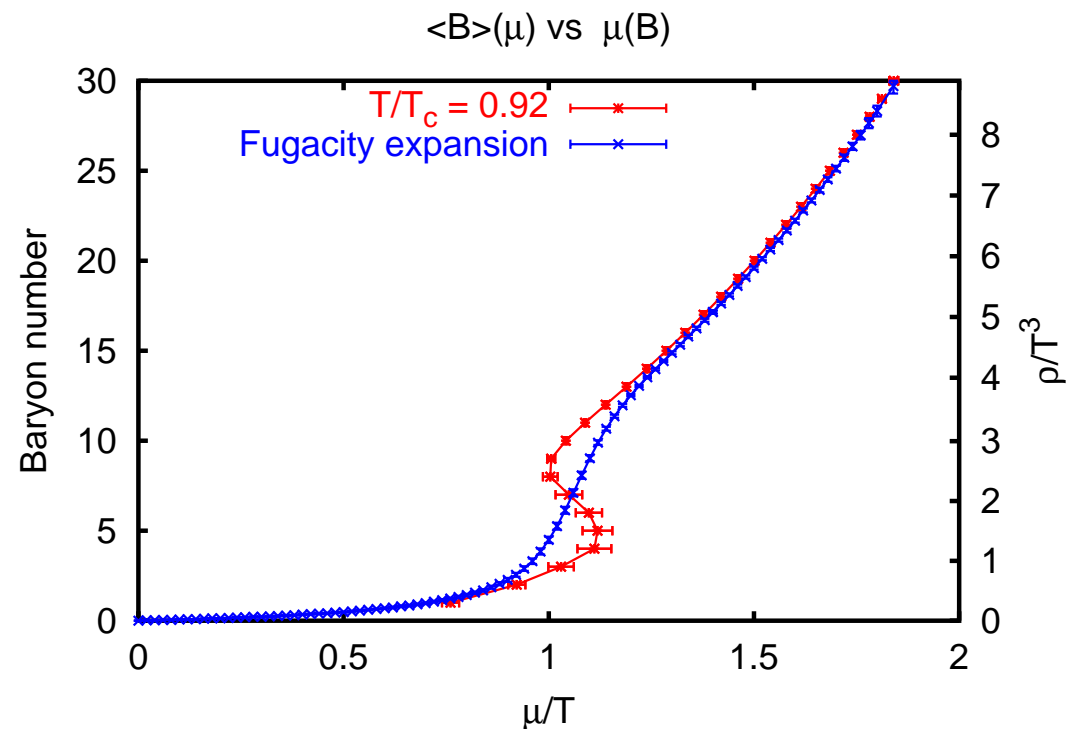
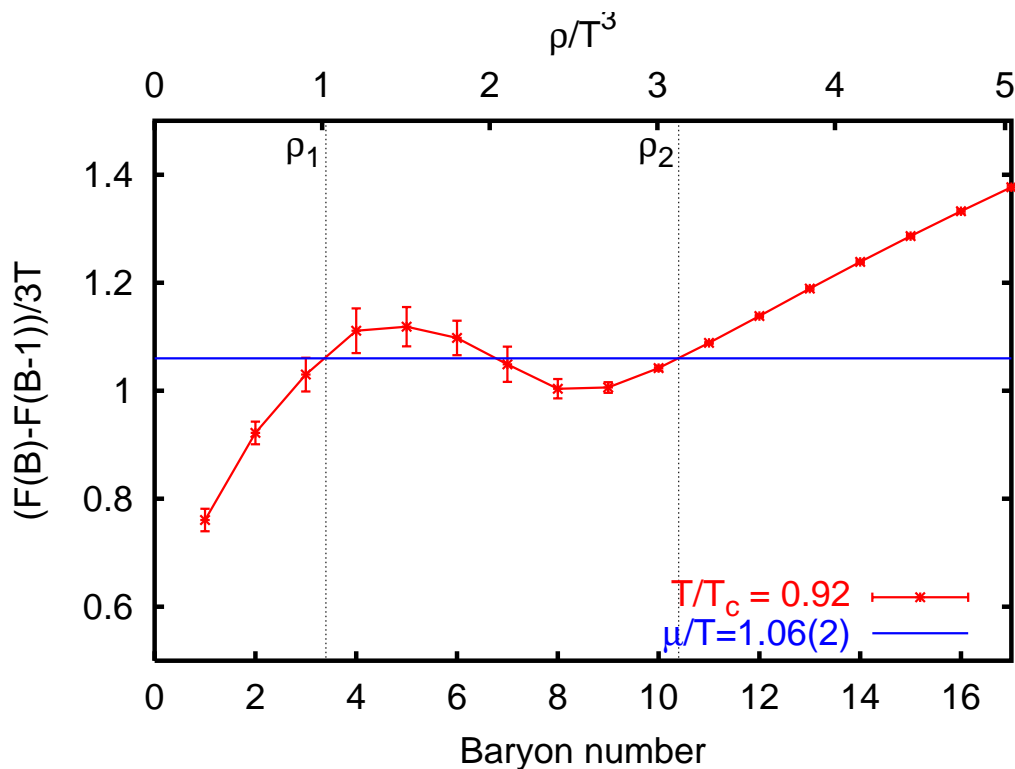
A. Alexandru, M. Faber, I. Horvath and K. F. Liu, hep-lat/0507020

Kentucky group :

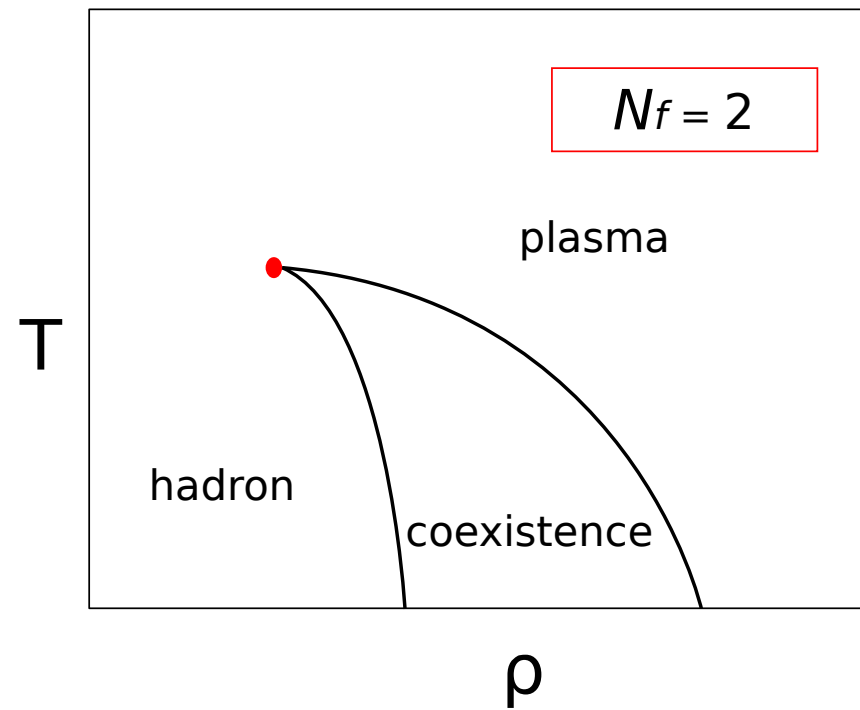
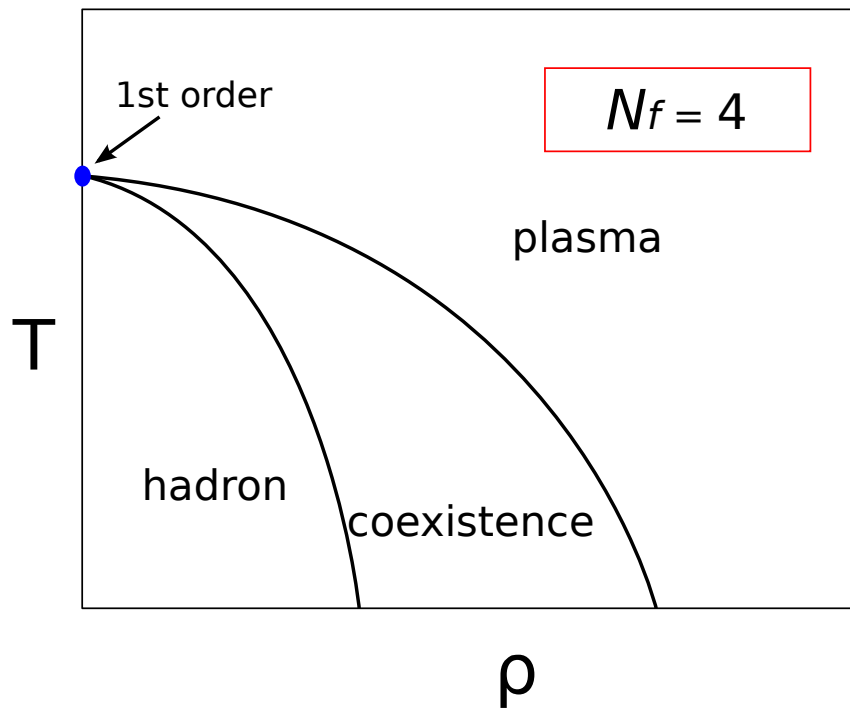
$6^3 \times 4$  lattice, clover-improved Wilson fermions  $N_f = 2, 3$  and  $4$ .

Left: The Maxwell construction allows to extract the critical chemical potential and the boundaries of the co-existence region. Right: Comparing the saddle point approximation (red) with the fugacity expansion (blue). Strong finite-size effects in the latter obscure the first-order transition.

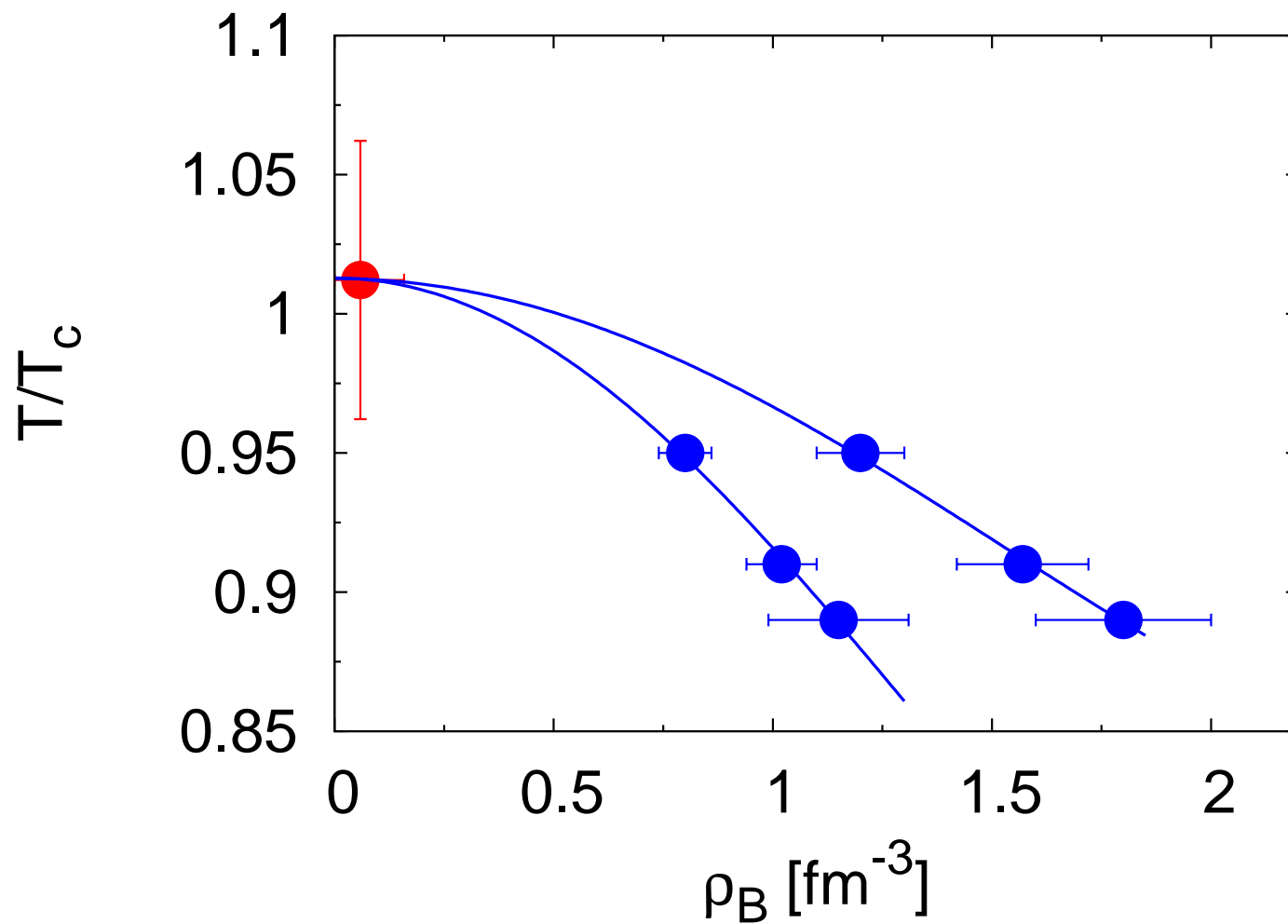
from S. Kratochvila and Ph. de Forcrand hep-lat/0509143



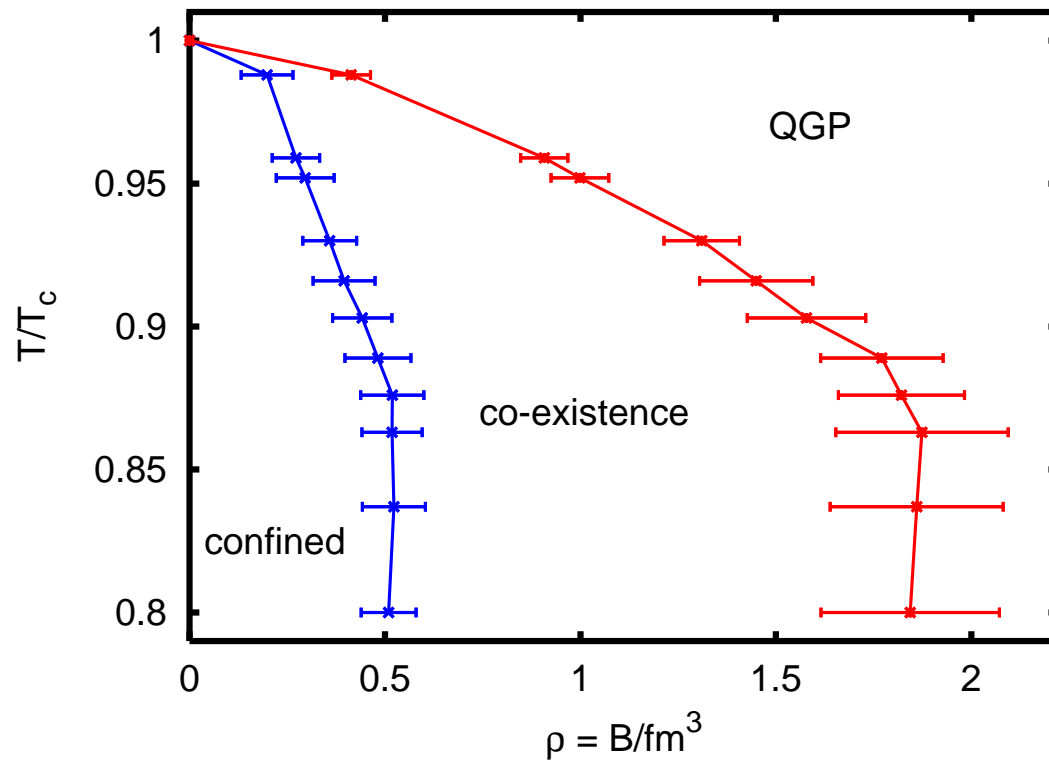
The number of flavors is extremely important :  $N_f = 4$  vs.  $N_f = 2$   
from Anyi Li arXiv:1002:4459



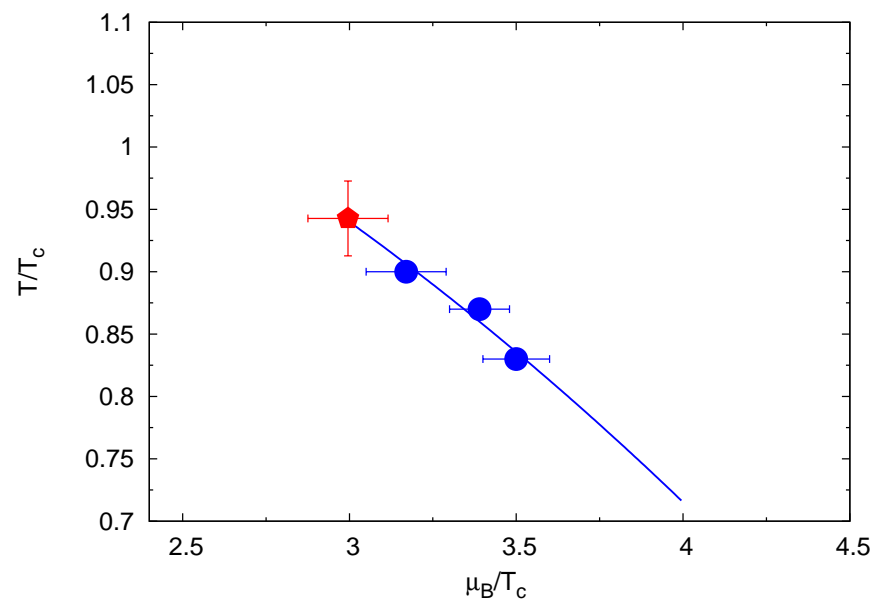
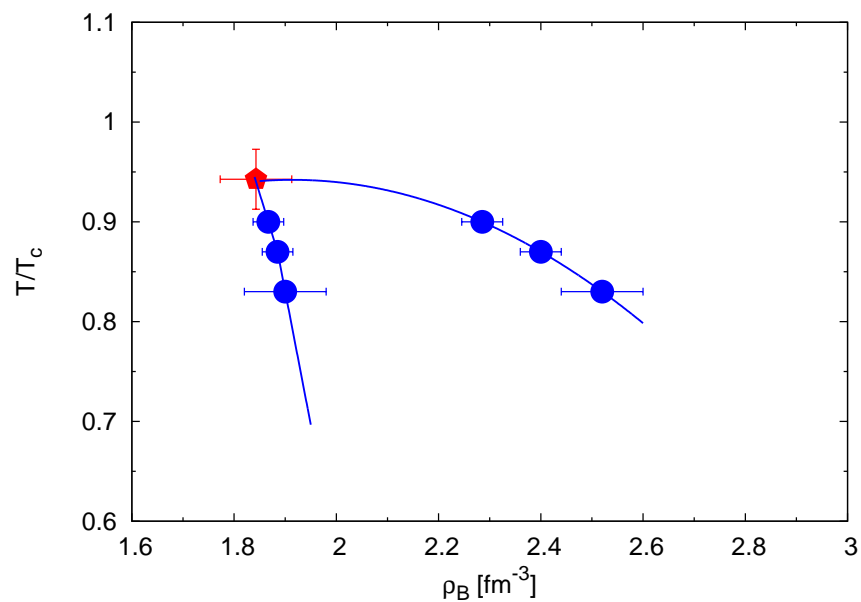
Phase boundaries in the temperature vs. density plot for  $N_f = 4$ .  
from Anyi Li arXiv:1002:4459



Phase boundaries in the temperature vs. density plot for  $N_f = 4$ .  
from S. Kratochvila and Ph. de Forcrand hep-lat/0509143



Left: Phase boundaries in the temperature vs. density plot for  $N_f = 3$ .  
Right: Transition line in the temperature vs. chemical potential plot.  
from Anyi Li arXiv:1002:4459





This looks rather systematic, however the lattices are too small.

There are possible systematic effects of the canonical ensemble method.

One would like to confirm this in a more robust way, that works also for large lattices (Taylor expansion), in order to verify the first order character of the transition.

## 7.2. Phase quenching

Consider the exact partition function with  $n_B \neq 0$ , i.e.  $\mu_q \neq 0$  :

$$Z_B(\beta, \mu_q) = \int D[U] (\det D(U, \mu_q))^{N_f} e^{-\beta S_G}$$

Factorize the complex determinant into **modulus and phase factor**

$$Z_B(\beta, \mu_q) = \int D[U] |\det D(U, \mu_q)|^{N_f} e^{i N_f \theta} e^{-\beta S_G}$$

**Phase-quenched ensemble :**

$$Z_{pq}(\beta, \mu_q) = \int D[U] |\det D(U, \mu_q)|^{N_f} e^{-\beta S_G}$$

Fortunately, this ensemble can also be sampled according to HMC; since it can be interpreted as the **fixed-isospin ensemble** with  $\mu_I = \mu_q$

$$Z_{pq}(\beta, \mu) = Z_I(\beta, \mu_I = \mu)$$

For even  $N_f$

$$|\det D(U, \mu_q)^{N_f}| = \det D(U, +\mu_q)^{\frac{N_f}{2}} \det D(U, -\mu_q)^{\frac{N_f}{2}}$$

such that phase quenching is equivalent to fixed isospin with  $\mu_I = \mu_q$ .

For  $N_f = 2$

$$(\det D(U, \mu_q))^2 = |\det D(U, \mu_q)|^2 e^{2i\theta}$$

For some observable  $\mathcal{O}$  we can consider **two expectation values**

$$\langle \mathcal{O} \rangle_I = \frac{1}{Z_I} \int D[U] \mathcal{O} |\det D(U, \mu_q)|^2 e^{-\beta S_G} \quad (\text{simulation possible})$$

$$\langle \mathcal{O} \rangle_B = \frac{1}{Z_B} \int D[U] \mathcal{O} (\det D(U, \mu_q))^2 e^{-\beta S_G} \quad (\text{simulation impossible})$$

Nevertheless, the last **average can be estimated** by including the missing phase factor into the observable : estimator

$$\langle \mathcal{O} \rangle_B = \frac{\langle \mathcal{O} e^{2i\theta} \rangle_I}{\langle e^{2i\theta} \rangle_I}$$

where the averages are taken w.r.t. the phase quenched (pq), i.e. the fixed-isospin (I) ensemble. **Phase quenching is applied more generally !**

While the **Monte Carlo process is guided by the fixed isospin ensemble**, the global phase factor has to be evaluated only after the trajectory is finished, simultaneously with the observable  $\mathcal{O}$  on the configuration.

The smallness of the denominator (“average phase factor”) quantifies the severity of the sign problem !

When the denominator is small due to phase cancellations, the error of the numerator is also big, and the estimate not reliable.

The denominator decreases exponentially with volume and  $1/T$

$$\langle e^{2i\theta} \rangle_I \propto e^{-\frac{V}{T}\Delta f}$$

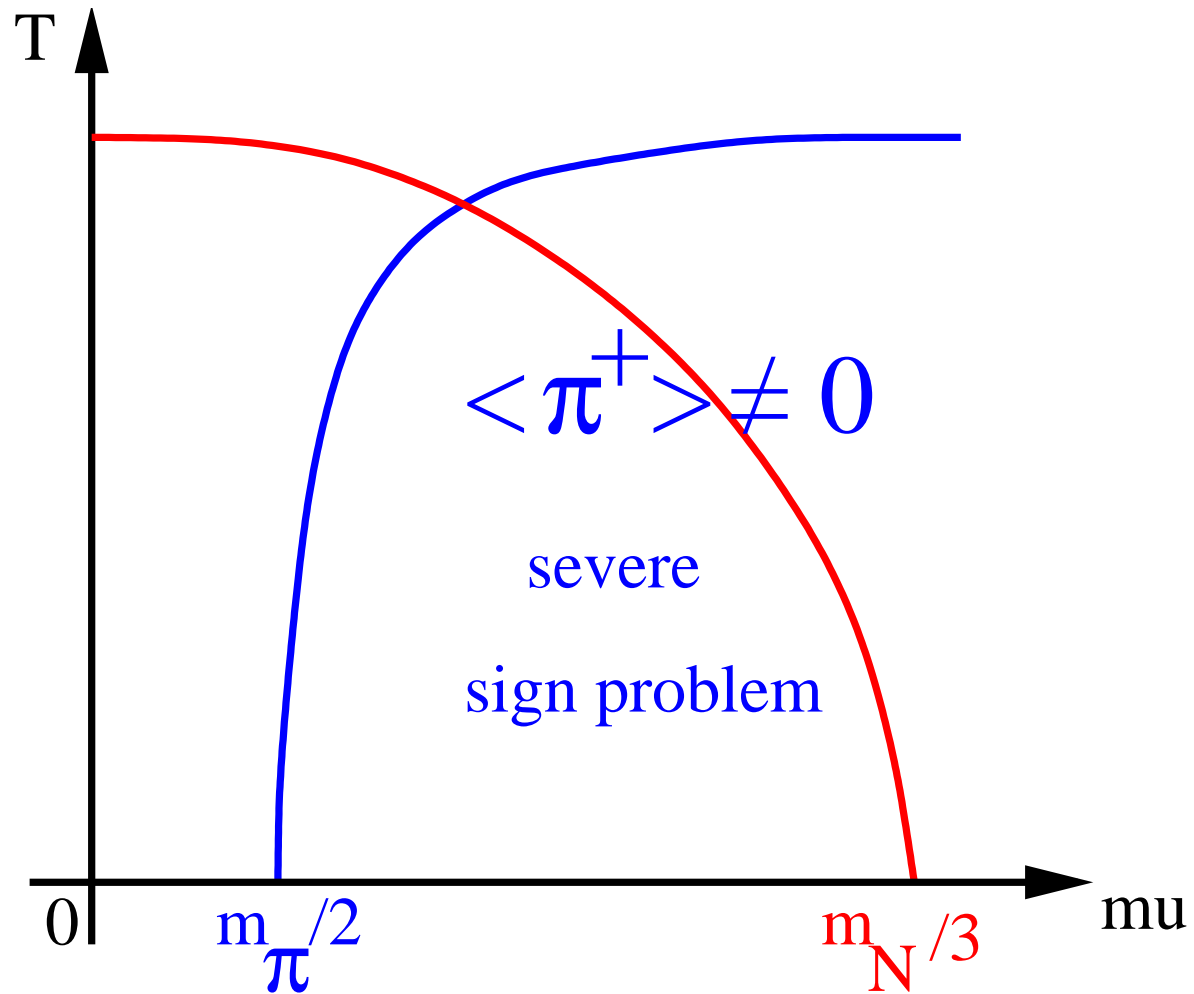
where  $\Delta f$  is the difference in free energy density between the systems described by  $Z_B$  and  $Z_I = Z_{pq}$ . This (intensive) difference  $\Delta f$  is non-uniform over the  $\beta$ - $\mu_q$ -plane ! This limits the reliable range there (low  $\mu_q$ , high  $T$ ).

## Results of a systematic investigation of the average phase factor :

- The sign problem is not severe for  $\mu_q < \frac{m_\pi}{2}$
- Large differences exist between the free energy densities of the phase-quenched and full theory for  $\mu_q > \frac{m_\pi}{2}$ .
- The method becomes problematic, anyway, for large volumes.
- For high temperature the average phase factor doesn't drop as fast with volume as for  $T \leq T_\chi$

“Phase quenching is problematic at low temperature and high density !”

Where the phase-quenched simulation fails  
from Ph. de Forcrand arXiv:1005.0539



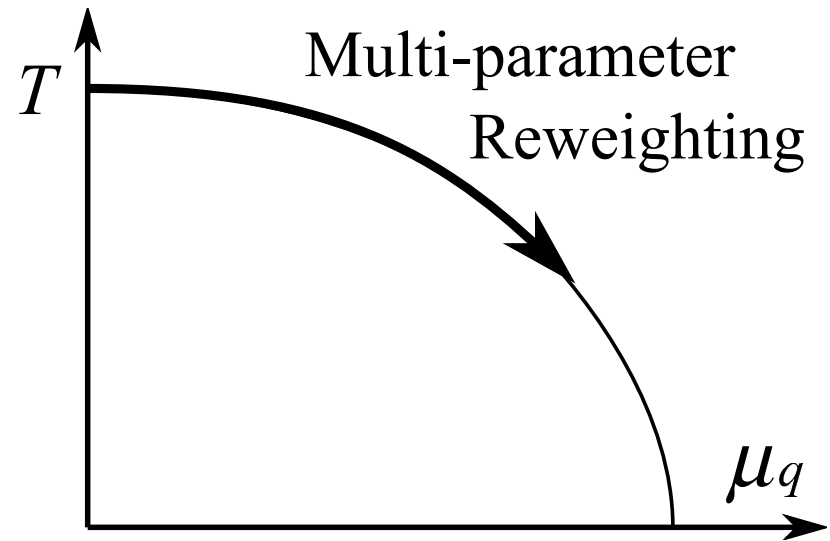
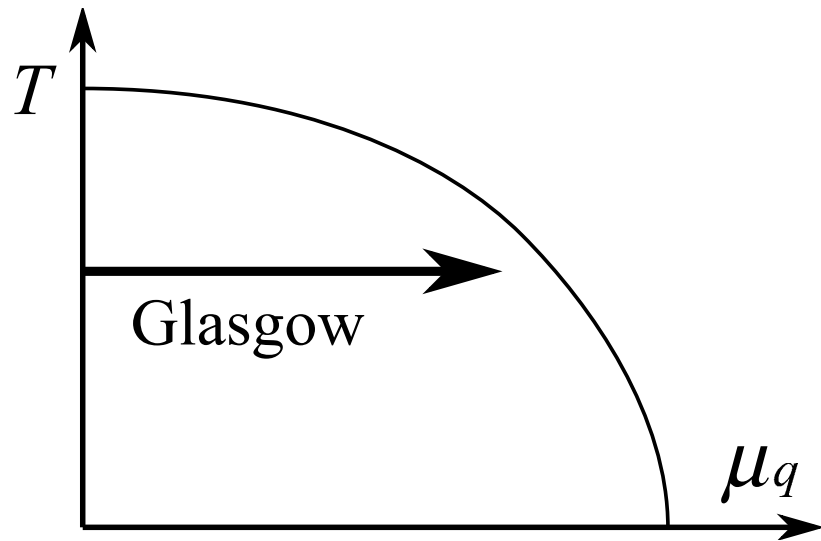
### 7.3. Reweighting across the $\beta$ - $\mu_q$ plane

An attempt to find curvature and critical endpoint (Fodor, Katz et al.)

What is the best reference ensemble ?

1. Replace  $(\beta, \mu_q)$  by  $(\beta, 0)$  ! “horizontal reweighting”  
“Glasgow method”, failed because of bad overlap between the simulated and the (unknown) target ensemble
2. Replace  $(\beta, \mu_q)$  by  $(\beta', 0)$  (with some suitable  $\beta'$ ) !  
“multiparameter reweighting” or “Budapest method”, working successfully.
3. A convincing example for  $\mu \rightarrow i \eta$  : (accessible to direct simulation) condensate  $\langle \bar{\psi}\psi \rangle$  should rise with  $\eta$  (as seen in direct simulation), opposite to real  $\mu_q$  !

Glasgow (horizontal) vs. Budapest (multiparameter) reweighting





In both cases the reference ensemble is on the  $\beta$  axis, with real determinant.

The role of the “phase” above is played here by the reweighting factor

$$R = \frac{\det D(U, \mu_q) e^{-\beta S_G}}{\det D(U, 0) e^{-\beta' S_G}}$$

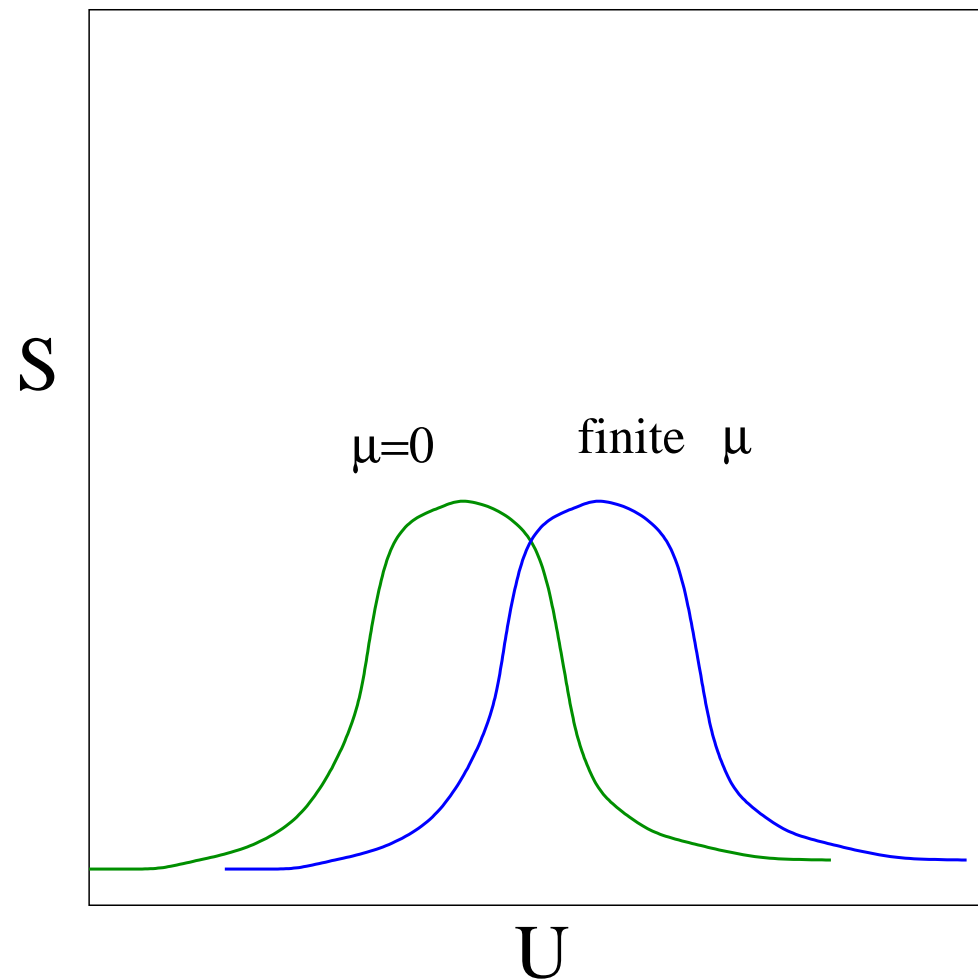
While the **Monte Carlo process is guided by the  $(\beta', \mu = 0)$  ensemble** the global reweighting factor  $R$  has to be evaluated only after each trajectory is finished, simultaneously with the observable  $\mathcal{O}$ .

**estimator :**

$$\langle \mathcal{O} \rangle_B = \frac{\langle \mathcal{O} R \rangle_{\text{reference}}}{\langle R \rangle_{\text{reference}}}$$

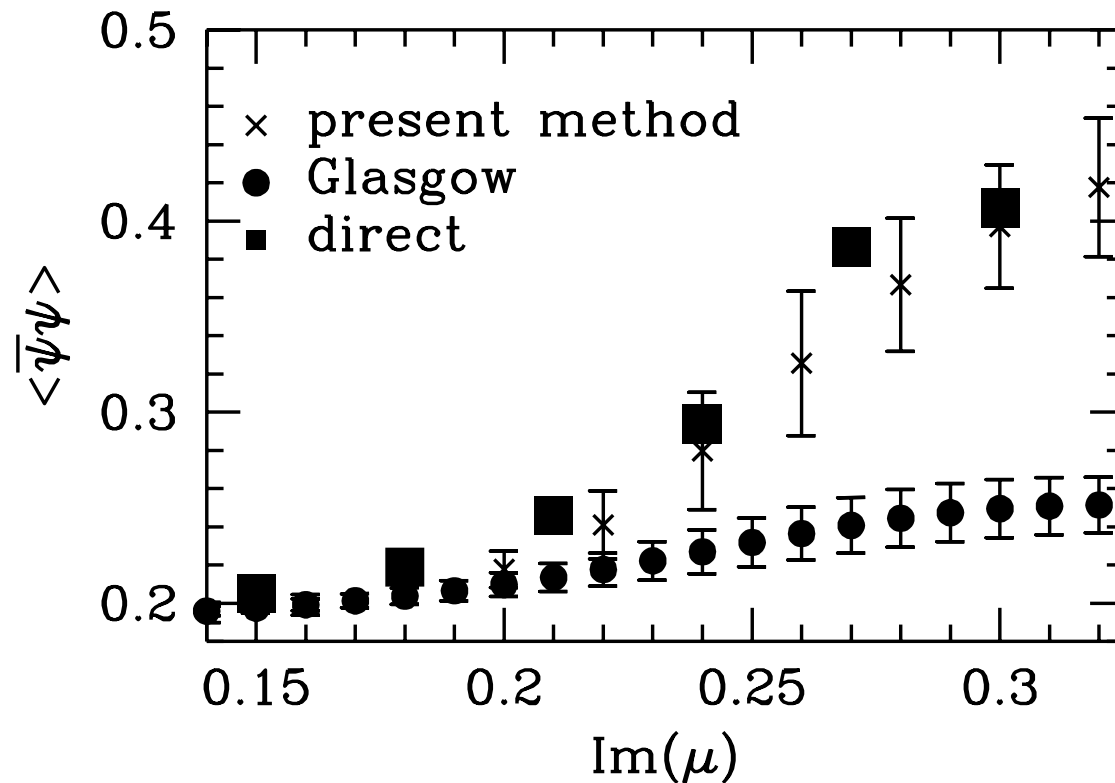
**Hidden problem :** “overlap problem” or better: “problem of insufficient overlap”

The “reference ensemble” might not contain enough configurations falling into the “target ensemble”, such that this bias cannot be corrected simply by reweighting.



Testing the methods at imaginary  $\mu$  by comparison with direct simulation. Failure of the Glasgow method due to the overlap problem. (from Z. Fodor and S. D. Katz hep-lat/0111064)

Budapest method reproduces the exact result, Glasgow method not !



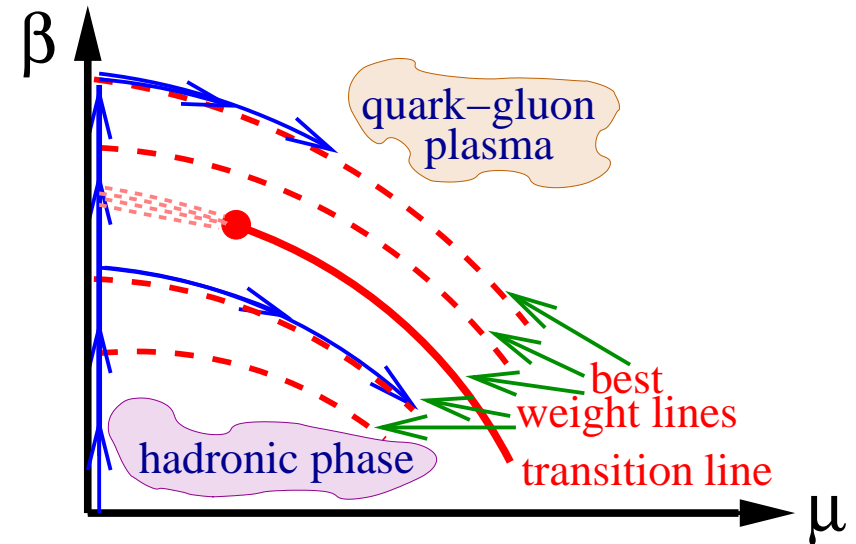
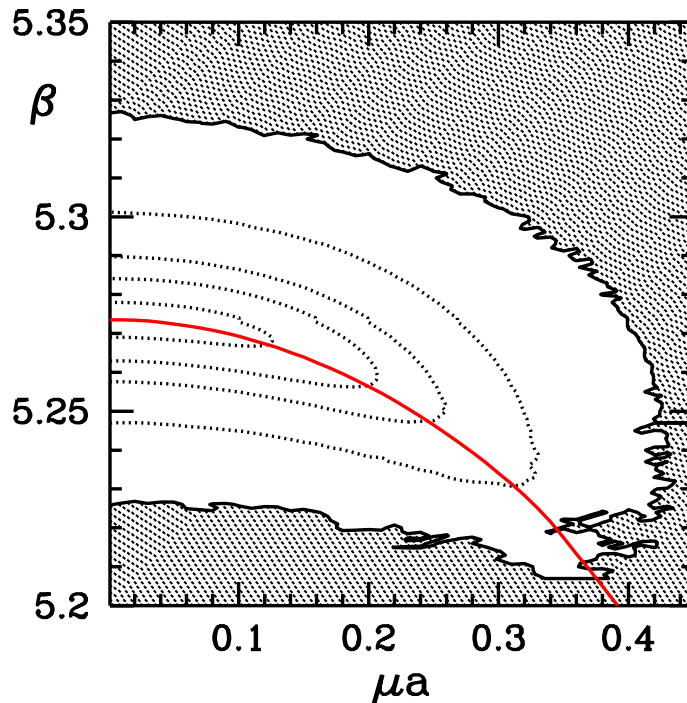
A useful tool for quality assessment : the “overlap measure”  $\alpha$

**Definition** :  $\alpha$  is the overlap measure, if a randomly selected fraction  $\alpha$  of configurations of the “reference ensemble” (where they occur equally weighted) acquires a weight  $1 - \alpha$  when taken as members of the “target ensemble” (where they are not equally weighted).

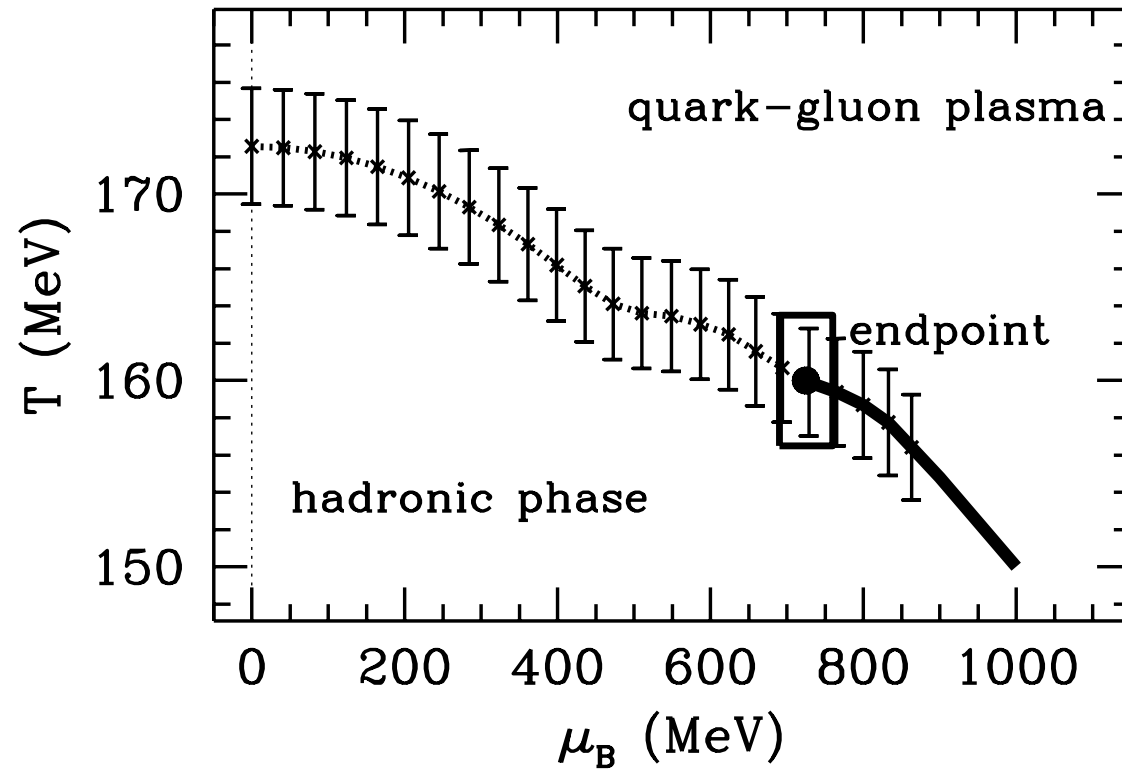
The optimal overlap is  $\alpha = 50 \%$

The grey area (next figure) is not accessible by reweighting from the reference point  $(\beta', \mu_q = 0)$ .

Left: Relief map of the overlap measure. The red line (the line of the crossover !) is determined by the peaks of susceptibility. (from F. Csikor et al. hep-lat/0401016) Right: Best pathes for reweighting in  $\beta$ - $\mu$  plane. (schematically from F. Csikor et al. hep-lat/0301027)



Finding the line of the crossover and fixing the critical endpoint ...  
from F. Csikor et al. hep-lat/0301027



... by the method of Lee-Yang zeroes :

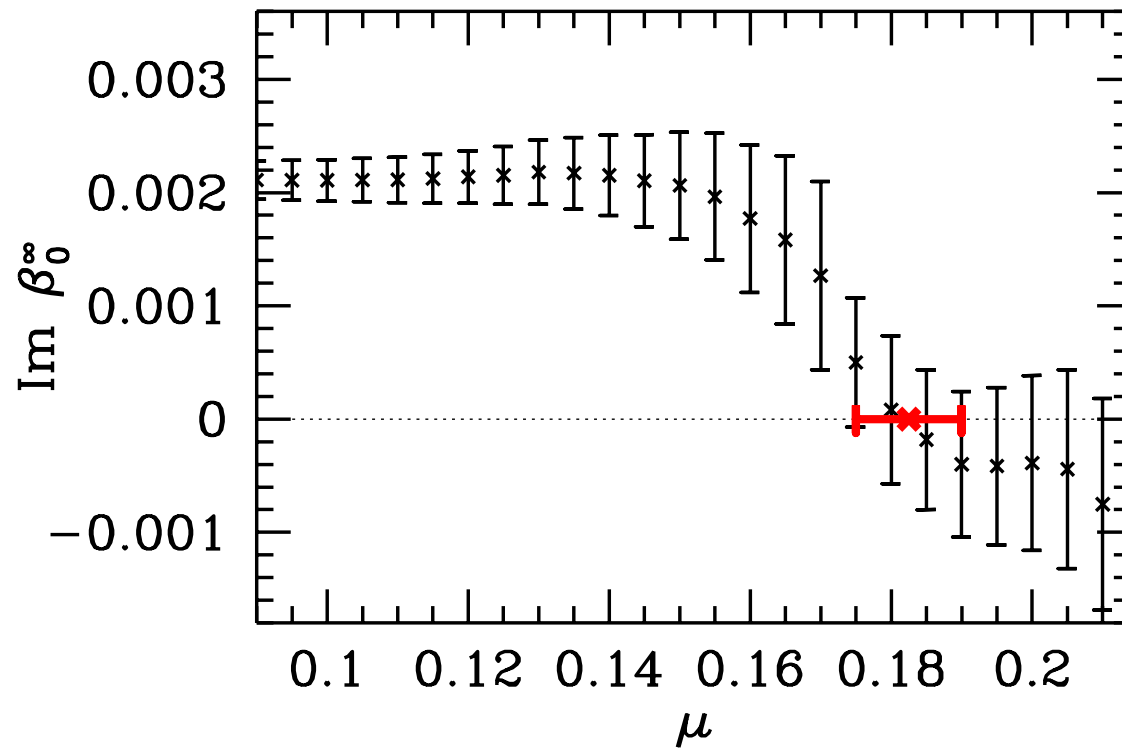
**Adding an imaginary part to  $\beta$**  allows to study the Lee-Yang zeroes of the theory : **these are the zeroes of the partition function.**

**When the Lee-Yang zeroes** in the limit  $V \rightarrow \infty$  **approach the real axis** this signals that a **real singularity (phase transition)** appears.

At finite volume, the pattern of the  $n^{\text{th}}$  Lee-Yang zeroes  $\beta_{LY}^n$  is  $\text{Im } \beta_{LY}^{(n)} = C(2n + 1)$ .

**When a crossover turns into a first order transition, the location of the (extrapolated) lowest Lee-Yang zero touches the real axis,  $C \rightarrow 0$ .**

Locating the critical endpoint by the lowest Lee-Yang zero  
(extrapolated to  $V \rightarrow \infty$ ) ( $\text{Im } \beta_{LY}^{(0)}$ ) in the complex  $\beta$  plane.  
from Z. Fodor and S. D. Katz hep-lat/0111064





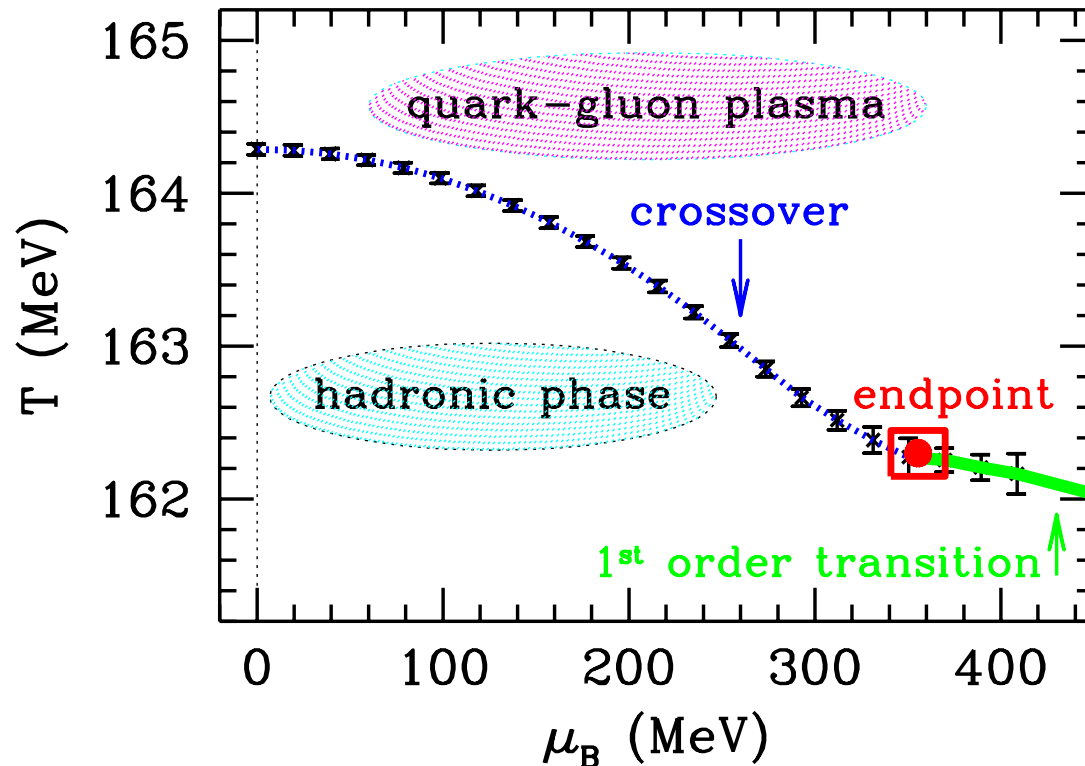
**This fixes the critical endpoint : F. Csikor et al. hep-lat/0301027**

**For 2 + 1 flavors the Wuppertal-Budapest group has obtained**

$$\mu_B^E = 725 \pm 35 \text{ MeV} \quad T^E \approx 160 \pm 3.5 \text{ MeV} \quad T_c(\mu = 0) = 172 \pm 3 \text{ MeV}$$

**(has been later updated !)**

Update of the critical point (small square) in physical units.  
Dotted line for the crossover, solid line for the first order phase transition.  
The small square shows the endpoint. Combining all uncertainties one obtains  $T_E = 162 \pm 2$  MeV and  $\mu_E = 360 \pm 40$  MeV.  
from Z. Fodor and S. D. Katz hep-lat/0402006

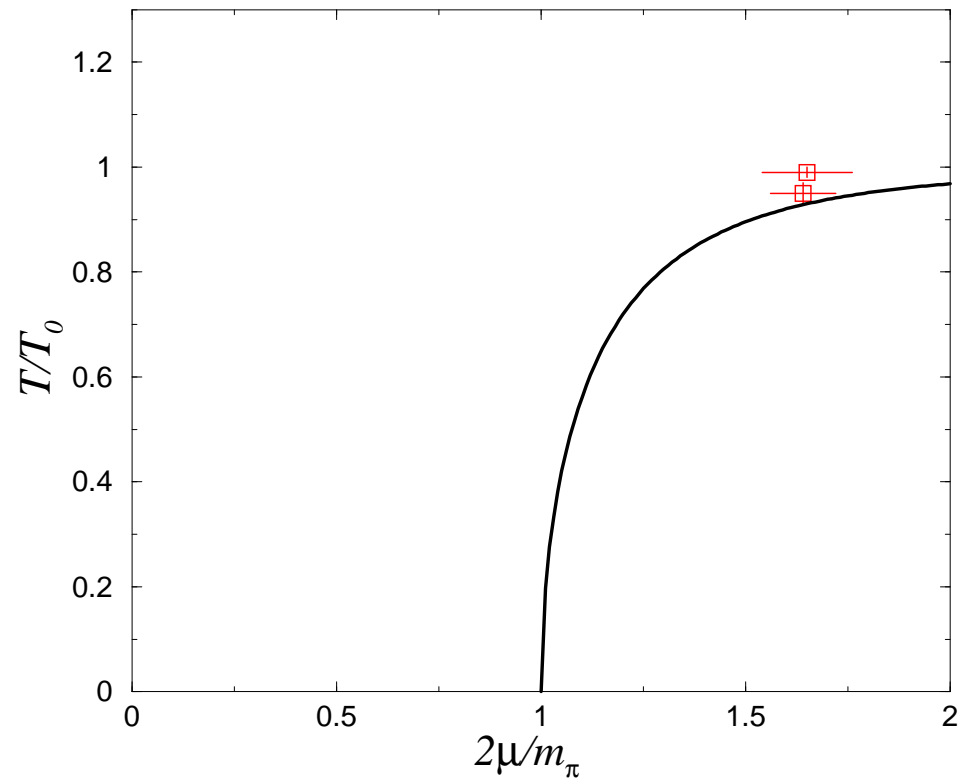


Compared to the previous finding, the light quark masses were reduced by a factor three, while the largest volume has been increased by a factor three.

This (rather old) simulation was **far from the continuum limit** ( $N_t = 4$ ) :

$$a = \frac{1}{4T_c} \sim \mathcal{O}(0.25 \text{ fm}) \quad (1)$$

Doubts are still allowed : The critical endpoint lies too close to the critical line for pion condensation (in phase-quenched simulations).  
from Splittorff hep-lat/0505001



## 7.4. Taylor expansion in $\mu_q$ , from points along the $\beta$ -axis

- The chemical potential enters always in the combination  $\mu_q/T$ .
- Reweighting gives  $\mu_q$ -dependence (in principle, at least).
- In fact, reweighting is **restricted to small  $\mu_q/T$  and small  $V$** .
- The error analysis of results of reweighting is difficult, a breakdown might even not be noticed (Glasgow method).

**Rescue : Observables can be obtained as power series in  $\mu_q/T$ .**

By now, this has become the “bread and butter method”.

**Only by Taylor expansion a reliable  $V \rightarrow \infty$  behavior can be determined giving access to intensive quantities like  $p$ .**

$$p(T, \mu_q) = p(T, 0) + \Delta p(T, \mu_q)$$

$\Delta p$  is an even function of  $\mu_q/T$  (since  $Z(\mu_q/T) = Z(-\mu_q/T)$ )

$$\frac{\Delta p(T, \mu_q)}{T^4} = \sum_{k=1}^{\infty} c_{2k}(T) \left(\frac{\mu_q}{T}\right)^{2k}$$

The Taylor coefficients stem from derivatives w.r.t.  $\mu_q$  of the determinant, more precisely

$$\frac{\partial \ln \det D(\mu_q)}{\partial \mu_q} = \text{tr} \left[ D^{-1} \frac{\partial D}{\partial \mu_q} \right]$$

and higher derivatives. Only even derivatives are non-vanishing.

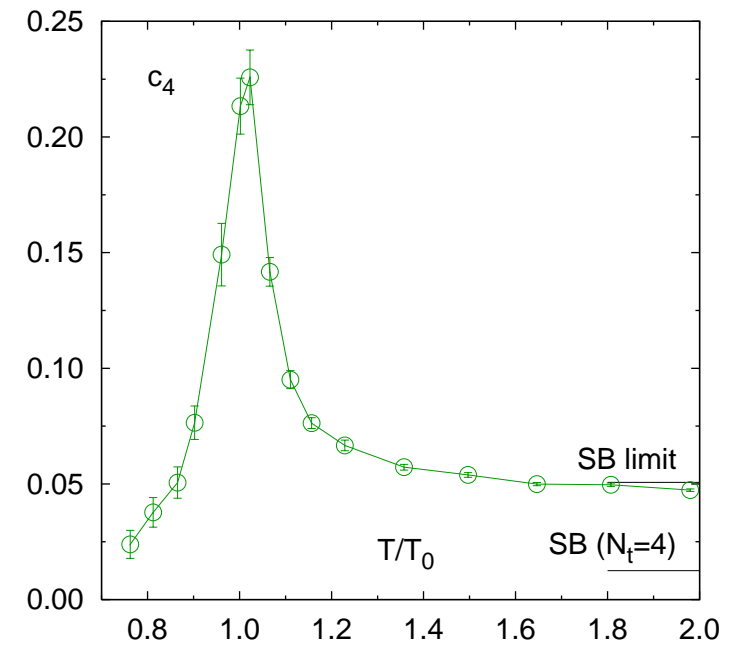
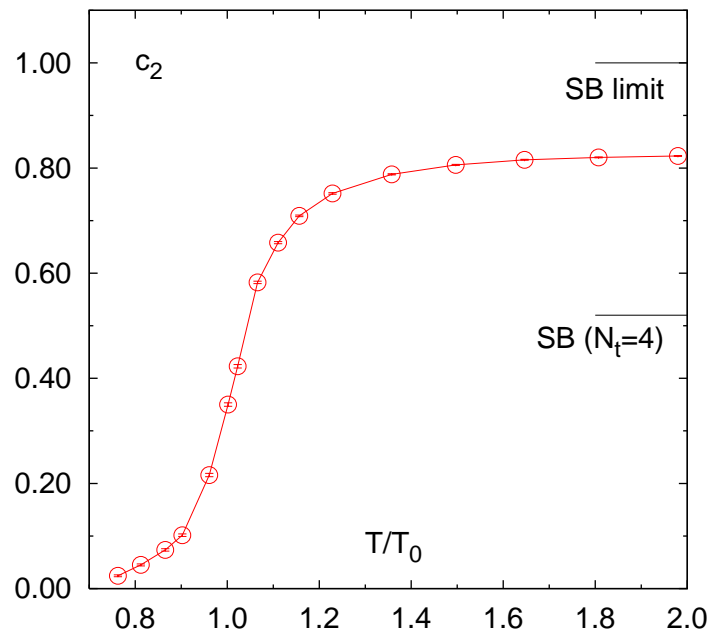
Therefore

$$c_{2k} = \left\langle \text{tr} \left( \text{polynomial of order } 2k \text{ in } D^{-1} \text{ and } \frac{\partial D}{\partial \mu_q} \right) \right\rangle_{|\mu_q=0}$$

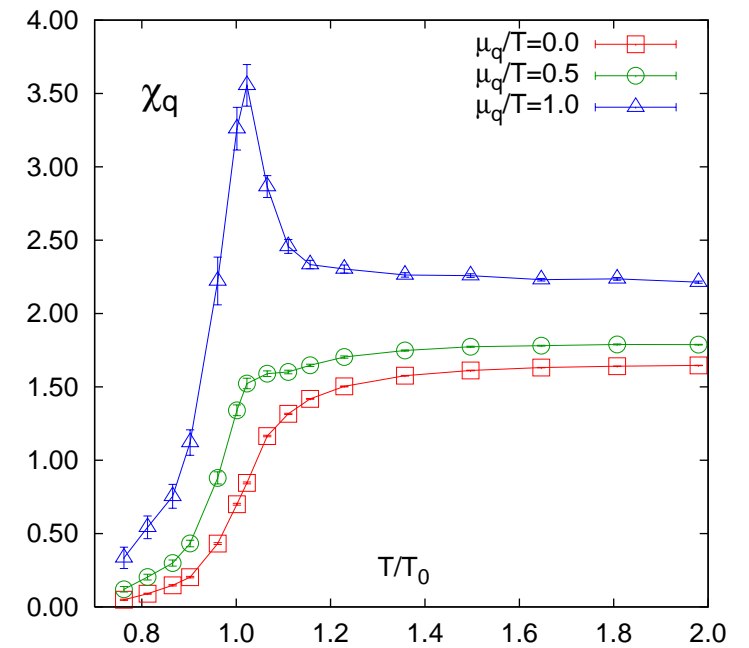
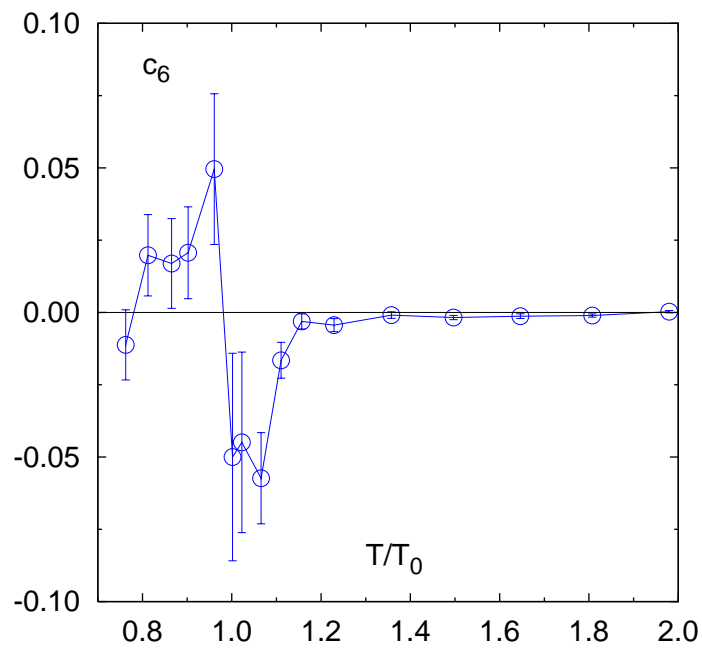
Taylor coefficients are easily calculable (in principle !) in simulations at  $\mu_q = 0$ , practically obtained by means of stochastic estimators.

Unfortunately, these observables become increasingly noisy with larger  $k$ .

The first two Taylor coefficients  $c_2$  and  $c_4$  as functions of temperature look very nice. (shown before for the  $\mu_q = 0$  transition)  
from Ch. Schmidt hep-lat/0610116



The Taylor coefficient  $c_6$  and the quark number susceptibility  $\chi_q$  (expanded for three values of  $\mu_q$ ), all as functions of temperature. from Ch. Schmidt hep-lat/0610116





In principle, **knowledge of  $c_{2k}$  should give all thermodynamics :**

- The equation of state (EoS)
- The transition line  $T_c(\mu_q)$
- The critical endpoint  $(\mu_c^E, T_c^E)$

For **all bulk quantities similar** series expansions exist :

$$\frac{n_q}{T^3} = 2c_2 \frac{\mu_q}{T} + 4c_4 \left(\frac{\mu_q}{T}\right)^3 + 6c_6 \left(\frac{\mu_q}{T}\right)^5 + \dots$$
$$\frac{\chi_q}{T^2} = 2c_2 + 12c_4 \left(\frac{\mu_q}{T}\right)^2 + 30c_6 \left(\frac{\mu_q}{T}\right)^4 + \dots$$

Going to higher density (higher  $\mu_q/T$ ) meets difficulties :

- higher order  $k$  is required
- the coefficients become more noisy
- the computation needs large volumes

A better way by simulations at

- imaginary baryonic chemical potential ( $\mu_q = i\eta_q$ )
- imaginary isospin chemical potential ( $\mu_I = i\eta_I$ )

has been proposed/explored.

(see M. D'Elia and F. Sanfilippo arXiv:0904.1400)

For the prediction of quantum number fluctuations it is important to discriminate between **different quarks** :

$$\frac{p}{T^4} = \frac{1}{VT^3} \ln Z(T, \mu_u, \mu_d, \mu_s) = \sum_{ijk} \frac{1}{i!j!k!} \chi_{ijk}^{uds} \left(\frac{\mu_u}{T}\right)^i \left(\frac{\mu_u}{T}\right)^i \left(\frac{\mu_d}{T}\right)^j$$

$$\chi_{ijk}^{uds} = \frac{\partial^{i+j+k} p/T^4}{\partial(\mu_u/T)^i \partial(\mu_d/T)^j \partial(\mu_s/T)^k}$$

or carriers of **different charges** (baryon charge, strangeness, electric charge) ;

$$\frac{p}{T^4} = \frac{1}{VT^3} \ln Z(T, \mu_B, \mu_S, \mu_Q) = \sum_{ijk} \frac{1}{i!j!k!} \chi_{ijk}^{uds} \left(\frac{\mu_u}{T}\right)^i \left(\frac{\mu_u}{T}\right)^i \left(\frac{\mu_d}{T}\right)^j$$

$$\chi_{ijk}^{BQS} = \frac{\partial^{i+j+k} p/T^4}{\partial(\mu_B/T)^i \partial(\mu_Q/T)^j \partial(\mu_S/T)^k}$$

Meaning of the first two expansion coefficients for some charge  $X$  :

$$2c_2^X = \frac{1}{VT^3} \langle N_X^2 \rangle$$
$$24c_4^X = \frac{1}{VT^3} (\langle N_X^4 \rangle - 3\langle N_X^2 \rangle^2)$$

called “variance” and “kurtosis”.

Studied also in effective models like PQM or PNJL models.

Intensively discussed in experimental searches for the critical endpoint.

## 8. Deep inside the phase diagram : properties of dense matter

### Results of two collaboration for the Equation of State (EoS)

#### 1) MILC and hotQCD collaborations,

light and strange quarks at almost physical quark masses  $\mu_l$  and  $\mu_s$

Temporal extent  $N_t = 4$  and  $6$  (yet at distance from continuum limit):  
differences are visible !

Calculations up to  $\mathcal{O}(\mu^6)$  (up to  $c_6$ )

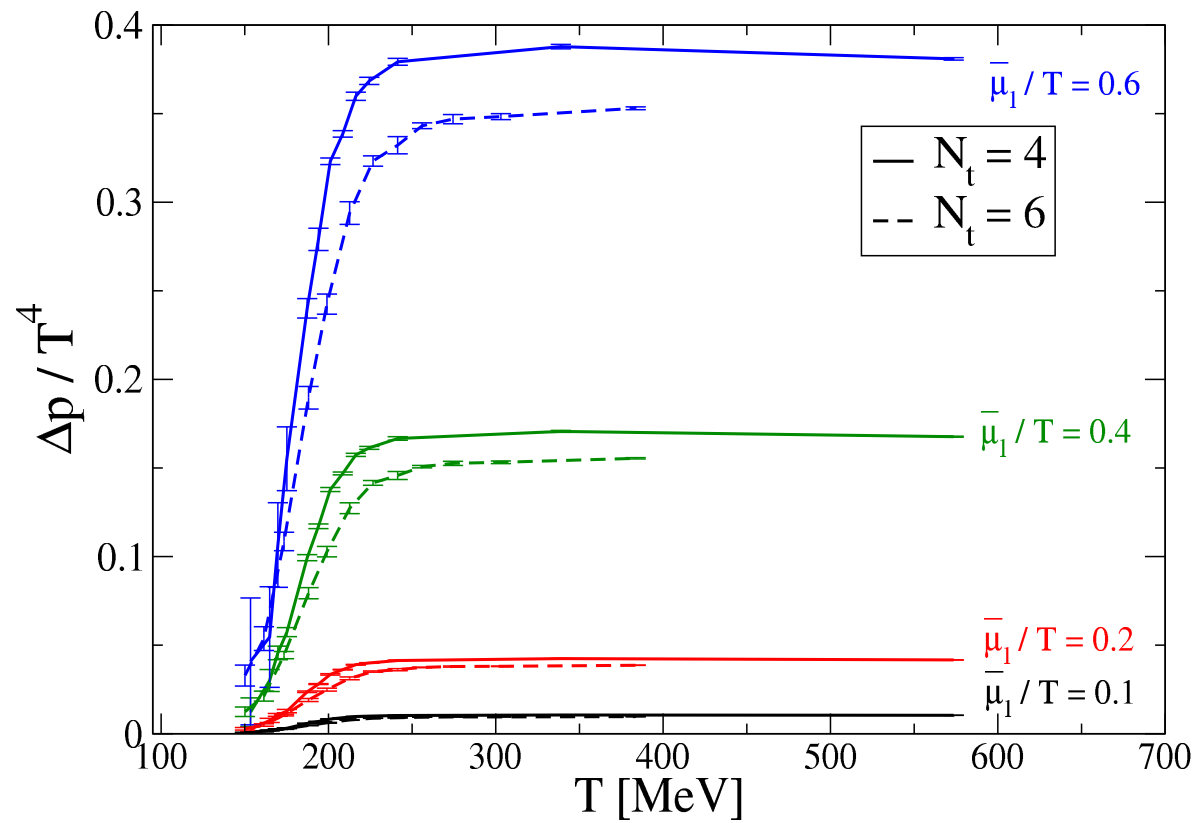
Comparison with HRG (Hadron Resonance Gas, taking the empirical hadron masses [to several GeV] with their baryonic charge into account)

#### 2) BMW collaboration, light and strange quarks

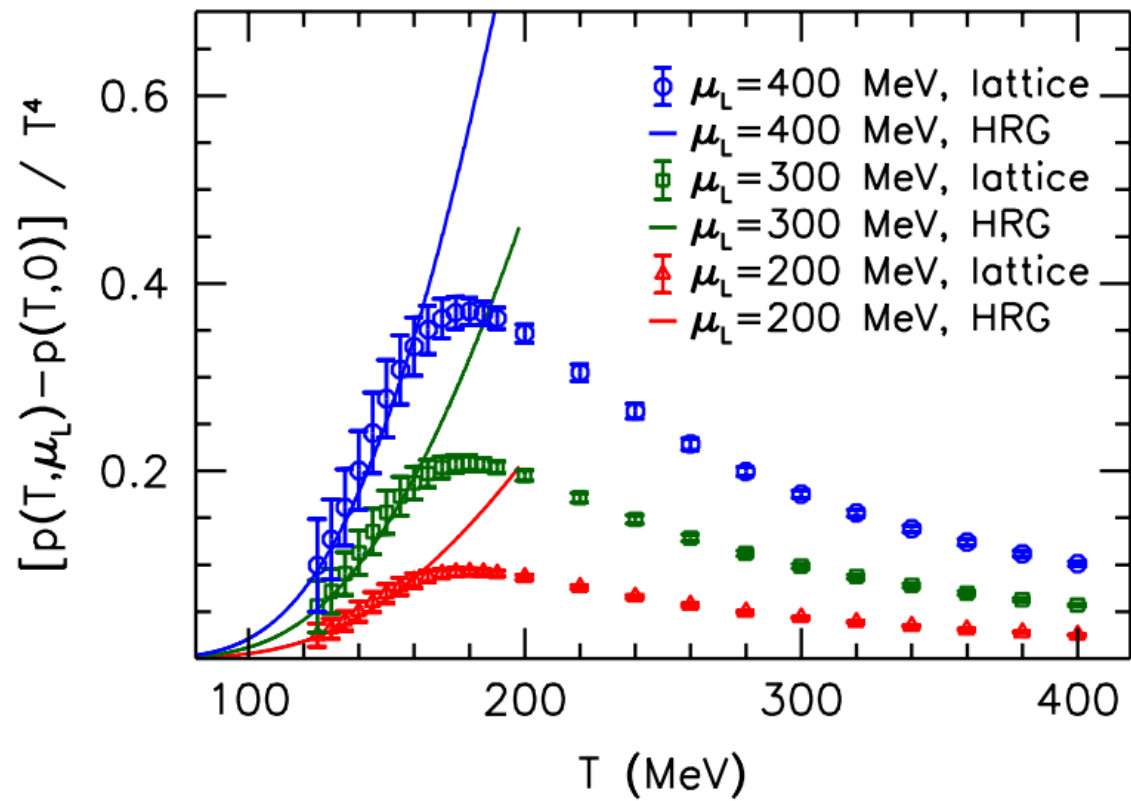
Calculations up to  $\mathcal{O}(\mu^2)$  (up to  $c_2$ )

Data for  $N_t = 6, 8, 10, 12$ , can be extrapolated to continuum limit !

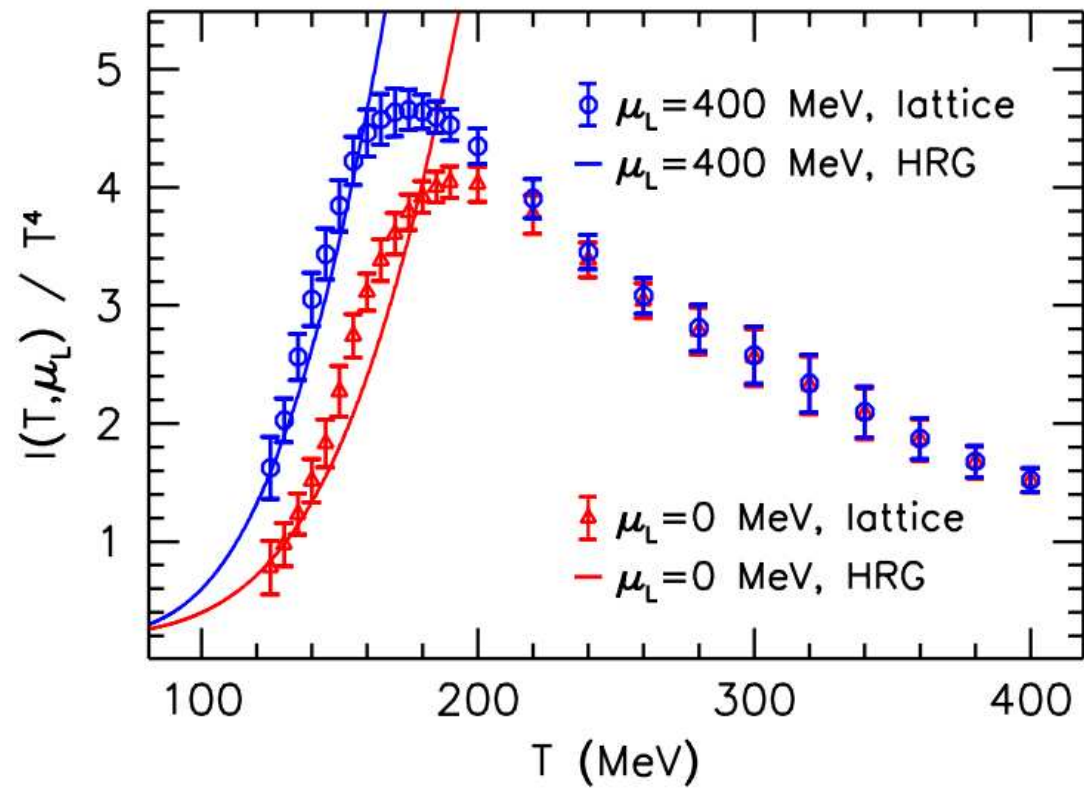
# Change in the pressure due to $\mu \neq 0$ (MILC+hotQCD)



## Difference between the pressure at $\mu > 0$ and $\mu = 0$ (BMW)



# The trace anomaly for non-zero $\mu_L$ (BMW, compared with HRG)





What else might be interesting to characterize the  $(T, \mu_q)$  point ?

For the hadronization process on top of the freeze-out curve (inside the “hadronic phase”) the following observables will be of interest:

- screening lengths
- quark condensate  $\langle \bar{q}q \rangle$ , other condensates ...
- hadron masses
- hadron radii

Imaginary  $\mu_q$  might be not too misleading !

see: A. Hart, M. Laine, and O. Philipsen,

hep-lat/0010008 hep-ph/0004060

## 9. Outlook

Much more should be said about properties of the quark-gluon plasma :  
(“functionality” of the plasma w.r.t. hard experimental probes)

- input for hydrodynamics : EoS under construction, velocity of sound
- quarkonium melting : the plasma “thermometer”
- many applications of Kubo-type formulae, like ...
  - viscosity : an ideal fluid ?
  - heat and electric conductivity
  - di-lepton spectral function
  - heavy quark diffusion
  - jet quenching